UNIVERSITA' DEGLI STUDI DI PADOVA

Dipartimento di Ingegneria Industriale DII

Master Course in Energy Engineering

Design and control of a standalone photovoltaic system with energy storage for household applications

Supervisor:

Ludovico Ortombina

Student:

Marianna Marcuzzi (2089405)

Accademic Year 2023-2024

Abstract

The integration of renewable energy sources (RES) with the electrical grid or directly with alternating current (AC) loads has gained importance in the context of global decarbonization initiatives. However, the inherent variability of RES, particularly solar energy, poses significant challenges for maintaining a stable and continuous power supply. This thesis investigates the design and control of a standalone photovoltaic (PV) system optimized for residential applications at the Shawinigan site, in Quebec. It specifically addresses critical issues such as frequency instability, voltage fluctuations, and harmonic distortion that derive from the stochastic nature of solar energy generation. The analysis includes the complexity associated with integrating energy storage systems, such as batteries, into standalone PV configurations, necessitating careful management of power flow between components and the assurance of stable voltage regulation. A notable contribution of this research is the development of a novel dual-loop current-voltage control algorithm for a single-phase inverter, utilizing the capacitor current of the LCL filter as a reference input. This method enhances system stability, power quality, and dynamic response. The efficacy of the control algorithm is evaluated through MATLAB/Simulink simulations, confirming the optimal performance of the overall system. This research illustrates the proposed solution's effectiveness in maintaining stable operation of the PV system under varying environmental conditions and offers valuable insights for improving the integration and control of RES in standalone applications.

Index

List of Figure

1. Introduction

The significance of renewable energy sources (RES) has slightly increased over the years due to heightened governmental interest from both developed and developing countries in combating climate change and achieving decarbonization goals. Over the past two decades, there has been a relevant increase in research and investment directed toward renewable energy technologies, including wind, solar, and biomass, to facilitate technological advancements [1]. Statistics indicate that RES will comprise 45 to 50 percent of the global power supply by 2030 and 60 to 70 percent by 2040, driven by the need for decarbonization. Consequently, the installed capacity of RES may expand significantly from 2020 to 2050. Many countries have established ambitious targets for transitioning their power sectors to renewable energy. However, the integration of RES into electrical grids presents significant challenges, including the inherent variability and unpredictability of energy generation from sources such as wind and solar, which depend on weather conditions. This variability makes it harder to ensure a stable energy supply. Furthermore, the low inertia of RES, derived from the reliance on power electronics in wind turbines and photovoltaic (PV) systems, contributes to frequency instability, reducing the grid's ability to handle sudden disturbances. Power quality issues, including voltage fluctuations and harmonic distortions caused by the switching components of RES technologies, affect negatively the grid performance and can damage sensitive equipment [2].

Renewable energy systems, such as photovoltaic (PV) systems and wind turbines, can also function in standalone mode, disconnected from the grid. Integrating these systems within a standalone configuration raises several technical challenges. While they are efficient in generating clean energy, they must address issues typically managed through grid connections, such as maintaining stable voltage and frequency for household appliances. Standalone PV or wind turbine systems must therefore ensure consistent power quality. Key challenges in this configuration include maintaining voltage stability, managing frequency fluctuations, and minimizing harmonic distortion. Power electronics in PV inverters can introduce harmonics that not only result in inefficiencies but also may damage sensitive electronic devices. Additionally, rapid changes in solar irradiance, such as those caused by a cloudy sky, can lead to voltage flickers and instability, disconnecting devices that necessitate of continuous power supply. Moreover, the system inertia in RES-based configurations is substantially lower than in conventional power plants, introducing issues about frequency stability during sudden changes in power demand or supply [3]. To address these challenges, the development of active power filters and advanced inverter designs is underway to reduce harmonics and ensure stable operation [4].

In standalone photovoltaic systems for household applications, variability in solar energy can result in inadequate power generation, potentially failing to meet user electricity requirements effectively. The incorporation of energy storage solutions is essential for ensuring a continuous power supply and addressing user demands during periods of low solar generation, such as cloudy days or nighttime. However, integrating battery management introduces added complexity to system control, necessitating the implementation of optimal energy storage management techniques to maximize system efficiency and reduce costs. Ineffective control can lead to higher power losses and necessitate the installation of larger battery banks, elevating investment costs and area coverage for the system.

This thesis project aims to investigate the performance of a standalone photovoltaic system integrated with energy storage for household applications. The design of the system and its requisite components will be conducted using the MATLAB/Simulink environment. A primary contribution of this research is the development of a novel control algorithm for a single-phase standalone inverter, a critical component that converts direct current (DC) from the photovoltaic system into alternating current (AC) for household use. Existing academic research has primarily focused on grid-connected inverters or three-phase systems used in high-power industrial applications, resulting in limited exploration of single-phase standalone inverters. Additionally, this inverter will be equipped with an LCL filter to attenuate high-frequency harmonics, enhancing power quality; however, the filter's integration also increases the complexity of inverter control. Therefore, this thesis emphasizes the formulation of an innovative control strategy for a single-phase standalone inverter. This new control approach leverages the current across the LCL filter capacitor as a reference signal, employing a dual-loop current-voltage control scheme. Utilizing Laplace transformations and control theory, the algorithm is developed, and its efficacy is validated through Simulink software. The performance of the control algorithms will be evaluated by comparing theoretical mathematical models with simulation results.

The structure of this master's thesis will comprise two main sections: the first section will provide a literature review with a comprehensive explanation of the system components and the theoretical mathematical models at the basis of algorithm implementation. The second section will focus on the computational methods employed in the design of the photovoltaic system tailored for the specified application, followed by the control implementation in Simulink. The design process for the photovoltaic array will initiate with an estimation of user electricity needs, coupled with an analysis of the solar irradiance available at the designated location over the years. This design phase is fundamental for the accurate sizing of other system components. Subsequently, several algorithms are implemented to ensure optimal control of the main electrical variables such as current, voltage, and power to minimize losses and guarantee a perfect interconnection between components.

2. Literature review: components description

The standalone system for residential applications comprises several interconnected components that collaboratively ensure a continuous and reliable power supply. Central to the system is a photovoltaic panel that captures solar energy and converts it into direct current electricity. However, the voltage output from the PV panel is generally insufficient for direct application; therefore, the output is routed through a boost converter. This converter steps up the DC voltage to an appropriate level suitable for both the battery and the load.

After the voltage has been increased, the output from the boost converter is directed to a DC bus, which functions as the primary energy distribution node for the system. To ensure voltage stability and mitigate any fluctuations or ripples, a capacitor is incorporated into the DC bus, to maintain consistent power delivery to downstream components.

In addition to the PV array and boost converter, a secondary boost converter is utilized to regulate the charging and discharging cycle of the battery. This converter is responsible for ensuring that the battery is charged correctly, facilitating the storage of excess energy generated by the PV panel during sunny conditions for later use. In scenarios of insufficient solar irradiation, the battery discharges to supply the necessary power to the load, thereby preserving the system's energy equilibrium.

The DC bus is also connected to a single-phase inverter, which converts the stored DC power from the PV or the battery into alternating current power, thereby rendering it suitable for household applications. The inverter is equipped with an LCL filter, which plays a pivotal role in attenuating high-frequency harmonics and smoothing the output, thus ensuring the delivery of clean and stable sinusoidal AC power to the resistive load.

The functioning of each component will be described in detail, outlining their roles and how they contribute to the overall operation of the system.

2.1 Photovoltaic panels
Solar panels are devices that convert sunlight into electricity, providing a renewable source of energy for homes, businesses, and utilities. They consist of numerous photovoltaic (PV) cells, typically made from materials like silicon, that capture and convert solar energy. Solar panels vary in size, efficiency, and application, from small residential arrays to large-scale solar farms. With advancements in technology, solar panels are becoming increasingly efficient and cost-effective, contributing to cleaner energy solutions and helping reduce reliance on fossil fuels in the fight against climate change.

Photovoltaic cells:
Photoelectric effect
Solar modules are made up of several photovoltaic cells connected in parallel and in series (usually, a standard PV panel used for a rooftop residential array will present almost 60 cells linked together) to generate enough electrical energy to satisfy the user's complete or partial electricity needs. But how solar energy is converted into electricity? The basic phenomenon of the process is the photovoltaic effect, from which the name "photovoltaic" panels.
It is possible to summarize the solar cell behavior in 3 main steps:
- Light absorption and production of free electrons: the sunlight hits the PV cells, made of semiconductor materials, and the energy from the sun is converted into heat which allows part of the electrons of the valence band to cross the energy gap and reach the conduction band where they can move freely.
- Free electrons flow and direct current production: the PV cell is made of two different layers of semiconductor material, as silicon, one of them contains some impurities (doping process),

creating an electric field, meaning one side has a net positive charge and one has a net negative charge. This leads to the creation of an electric field that functions like a diode, guiding freed electrons to flow in a single direction, thereby creating a steady electrical current.
- Electrical current capture and transfer through the wires: once the free electrons generate an electrical current, metal plates on the sides of each solar cell collect those electrons and transfer them to wires.

Other main components of the solar cells are the transparent glass which covers the silicon layer and usually presents also an anti-reflective coating to stop reflection, and metal contacts that act as a conduction funnel for the electricity generation from the cell, connecting that current to the overall wiring and electrical systems of a solar system.

Semiconductor materials and p-n junction

As already said, solar cells are made mainly of semiconductor materials such as silicon. This kind of material is fundamental for cell functioning: the band gap between the conduction and valence level is thin enough (1-2 eV for Si) to allow the flow of electrons if enough energy is supplied by the sun but, contrarily to the conductor materials, these levels are not superimposed, and it is possible to control the flow of electrons. Conductors, on the other hand, have free electrons that are not as easily controlled for this purpose, making them unsuitable for efficient energy conversion in solar cells.

The doping of silicon is a key process in creating the p-n junction that is essential for photovoltaic cells. By adding specific impurities to pure silicon, such as boron (which creates a p-type material with "holes" or positive charge carriers) and phosphorus (which adds extra electrons, creating an n-type material), the resulting structure forms a p-n junction. This junction establishes an electric field at the interface of the p-type and n-type materials, which is critical in the separation of charge carriers generated by the photoelectric effect.
When sunlight strikes the cell, photons excite electrons, knocking them loose from their atomic bonds. This creates electron-hole pairs that are naturally separated by the electric field at the p-n junction. Without this separation, the excited electrons would quickly recombine with the holes, and no current would flow. The p-n junction ensures that the electrons are pushed toward the n-type side and the holes toward the p-type side, creating a flow of electrons through an external circuit. This flow of electrons is what generates electrical current and allows the solar cell to convert sunlight into electricity.

Thus, the p-n junction is fundamental to the operation of photovoltaic cells, as it not only separates the charge carriers but also ensures that the energy from the sun is converted into usable electrical energy. Without the doping process and the formation of the p-n junction, the photovoltaic effect would be ineffective.

The main type of solar cells

- **Monocrystalline Solar Cells**: These are made from a single continuous crystal of silicon. Monocrystalline cells are more efficient due to their uniform structure, which allows electrons to flow more easily, improving electricity generation. They are also more expensive to produce due to the manufacturing process.
- **Polycrystalline Solar Cells**: These cells are made by melting silicon fragments together. Although they are less efficient than monocrystalline cells, they are cheaper to produce. The electron flow is less efficient because the silicon crystals are misaligned but they are still the most used, especially in household applications, thanks to their affordable price.

4

- **Thin-film Solar Cells**: These are made from materials like cadmium telluride (CdTe), copper indium gallium selenide (CIGS), or amorphous silicon. Thin-film cells are lightweight and flexible, making them suitable for unique applications. However, their efficiency is lower than that of crystalline silicon cells, so they are mainly used in large-scale installations.
- **Organic Solar Cells**: These cells are made from carbon-based materials, offering flexibility and potential for transparent solar panels, like solar windows. Although they are not commercially viable yet due to lower efficiency, they hold promise for lightweight, low-cost solar technology.
- **Perovskite Solar Cells**: Perovskites are materials with a unique crystal structure, which can be used to create thin-film solar cells. These cells offer high potential efficiencies and low production costs, but they are still in the development phase. Perovskites could be a game-changer in solar technology.

Each type has its own advantages and trade-offs in terms of efficiency, cost, and applications, and ongoing research is focusing on improving their performance and affordability.

The future of solar panel efficiency is advancing through two main strategies: multijunction solar cells and improvements in p-type cells using gallium. Multijunction cells layer different semiconductors with varying bandgaps to absorb a broader range of the solar spectrum, achieving higher efficiency, with a world record of 39.5%. Additionally, gallium is being used to replace boron in p-type silicon cells, preventing degradation caused by oxygen and improving long-term performance, leading to higher efficiencies in solar panels.

Single diode model

To evaluate the electrical performance of a PV cell, different equivalent circuit models can be used. In this case, the simple model of the single diode will be used to plot the I-V and P-V curves and to analyze the variation of performance caused by external disturbances as temperature and irradiance changes. The equivalent circuit (**Figure 2.1**) of an ideal PV cell consists of a current source that represents the PV panels, a diode connected anti-parallel with it, a series resistance (to show the voltage drops and internal losses due to the current flow), and a parallel resistance which takes into account the leakage current to the ground when the diode is reverse biased [5].
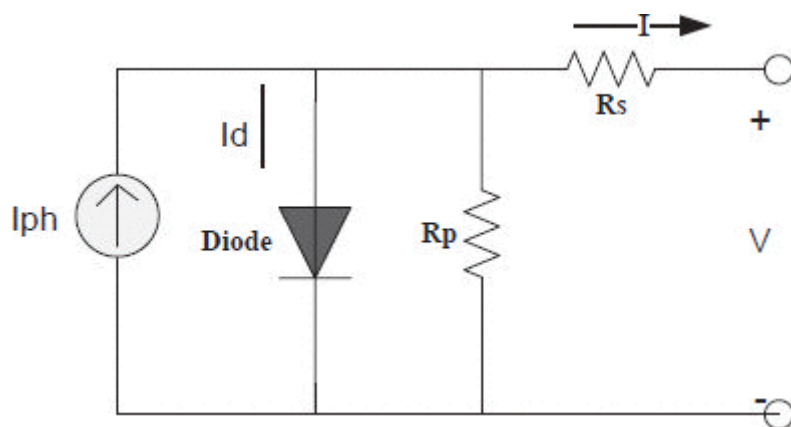
Figure 2.1: Equivalent Circuit of an ideal PV cell, Source: [5]

The main equation can be derived from the model:

1) $I = Iph - Id - Ip$

Where I is the output current, Iph is the photocurrent from the PV array, Id is the diode current, and Ip the current through the parallel resistance.

The pv current is expressed as

2) $I_{ph} = (I_{ph})_{T1} + K_0(T - T1)$ where the 1st term is the photovoltaic current, the normal temperature T1= 25°C and Ko is a constant which takes into account how the irradiance and temperature effect the PV current production.

3) $I_d = I_s \left(e^{\frac{qV}{AkTc}} - 1 \right)$ with Id diode current, Is is the saturation current of the diode, q is the charge of the electron, k is the Boltzmann constant, Tc is the temperature of the cell and A is the ideality factor of the diode.

Since usually the parallel resistance Rp is high, the current Ip can be neglected.

From these main equations is possible to note that the temperature of the cell which is a consequence of the incidence irradiation on the panel has a huge impact on the current flow and so it will affect the performance of the panel.

Moreover, the Fill Factor (FF) is another important parameter to consider in the efficiency of the cell evaluations. It measures the intrinsic efficiency of a photovoltaic (PV) cell in terms of the quality of its current-voltage (I-V) characteristics. For value of 0.7 or higher is considered a good cell. FF increases with temperature decrease [6].

It can be defined as:

4) $FF = \frac{P_{max}}{Voc * Isc}$

where Pmax is the power at the maximum power point, Voc is the open circuit voltage and Isc is the short circuit current.

The characteristic curves I-V and P-V can be seen below.
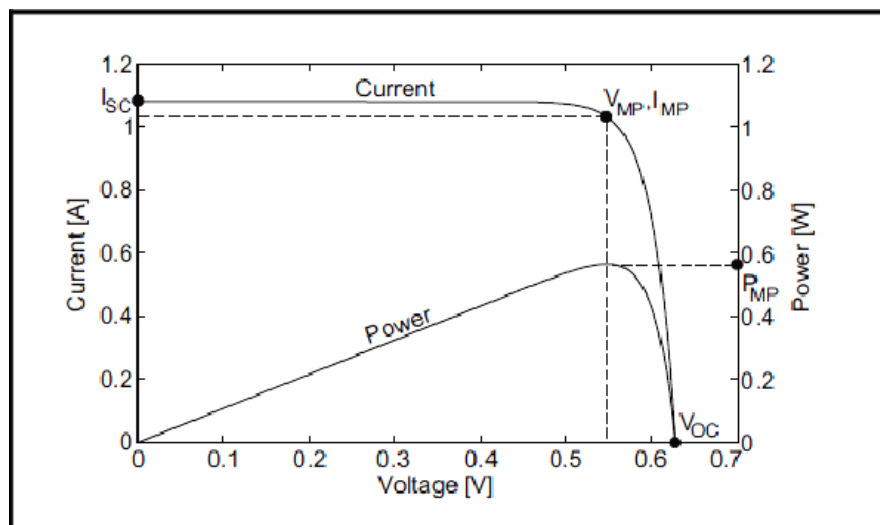
Figure 2.2: Characteristic curve for a PV module, Source: Reasearchgate.net

6

The effect of temperature and irradiance variation is shown below considering the Jinko Solar Co. Ltd JKM250P-60 panels, whose curves are plotted in MATLAB/Simulink environment.

The irradiance dependence is shown in **Figure 2.3.**
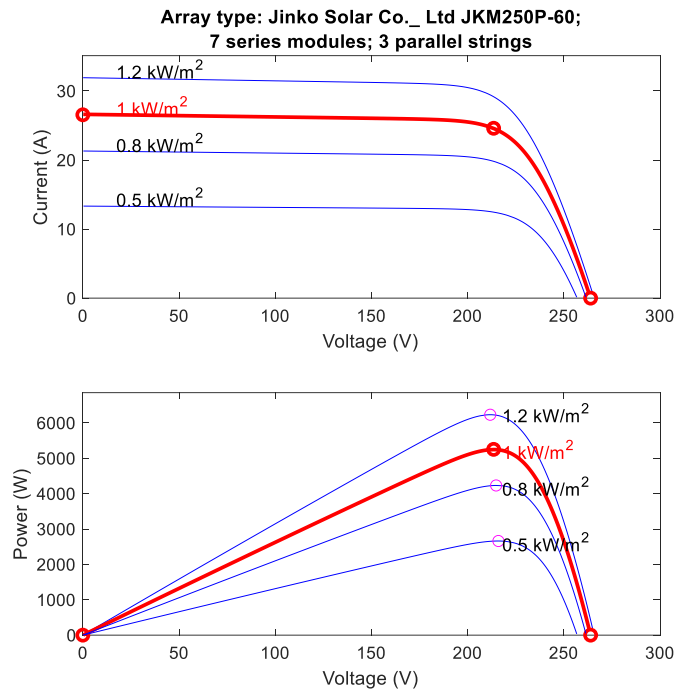
Figure 2.3: Characteristic curve for a PV panel (Irradiance Dependence), Source: Simulink

The temperature dependence of the array current and voltage is shown in **Figure 2.4.**
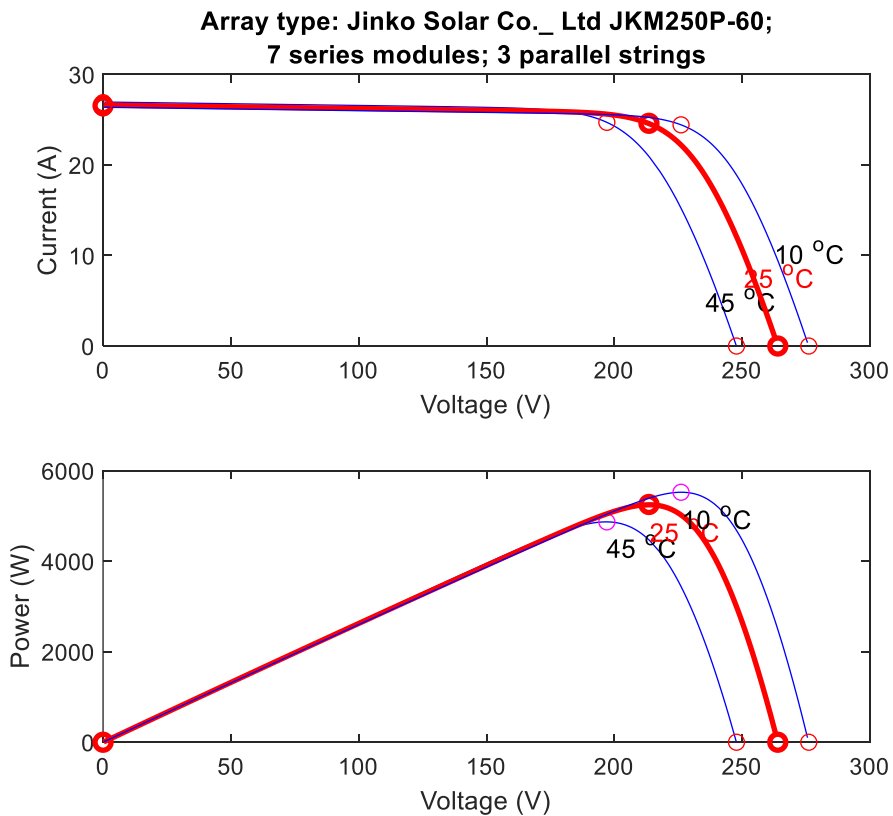
Figure 2.4: Characteristic curve for a PV panel (Temperature Dependence), Source: Simulink

In situations where some parts of a solar panel system are shaded, the power-voltage (P-V) curve can show multiple peaks. This happens because the amount of sunlight hitting different panels varies, which affects the overall power output. Finding the global maximum power point (GMPP), or the highest power the system can produce, becomes complex because of these smaller peaks. The issue arises when bypass diodes in the shaded panels activate to prevent overheating and loss of power. Additionally, the current-voltage (I-V) curve will show sudden drops as shaded panels reduce the total current [7]. The characteristic curves of partially shaded PV modules are shown below:
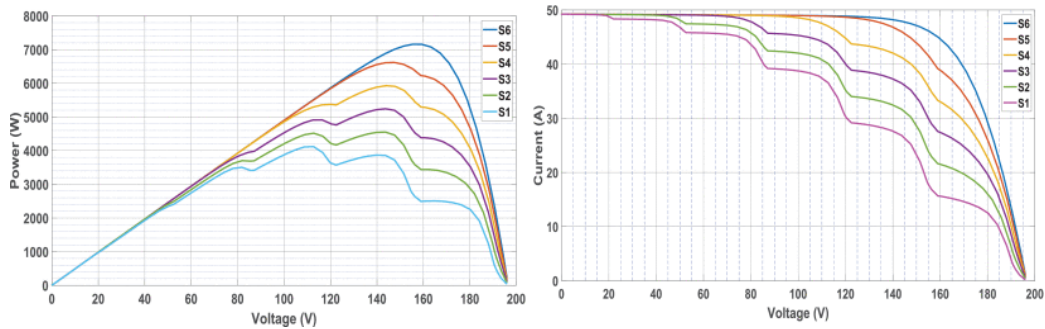
Figure 2.5: *Characteristic curve for a PV module in case of partial shadowing, Source: [7]*

In summary:

- As temperature increases, the open-circuit voltage (V_oc) decreases, which in turn lowers the efficiency of the PV cell. This is because higher temperatures increase the recombination rate of charge carriers, which diminishes the electrical output. On the other hand, the short-circuit current (I_sc) increases slightly with temperature, but the net effect is still a reduction in overall performance, especially as the temperature rises beyond the optimal operating range.
- Irradiance, or the intensity of sunlight, directly impacts the amount of energy that a PV cell can convert into electrical power. As irradiance increases, the available energy for conversion grows, leading to higher current output and power generation. This causes an upward shift in the characteristic curve, improving the cell's performance. Conversely, lower irradiance results in reduced current and power output.

In typical operating conditions, the maximum power point is highly sensitive to both temperature and irradiance. Under high irradiance, the MPP is usually achieved at a higher voltage and current, whereas at low irradiance, the voltage remains relatively stable, but the current decreases significantly. The combined effects of temperature and irradiance variations must be accounted for in the design and operation of PV systems to maximize their efficiency across varying environmental conditions [8].

2.2 Maximum Power Point Tracking (MPPT) Algorithm

To maximize power output, PV systems must operate near their MPP. This is particularly important because photovoltaic modules have a relatively low solar-to-electrical energy conversion efficiency, typically around 16-17% for a single module. By operating at the MPP, the system ensures optimal utilization of the available solar energy, compensating for the inherent limitations in efficiency. When a PV system doesn't consistently operate at this optimal point, power production decreases. To compensate for this, additional panels would be required to achieve the same energy output, which increases both the space needed for installation and the overall system cost. This issue is especially problematic for household applications, where space is limited, and affordability is a key concern.

From the power-voltage characteristic curve, even slight voltage changes can lead to substantial power losses, particularly as the array's output voltage rises. These losses drastically impact efficiency, emphasizing the importance of a maximum power point tracking-algorithm. By continuously adjusting the operating point, MPPT algorithms ensure that PV systems maximize power production, making them a more viable and cost-effective solution, even with space and budget constraints.

Due to their importance, several MPPT algorithms have been proposed and implemented over the years. In the case of uniform irradiance, there is a unique maximum power point and the conventional MPPT technique works well. However, when the temperature or the irradiance changes, or in partial shading conditions which leads to different maximum power points formation, the conventional techniques are replaced by more complex algorithms.

Choosing an effective MPPT method depends primarily on three key criteria: performance, system complexity, and cost. Performance identifies the algorithm's tracking speed and accuracy in reaching the maximum power point, system complexity involves the sophistication of the control system, the types and quantities of voltage and current sensors required, the tuning of parameters, and the ability to detect partial shading while the cost refers to the overall expense of implementing the MPPT system, balancing performance with budget constraints to ensure a cost-effective solution [9].

The main MPPT control techniques are considered and compared.

The Perturb and Observe Algorithm

Figure 2.3 clearly shows that PV power as a function of the voltage decreases on the right of MPP and increases on the left: this is the basis for the MPP algorithm. A perturbation is applied to a variable (PV current, voltage or duty cycle) and the newly reached power is evaluated**.**

If an increase in voltage leads to an increase in power, the operating point is to the left of the Maximum Power Point, and the perturbation proceeds in the same direction. On the contrary, if an increase in voltage results in a decrease in power, the operating point is to the right of the MPP, and the perturbation reverses direction. After a certain number of iterations, the maximum power point is found.

This algorithm is intuitive and easy to implement, for these reasons, it is widely used and several researches are carried out on this topic. However, the conventional P&O algorithm presents some disadvantages:

- The continuous oscillations around the MPP lead to losses and may reduce system efficiency.
- When the external conditions, such as temperature and irradiance, vary suddenly, this algorithm can be slow in tracking the new MPP, which can negatively affect performance. Moreover, under rapidly changing external conditions, the classical P&O algorithm might misinterpret the power variation as being caused by external changes and may continue to increase or decrease the control variable in the wrong direction.

- It is highly affected by the design parameters, such as the step size: a large perturbation of the control variable speeds up the tracking process but introduces higher oscillations, while a small step size slows down the tracking process and negatively impacts performance.

Incremental Conductance (InC)

The method uses the shape of the characteristic curve to determine the MPP. In particular, the slope of the P-V curve is equal to 0 at MPP, greater than 0 for the points lying on the left of MPP, and smaller than 0 on its right. The main equations to describe the process are:

5) $\quad \frac{dP}{dV} = \frac{d(VI)}{dV} = I + V\frac{dI}{dV}$

From the equation above:

6) $\quad \frac{dI}{dV} > -\frac{I}{V} \quad$ at MPP left

7) $\quad \frac{dI}{dV} = -\frac{I}{V} \quad$ at MPP

8) $\quad \frac{dI}{dV} < -\frac{I}{V} \quad$ at MPP right

The Incremental Conductance (InC) algorithm operates by comparing the incremental conductance (dI/dV) with the instantaneous conductance (I/V) at each iteration, adjusting the duty cycle of the DC-DC converter connected to the photovoltaic (PV) array to continuously extract the maximum possible power.

This method is both simple to implement and robust, similar to the Perturb and Observe (P&O) algorithm, but with the added benefit of performing reliably even under partial shading conditions or when external conditions change rapidly. In fact, the InC algorithm can recognize shifts in the Maximum Power Point (MPP) caused by varying environmental factors and adapt accordingly to maintain optimal power extraction. Moreover, it reduces power losses by minimizing oscillations around the MPP, resulting in better overall efficiency.

Artificial Neural Networks (ANN)

This technique uses artificial intelligence to achieve high performance. The ANN is usually made up of 3 layers: the input layer, one or several inner layers, and the output layer. The layers comprise different neurons, that are connected with the neighbor layers by different paths, each of them defined by different weights. An Artificial Neural Network (ANN) processes inputs into outputs through non-linear functions. The structure of the network, including the number of neurons in the input and output layers, depends on the specific problem being addressed. Meanwhile, the configuration of the hidden layers, including the number of neurons and the choice of activation function, is determined based on the values that minimize the error during the training process. These parameters are optimized to achieve the best possible performance for the given task. The general architecture of an ANN is shown below.
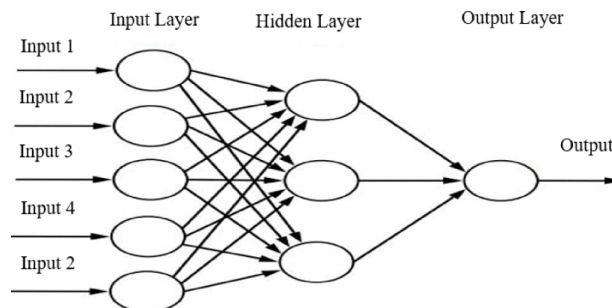
Figure 2.6: Architecture scheme of an Artificial Neural Network, Source: [10]

10

Simulations demonstrate that this kind of algorithm, provides brilliant tracking accuracy, high performance, and fast response time. ANNs can improve their performance over time through training, making them adaptable to new data or changing conditions however training ANNs often requires large amounts of high-quality labeled data, which may not always be readily available for certain tasks or can lead to a too high computational cost. The lack of sufficient data the network's ability to generalize effectively.

Fuzzy Logic

Fuzzy logic control (FLC) for Maximum Power Point Tracking (MPPT) in photovoltaic systems involves three main stages. The first stage, called fuzzification, converts the system's input values into linguistic variables based on their membership functions. In the second stage, decision-making, the system applies a set of "if-then" rules to process the fuzzified inputs. Finally, the defuzzification stage transforms the fuzzy output into a numerical value using a specific membership function. The fuzzification basic process is shown below.
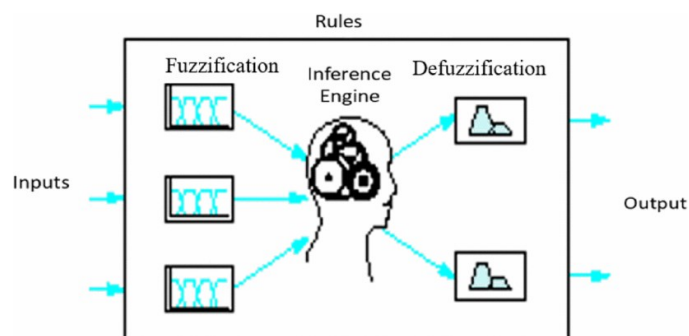
Figure 2.7: Fuzzification basic process, Source: [10]

The literature compares various MPPT techniques:

- P&O Algorithm: While simple to implement, the basic P&O algorithm suffers from steady-state oscillations that hinder accurate MPP tracking. Modifications with variable step sizes have been proposed to address this issue.
- InC Algorithm: InC method tracks the MPP without oscillations and performs well under sudden changes in atmospheric conditions. However, its implementation is relatively complex.
- AI-Based Methods: These techniques offer efficient MPP tracking without oscillations. They are advantageous because they do not require the system's real model or equations and can handle nonlinear relationships between inputs and outputs effectively [10].

2.3 DC-DC Converters

DC-DC converters are essential components in photovoltaic (PV) systems, mainly for regulating and optimizing the power output. Solar panels generate direct current (DC) electricity, but their output voltage and current vary significantly based on factors such as sunlight intensity and temperature. These fluctuations can result in inefficient power transfer to the load or battery.

A DC-DC converter addresses these challenges by adjusting the voltage to match the load requirements, ensuring that the PV system operates at its Maximum Power Point (MPP). This is critical because the MPP changes with varying environmental conditions, and without a converter, the system would be unable to consistently deliver the maximum power that the PV system can provide. In addition, the converter stabilizes the output voltage, either boosting it up or stepping it down, depending on the application.

In a nutshell, DC-DC converters must be used to:

- match the impedance between the PV panel and the load to ensure the system operates at MPP,
- keep V constant and close to the magnitude required by load and battery,
- allow the PV system to function effectively across a wide range of operational conditions.

Type of DC-DC converters

The first classification can be done between Linear and Switching DC-DC Converters.

A DC-DC linear convert decreases a higher input DC voltage into a lower stable output voltage using a linear regulation method. A transistor or a MOSFET acts like a variable resistor, and they dissipate excess energy as heat to reach the desired output voltage regardless of load or input voltage variations. The voltage regulation is stable and precise, but it has a low efficiency: there are high power losses due to energy dissipation. In the case of integration between PV panels or batteries with a DC-DC converter, efficiency is a key factor so linear converters are not suitable and switching DC-DC converter are used.

A switching DC-DC converter consists of a semiconductor device (transistor, MOSFET, IGBT, etc.) that switches rapidly between the ON and OFF states. During the ON state, the inductor coil L stores electrical energy in the form of a magnetic field, which is then transferred to the load during the OFF state. By adjusting the duty cycle (the proportion of the switching period during which the switch is ON), the desired output voltage is achieved.

The switching introduces a voltage ripple, and a capacitor is used in parallel with the load to smooth the output voltage. These devices typically achieve an efficiency of 95% or higher, making them ideal for high-power applications or battery-powered devices. However, they generate more electromagnetic noise and require additional components, which makes them more complex and expensive compared to linear converters.

Within the class of switching converters, there are two main types: non-isolated and isolated DC-DC converters. Isolated converters use a transformer to electrically separate the input and output circuits, ensuring there is no direct current flow between the two. This separation enhances safety by preventing electrical faults or surges from the input side (such as high-voltage spikes or short circuits) from reaching the output side, where sensitive electronic components might be damaged. Additionally, this isolation helps reduce noise improving the performance of the system.

On the other hand, non-isolated DC-DC converters directly connect the input and output through a single electrical path. These converters are often used in low-power devices because they are simpler, less expensive, and more compact. They are also more efficient compared to isolated models, as they do not require a transformer, eliminating the energy losses associated with electromagnetic induction. The electrical circuit of the isolated and non-isolated DC-DC converter is in **Figure 2.8**.
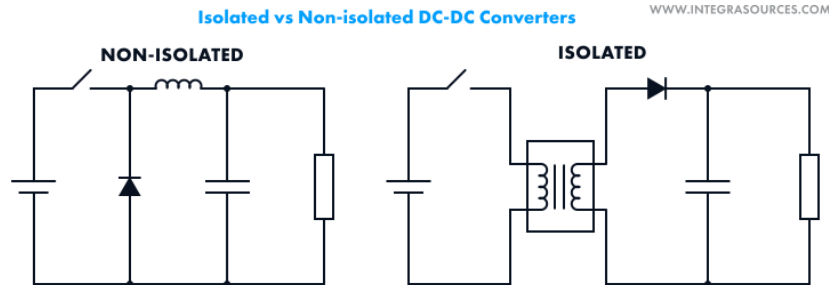
Figure 2.8: Isolated and Non-isolated DC-DC Converters, Source: [11]

The most classical classification of the switching converter regards the relation between the input and output voltage. The three main types of converters are buck (or step-down) converters, boost (or step-up) converters, and buck-boost converters.

Buck Converters

These types of converters reduce the input voltage to a lower output voltage, for this reason, they are also called step-down converters. During Ton (the portion of the switching period in which the switch is on), the energy from the input voltage source is accumulated in inductor L and capacitor C (which smooths also the output voltage ripple). Then the switch is switched off, and the energy stored in the inductor coils and in the capacitor goes to the load. The circuital model of the Buck Converter shown in **Figure 2.9** will help clarify its behavior.
The input and output voltage are linked by the following relationship:

9) $V_{in} = V_{out} D$

where D is the duty cycle defined as

10) $D = \frac{t_{on}}{Ts} \in [0; 1]$

 where ton is the percentage of the switching period Ts in which the switch is ON
These converters are mainly used as power supplies for low-voltage devices (multimedia players, game consoles, monitors, and television sets) and battery chargers.

Boost Converter
These types of converters increase the input voltage to a higher output voltage, for this reason, they are also called step-up converters. They usually have a bigger inductance L and capacitor C compared to the buck converters. Although the input current is smoother compared to buck converters and the current Total Harmonic Distortion (THD) is smaller, larger capacitors are required because the capacitor current is discontinuous. In a typical boost converter, the inductor initially receives the input current from the source while the diode remains in a non-conductive state, preventing current from flowing to the capacitor and load. When the switching device turns off, the diode becomes conductive, allowing

the stored energy in the inductor to combine with the input voltage. This combined energy is delivered to the output, resulting in an output voltage higher than the input.

The fundamental relationship between input and output voltage is:

11) $V_{in} = (1 - D)V_{out}$

With the duty cycle defined as in equation 10).

Boost converters are commonly used in situations where a high enough input voltage cannot be provided by batteries or when there is limited space for additional batteries. Typical applications include hybrid vehicles, energy-efficient lighting systems, portable lighting devices, PV systems, etc.

Buck-Boost Converter

Buck-Boost converters can both increase and decrease the input voltage to get a higher or smaller output voltage. They are particularly used in systems with varying input and output voltage requirements for example, devices powered by Li-ion batteries or measuring instruments, cameras, MP3 players, GPS devices, wireless peripherals, LED lighting, and other similar applications.

The fundamental relationship between input and output voltage

12) $V_{out} = \frac{D}{1-D} V_{in}$

Note that this kind of converter uses the same components (a switching element, conductor coil, diode, and capacitor), but they are arranged differently [11]. The basic schematic of these converters is shown in **Figure 2.9**.

a) Buck converter b) Boost converter c) Buck-Boost converter
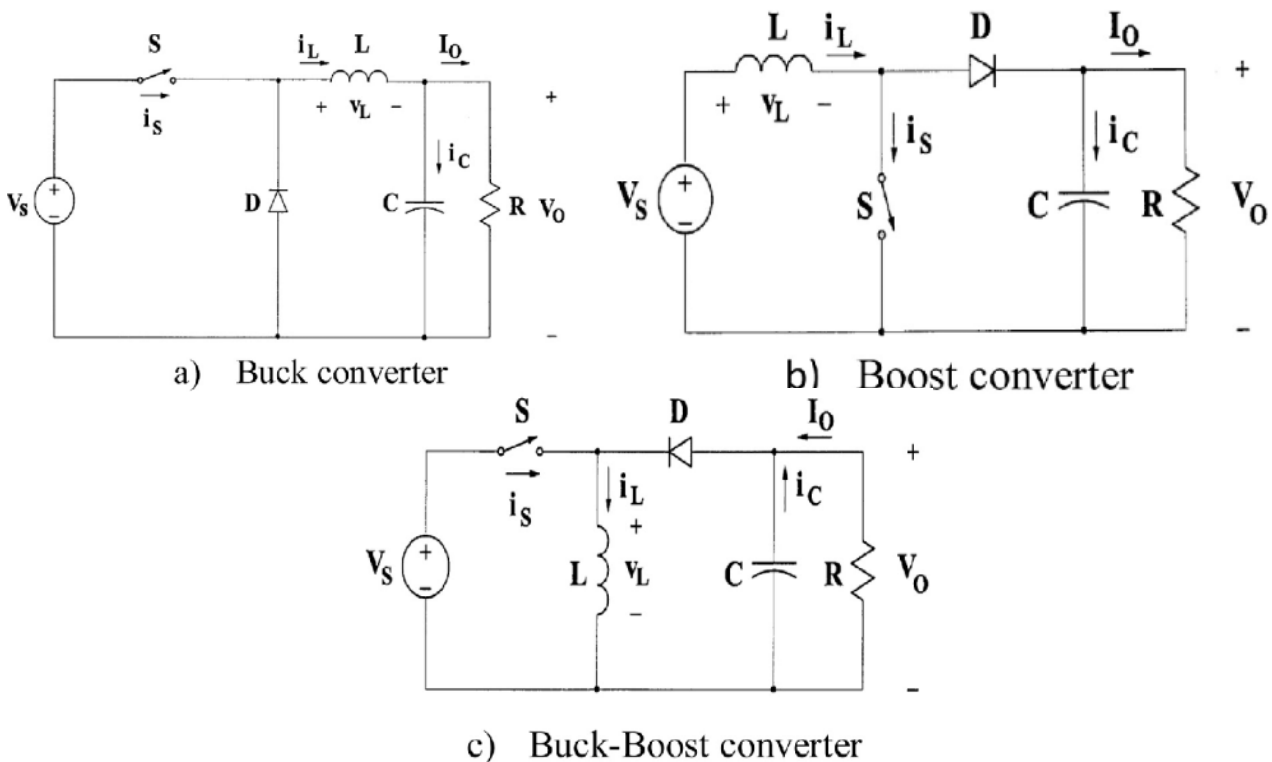
Figure 2.9: DC-DC Converters Circuital Model, Source: [11]

14

Boost Converters

Usually, in photovoltaic systems is preferable to use Boost converters, which would raise the input voltage to the desired output one. The input voltage, measured directly from the PV array, is usually too low and must be boosted to feed correctly the load and the battery. Moreover, a higher voltage level and a lower current lead to a more efficient power transfer between electrical devices, due to the smaller conduction losses in the wires. Finally, since the photovoltaic (PV) panel is represented as a current source, with its output current being directly proportional to solar irradiance, variations in irradiance result in corresponding fluctuations in the output current. This issue can be effectively addressed by the boost converter, which incorporates inductance that is directly connected to the current source. As a result, the boost converter filters the input current and mitigates ripple from the outset, ensuring a more stable current supply to the load despite variations in solar conditions.

There are two different modes of operation:
- **Continuous Conduction Mode (CCM):** The inductor current never falls to zero throughout the entire switching period. Energy transfer between the source and load is constant, allowing for reduced ripple in the output voltage and generally higher efficiency under heavy loads. CCM often requires more complex control circuits to handle stability across different load conditions.
- **Discontinuous Conduction Mode (DCM):** The inductor current falls to zero before the end of the switching cycle. This happens when the load demand is low, causing all stored energy in the inductor to transfer to the load before the next cycle. While simpler to control, DCM can lead to higher peak currents, increased ripple, and potentially greater electrical disturbances [12].
A particular focus must be maintained during the sizing of the boost, to guarantee that the DC-DC converter works always in CCM mode, no matter which are external solar conditions.

Boost Converters' basic equations and models

Boost Converters' behavior can be analyzed using various models depending on the level of detail and the application focus. Each model offers unique insights into different aspects of the converter's operation. The first to be analyzed is the Switching Model, which captures the ON/OFF states of the switch and diode during each switching cycle, offering a precise representation of the converter's time-domain behavior, including switching transients. While highly accurate, it is computationally demanding and less suited for control design or long-term performance evaluations.

The following hypotheses are done:
- The input voltage Vin is constant
- Every component is ideal (so there are no losses, so the input power is equal to the output one)
- The output voltage ripple is negligible (means ΔVo << Vo)
- The system is periodic and the switching period (how often the switch opens and closes) Ts is defined as

13) $T_s = t_{on} + t_{off}$ where

14) $t_{on} = \frac{D}{Ts}$

Switching Model
The main equations describing the relationship between circuit variables are calculated using the Kirchhoff law, applied to the model of the Boost Converter shown in **Figure 2.9**.

In CCM, the equations must be calculated separately for the two different states - ON and OFF - because the model is discontinuous.

When the switch is ON (diode OFF):

The switch is ON so the input DC voltage source is applied to the inductor L, which accumulates energy. The input voltage Vin equalized the inductor voltage V_L, and the following equation can be written:

15) $V_{IN} = V_L = L\frac{di}{dt}$ where di/dt is the variation of inductor current over time

Instead, the diode is OFF and it works as an open circuit, the relationship between the output voltage and the voltage across the diode is:

16) $V_D = -V_o$

When the switch is OFF (diode ON):

In this case, the diode is forward biases and works as a closed circuit, connecting the inductor L to the load. The energy flows from the inductor to the load R, increasing the output voltage. Since the switch is OFF, the input DC source is disconnected from the circuit.

The main equation that describes this situation is:

17) $V_L = V_{IN} - V_o = L\frac{di}{dt}$

From these previous equations and considering the periodicity of the system, the conversion ratio M can be computed, and it is:

18) $M = \frac{V_o}{V_{IN}} = \frac{1}{1-D}$ always bigger or equal to one since $D \in$ [0;1].

The hypothesis of ideal components, which lead to energy conservation, allows us to find the relationship between the mean inductor IL, output Io, and diode Id current values:

19) $I_o = I_D = I_L(1-D)$

The equations governing the operation of circuits in DCM differ significantly from those in CCM. This distinction arises because, in DCM, the inductor current falls to zero during each switching cycle, whereas in CCM, the inductor current never reaches zero. In DCM, the system exhibits additional complexity as it operates in three distinct intervals: energizing the inductor, depleting its energy, and the period where the inductor current remains zero. As a result, the equations for voltage and current involve different boundary conditions and require consideration of these intervals. Moreover, DCM often involves higher peak currents, increased ripple, and dependency on the load, leading to changes in efficiency and dynamic behavior compared to CCM.

In DCM, the conversion ratio is

20) $M = 1 + \frac{I_N}{I_o}D^2$ where

21) $I_N = \frac{V_{in}T_s}{2L}$ called normalization current.

Note, that M is a function of Io, and if Io≈0, its value tends toward infinity regardless of the duty cycle. This is because, in DCM, the inductor's energy is not fully utilized when there is no load, allowing the output voltage to rise uncontrollably in an ideal scenario. In a real scenario, parasitic elements and component limits prevent M from reaching infinity, but significant voltage overshoots can still occur.

This makes the design of Boost converters working in DCM, very challenging, and usually, protection mechanisms must be adopted.

<u>Average Model</u>

The Average Model instead simplifies the converter's operation by averaging the inductor current and capacitor voltage over a switching period. It provides a continuous representation of the system and is suitable for analyzing dynamic performance and designing control systems while neglecting high-frequency switching effects.

The switching model analyzed before is an example of Variable Structure Systems (VSS), where the topology changes periodically due to the opening and closing of the switches. For this reason, there are nonlinear time-variant systems, and their dynamic analysis is complex. However, it is possible to get simpler linear systems of converters if only the average magnitudes of the system variables are considered. Note that this leads to a lack of information linked to the switching frequency (fs), but sometimes it is a good compromise.

The average value $\bar{x}$ of a variable x is defined as:

22) $\bar{x}(t) = \frac{1}{T}\int_{t-T}^{t} x(\tau)d\tau$ where T is the smallest regular switching period

The basic equations found for the Switching model hold in the Average model case too.

To analyze the average quantities of the circuits, it is necessary to find the equations that link input and control variables. For example, the mean diode current can be expressed as

23) $\bar{\iota_D} = (1 - \delta)\bar{\iota_L}$

Under the hypothesis that input and output voltage have a small ripple, the average voltage across the inductor is

24) $\overline{u_L} = \overline{u_\iota} - (1 - \delta)\overline{u_o}$

The circuit describing equations *21)* and *22)* is shown in **Figure 2.10.**
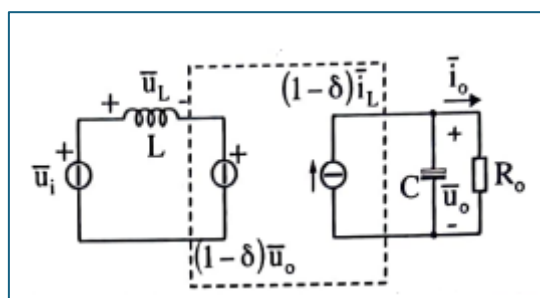
Figure 2.10: Boost Average Model Circuit, Source: [13]

<u>Steady State and small signal Model</u>

The given circuit, which represents the average value of variables over switching periods, is valid for large-signal analysis as well. When the duty cycle is constant, the model behaves linearly. This circuit model can be employed to analyze the dynamic behavior of the converter under large-signal conditions. If a small perturbation is applied around the operating point, a linearized model can be derived. This

linear model can be divided into two sub-models: one corresponding to the steady-state behavior and the other to the small-signal dynamics. The two models are illustrated below. On the left, there is the steady state average model, and on the right the small signal model.
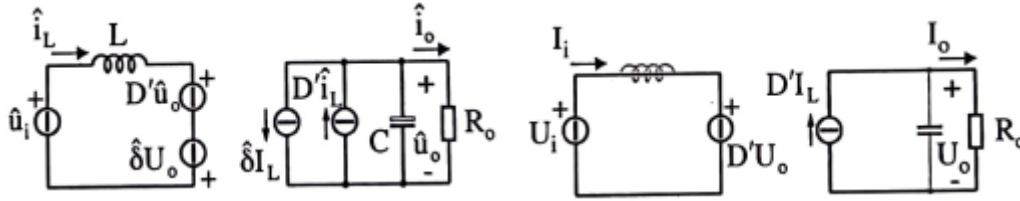
Figure 2.11: a) Steady State Model and b) Small Signal Model of a Boost Converter, Source: [13]

The small signal model is obtained considering every x variable as the sum of a constant term X from the steady state model and the perturbed variable $\hat{x}$ so:

25) $\bar{x} = X + \hat{x}$

And equations 22) and 23) becomes:

26) $(1 - \delta)\overline{\iota_L} = D'I_L + D'\hat{\iota_L} - I_L\hat{d}$

27) $(1 - \delta)\overline{v_o} = D'V_o + D'\widehat{v_o} - V_o\hat{d}$
where D'=1-D, the uppercase letters indicate steady state variables and lowercase letters represent perturbed variables (^) or average value (-).

In summary,

- **Switching Model**: Captures the converter's time-domain behavior by explicitly considering the on/off states of the switch and diode. It's highly accurate but computationally intensive, making it impractical for control design or long-term analysis.

- **Average Model**: Simplifies the converter by averaging key quantities (like inductor current and capacitor voltage) over a switching period. It provides a continuous representation, ideal for dynamic performance analysis and control design while neglecting high-frequency switching effects.

- **Steady-State Model**: Focuses on the converter's behavior under constant conditions, using algebraic equations to relate input/output voltages, currents, and duty cycle. It is useful for understanding voltage gain, efficiency, and component sizing.

- **Small-Signal Model**: Linearizes the average model around a specific operating point, allowing for frequency response analysis. It's crucial for control design and stability analysis, revealing how the system reacts to small disturbances.

The equations and analysis in DCM for the average and small-signal models are not considered, as they are not relevant to our application since our boost converter is designed to operate exclusively in CCM [13].

2.4 Battery

A battery is a device that stores electrical energy chemically and releases it as needed. It consists of one or more electrochemical cells, each containing two electrodes (an anode and a cathode) and an electrolyte that allows the flow of ions. Additionally, a separator is used between the electrodes to prevent the direct flow of electrons within the battery, thereby limiting self-discharge and enhancing efficiency. When the battery is discharging (i.e., providing power), the chemical reaction between the electrodes releases electrons, which flow through the external circuit to supply electricity. When charging, the process is reversed, and energy is stored back into the battery. The battery's basic working process is shown below.
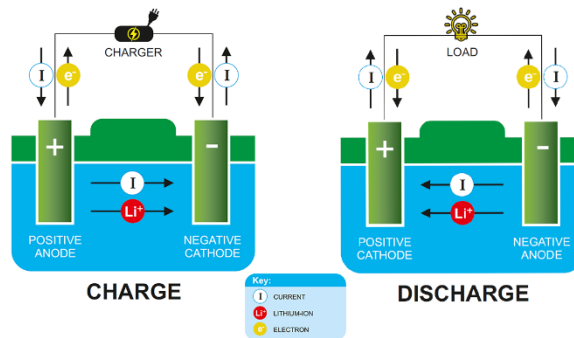
Figure 2.12: Battery's Charging and Discharging Processes, Source: NVClighting.me

Batteries play a crucial role in PV systems and renewable energy sources, especially due to their unpredictable behavior. In this context, batteries are necessary to decouple PV energy production from the load demand. Thanks to energy storage, the user's needs are satisfied even during cloudy days, characterized by lower solar irradiance and reduced electrical production. The excess energy is stored in the battery and used to meet the user's needs when PV power production is unavailable or insufficient.

Moreover, standalone systems must balance energy consumption, which depends on electrical load and production, both of which present high variability. Batteries help manage this variability by storing excess energy when generation is high and releasing it when demand exceeds supply. This balance ensures that the system continues to function smoothly, even with fluctuating energy inputs.

In an off-grid system, the battery also acts as a backup system. If no battery bank is present, other types of technology must be used to satisfy the user's electrical needs when solar energy is unavailable, such as diesel or other fossil fuel generators. Batteries, however, provide a cleaner and more environmentally friendly solution, contributing to a more sustainable energy supply and helping to combat climate change.

Even though the initial investment cost for standalone PV systems with batteries may be significant, this solution provides long-term savings by eliminating utility bills and providing reliable power, especially in hard-to-access or isolated locations. This technology has attracted considerable research interest in recent years, and batteries for solar household applications have become more efficient and economically accessible.

Key Performance Parameters of Batteries
Understanding the performance metrics of batteries is essential for selecting the right storage solution for a PV system. The key parameters include:
1. **Capacity (C):** It is defined as the battery's ability to hold and distribute electrical charge. It can be measured in Ah. which measures how much electric current a battery can produce for an

hour. The energy capacity can be calculated in watt-hours (Wh) by multiplying the capacity (Ah) by the average voltage (V) during discharge.

2. **Depth of Discharge (DoD):** The percentage of a battery's capacity that can be safely discharged without reducing its lifespan. Higher DoD values indicate better utilization of stored energy.
3. **Efficiency:** The ratio of energy retrieved from the battery to the energy stored in it. High-efficiency batteries minimize energy loss during charge and discharge cycles.
4. **Cycle Life:** The number of complete charge-discharge cycles a battery can undergo before its capacity significantly decreases. Batteries with a longer cycle life are more durable and cost-effective over time.
5. **Charge and Discharge Rates:** The speed at which a battery can be charged or discharged, typically expressed as a multiple of its capacity (as 1C or 5C).
6. **Self-Discharge Rate:** The rate at which a battery loses its charge when not in use. Lower self-discharge rates are desirable for energy storage applications.
7. **Temperature Sensitivity:** A battery's performance can vary significantly with temperature. Batteries with wider operational temperature ranges are more versatile.

Types of batteries

According to the U.S. DOE database, the most used batteries in the World are, in order, lithium (Li-Ion), lead acid, sodium sulfur (NaS), and flow batteries.

Lead Acid (LA) Batteries: they are made of 2 electrodes; the positive one is the lead dioxide (PbO_2) electrode, and the negative one contains lead (Pb). Both these electrodes are contained in a sulfuric acid electrolyte liquid, which makes possible the chemical reaction of charge and discharge. This battery type is the most mature technology on the market since it was commercialized in 1890, and it presents simple operation and low cost, making it very popular. LA batteries are mostly used in starter battery services for cars, Uninterruptible Power Supply units (UPS), and small PV systems. Even though they are commonly used, particularly for small-scale applications, they have several disadvantages that make other types of batteries more suitable for large-scale RES storage systems, where optimal performance and higher efficiency take precedence over cost considerations.
For example, LA batteries have a shorter life cycle and lower efficiency compared to other types. They can be discharged to about 70-80% Depth of Discharge (DoD), their efficiency is around 85%, and they are generally oversized due to their lower efficiency and shorter cycle life. Moreover, they do not perform well at low temperatures and cannot endure discharging for a long period without being damaged. Recent studies on advanced lead-acid batteries explore incorporating carbon into one of the electrodes to enhance energy density. Additionally, some research focuses on integrating supercapacitors to improve power capacity.

Sodium Sulphur (NaS) Batteries: the two electrodes (positive made of molten sulfur S and negative of molten sodium Na) are separated by a solid ceramic plate that works as an electrolyte. To keep the electrodes in a molten state, chemical reactions must occur at high temperatures so a heating system must be coupled with the battery. Similarly to the LA batteries, NaS batteries have been present in the market for several decades making them a well-known technology. Their main advantages are the high efficiency and energy density, high life cycles, and rapid response, while the disadvantages are the elevated working temperature of around 600K, the high cost, and the corrosion nature of sodium polysulphides makes them not suitable for all the applications.

Future research on this type of battery aims to address safety concerns by reducing the risk of fire incidents associated with its high operating temperature, by developing new battery technologies based on sodium, such as sodium-nickel chloride (NaNiCl) batteries and sodium-ion (Na-Ion) batteries.

Flow Batteries: The two electrodes, one positively charged and the other negatively charged, are in liquid form and are separated by an ion-selective membrane. During charging and discharging, this membrane enables the selective flow of ions, facilitating chemical reactions. The liquid electrolytes are stored in tanks and must be pumped into the battery during charging and discharging. The most promising technology of flow batteries is the Vanadium Redox Battery (VRB), which showed better performances than the others. Generally, flow batteries have a high life cycle (> 10.000 cycles), and good power/energy flexibility, and they are suitable for medium and large store sizes. An interesting feature of this battery is that its power (measured in kW) and energy capacity (measured in kWh) are independent of each other, a property known as decoupling. The power output depends on the number of modules or stacks of cells, which determines how quickly the energy can be delivered. On the other hand, the energy storage capacity depends on the volume of the electrolyte stored in the tanks. It is possible to increase the battery's power output by adding more modules or expand its energy capacity by increasing the size of the electrolyte tanks, allowing for flexible scaling based on specific needs.
The disadvantages are the large area required because of the low energy density and the need for an additional pumping system, which introduces further energy losses. These two factors make flow batteries not suitable for large-scale applications in non-mobile energy storage systems, peak shaving services, and energy time shifts.

Lithium-Ion (LI) Batteries: The two electrodes (the positive one made of lithium metal oxide and the negative one made of carbon material) are separated by a porous polymeric material, which allows the ion flow between them, during the charging and discharging processes. The electrodes are also immersed in an electrolyte made of lithium salts, such as LiPF6, which are dissolved in organic liquid. The number of projects where LI batteries are used has increased consistently in the last years, for example, from 2016 to 2017 their use has grown by 56%, thanks to their high efficiency and flexibility which makes them suitable for a large variety of applications. They have been especially utilized for electric vehicles, portable electronics, and large-scale energy storage systems. The main advantage is the high cost compared for example with LA batteries. Lithium-ion technology is expected to lead the market in the future, and with the rapid growth of the electric vehicle industry, the cost of these batteries is projected to decrease significantly (expected reduction from 54% to 61% by 2030 for stationary renewable energy applications) [14].

The table below shows a comparison between the performance of different battery types:

Characteristics/Technology	Li-Ion	NaS	Lead Acid	Flow Batteries
Power Range	1kW - 50 MW	0.5 - 50 MW	some MW	several kW to some MW
Energy Range	up to 10 MWh	up to 350 MWh	up to 10 MWh	from 100 kWh to some MWh
Discharg Time	10 min - 4h	6 -7 h	min to more than 20 h	some h
Cicle Life	2.000 - 10.000 cycles	2.000 - 5.000 cycles	500 - 3.000 cycles	>12.000 cycles
Life Duration	15-20 years	<15 years	5 - 15 years	10 - 20 years
Efficience	90 - 98%	75 - 85%	75 - 85%	70 - 75%
Energy Density	120 - 180 Wh/kg	100 - 120 Wh/kg	25 - 35 Wh/kg	10 - 25 Wh/liter
Reaction time	some milisec	some milisec (if hot)	some milisec	some milisec

Figure 2.13: Comparison between the performance of Different Battery Types, Source: [14]

2.5 Inverter

In a standalone PV system, an inverter is mainly used to convert the direct current (DC) from the PV panels to an alternating current (AC) that feeds most of the loads like household appliances. In addition, the inverter plays a crucial role in voltage regulation and manages the power flowing within the PV system (PV panels, DC-DC converters, batteries, load), ensuring higher performance and reliability of the system. Although the boost converter handles the DC voltage, the inverter regulates the AC output voltage to ensure it is stable and within acceptable load limits. This is fundamental, especially when the load demands vary or if the system includes sensitive electronic devices. Moreover, the inverter regulates how much voltage is used to charge the battery and how much is used to satisfy the load demand.

The inverter uses high-speed electronic switches (like MOSFETs or IGBTs) to rapidly switch the DC voltage's polarity. This creates a voltage that alternates between positive and negative, mimicking the behavior of AC.

Inverters are classified following different criteria as the applied input source, connection wise, number of voltage phases, etc.

Input Source Wise Classification

The inverter can be defined as the device that converts DC input supply into AC output where input may be a voltage source or current source. Inverters are mainly classified into two main categories.

A Voltage Source Inverter (VSI) operates with a constant DC voltage as its input, supplied by a stiff DC source—one with ideally zero impedance. The output AC voltage is determined by the switching states of the inverter and the applied DC voltage, making it unaffected by the load's influence.

A Current Source Inverter (CSI) uses a constant current as its input, derived from a high-impedance DC source. This stiffness in the current, maintained by a large inductor or a controlled current loop, ensures the output AC remains independent of the load, governed solely by the inverter's switching states.

Output voltage and current waveform of the inverter are AC quantities, and they are expressed as their Root Mean Square Value (RMS) because it provides a meaningful measure of the equivalent DC value that delivers the same power to a resistive load. This simplifies power calculations, ensures compatibility with equipment designed to respond to RMS values, and offers a standard way to compare AC and DC systems. For sinusoidal waveforms, RMS simplifies calculations by relating directly to peak values, making it the practical choice for analyzing and designing power systems.

The RMS quantity is calculated as:

28) $X_{rms} = \sqrt{\frac{1}{T}\int_0^T X(t)^2\, dt}$ where X is the variable

Instead, the deviation of the output quantities from their fundamental and sinusoidal components is represented in terms of Total Harmonic Distortion (THD) defined as:

29) $THD = \sqrt{\frac{\sum_1^{inf} Xn^2}{X1^2}}$ where X in the variable and the pedicle determines the harmonic

X1 is the RMS value at the fundamental frequency, while Xi is the RMS value of the harmonic components

The Total Harmonic Distortion (THD) formula measures the distortion in a signal caused by the presence of harmonics relative to its fundamental frequency. It is commonly used to evaluate the quality of

voltage or current waveform. A lower THD indicates a cleaner, more sinusoidal waveform, while a higher THD suggests significant waveform distortion, which can affect the efficiency and reliability of electrical systems.

Single Phase VS Three-Phase Inverter

Based on the output voltage and current phases, the inverters can be classified into single phase and three phase.

A single-phase inverter converts a DC input voltage into a single-phase AC output at a nominal frequency of 50Hz or 60Hz and a nominal voltage. The nominal voltage refers to the voltage level at which the electrical system operates, with typical values being 120V, 220V, and 440V. The voltage in a single-phase system continuously rises and falls (peaks and dips), which prevents the delivery of constant power to the load, thereby decreasing efficiency. The output voltage is typically around 230V, making it suitable only for low-load applications. Single-phase inverters are simpler, making them commonly used for household appliances that require low current. They require only two wires: a neutral wire, which acts as a return path for the current, and a phase wire, which carries the load. However, single-phase inverters are less reliable because a failure in the phase wire results in a total interruption of the power supply.

A three-phase inverter, on the other hand, converts a DC input into a three-phase AC output. The AC waves generated by this inverter have the same amplitude and frequency but are phase-shifted by 120° from one another. This phase shift compensates for peaks and troughs, allowing the inverter to deliver a constant power supply. Three-phase inverters generally operate with higher supply voltages, around 415V, and can handle larger power loads. These inverters are more complex, expensive, and physically larger than single-phase inverters. As a result, they are primarily used for industrial applications where higher power is required [15] [16].

The difference in AC output waveform of single and three-phase inverters is shown in **Figure 2.14.**
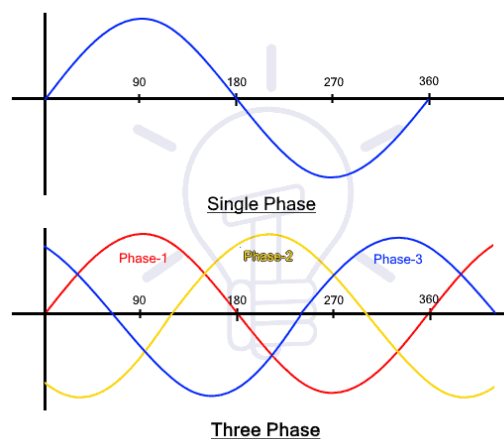

Figure 2.14: AC output waveform of single and three-phase inverters, Source: [18]

Since this thesis focuses on photovoltaic (PV) systems for household applications, I will primarily describe the single-phase inverter that I plan to implement in this work.

Bridge-Type Inverters

A bridge inverter is a type of power inverter that uses a bridge configuration of electronic switches to convert direct current (DC) into alternating current (AC). The most common types are half-bridge and full-bridge inverters.
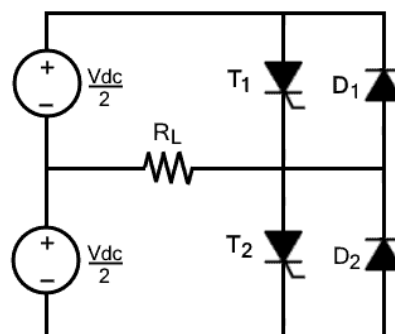
Half Bridge Inverter

The half bridge inverter uses two switches which can be Mosfet or BJT. The switches are complementary so when the first opens the second one is closed and vice-versa. The switching frequency influences the output frequency: for 50Hz frequency at the output, each thyristor is turned ON for 20ms at a time. If there is a simple resistive load, the circuit works in two modes:

- Mode 1: as soon as T1 is turned ON, current starts flowing from source to load. The current direction in this mode will be from right to left through the load. The load voltage in this mode is half of the applied input DC voltage which is $V_{DC}/2$.
- Mode 2: the thyristor T2 is turned ON and T1 is OFF. Note that a dead time is present before turning ON T2, the switch T1 should be allowed to turn OFF completely because turning ON both at a time will cause a short circuit which will permanently damage the circuit. The current in this mode will flow from left to right in the load and the output voltage is $-V_{DC}/2$.

Note that the two diodes D1 and D2 are added to the circuit. These diodes act as freewheeling diodes which help maintain continuous current flow and protect the switches from voltage spikes.

The half-bridge inverter circuit is shown in **Figure 2.15.**

Half Bridge Inverter

Figure 2.15: Half Bridge Inverter Circuit, Source: [18]

Full Bridge Inverter

The full bridge single-phase inverter has four controlled switches. The bridge inverter includes four freewheeling diodes, which return the stored energy from the load back to the source. These diodes work only when all thyristors are turned off, and they are necessary in case of capacitive or inductive loads. The functioning of the full bridge is similar to the half-bridge but since there are more switches the are four different operation modes instead of two. Only 2 switches will work at a time for any load. The 4 operations modes are:

- Mode 1: Initially all the thyristors are switched off. Then, T1 and T2 are tuned ON while T3, and T4 are OFF. The input current flow through T1, enters the load and returns to the DC source through T2.

- Mode 2: after transitioning from mode 1 to mode 2, the previously activated thyristors T1 and T2 are turned OFF. In this phase, the feedback diodes D1 and D2 begin to conduct, allowing current to flow in the opposite direction, from D2 to D1 through the load. These diodes are referred to as feedback diodes because they return the stored energy from the load back to the source.
- Mode 3: it is similar to Mode 1 but the current is reversed (opposite direction through the load). The switches T3 and T4 are ON, while T1 and T2 are OFF.
- Mode 4: the thyristors T3 and T4 are turned OFF to transition from Mode 3 to Mode 4. During this phase, the feedback diodes begin to conduct, causing the direction of the current to reverse. The current flows from the load back into the source through these feedback diodes. This reversal allows the stored energy in the load to be returned to the source.

The circuit scheme of a full bridge inverter is shown below.

As for the half-bridge, turning ON more than two thyristors at a time will cause a short circuit which will produce excessive heat, and it will burn the circuit.

Full Bridge Inverter
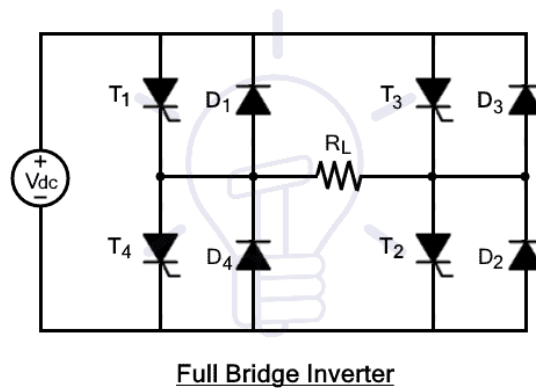
Figure 2.16: Full Bridge Inverter Circuit, Source: [18]

The main differences between half-bridge and full-bridge inverters lie in their power handling and complexity:

- Half-Bridge Inverter: Simpler and less costly, providing half of the DC voltage as AC output. It is suitable for low-power applications.

- Full-Bridge Inverter: More complex and capable of delivering higher output power (equal to the input DC voltage)

Standalone and Grid-Tied Inverter

Inverters can be classified based on their connection to the load and are generally divided into two categories: standalone inverters and grid-connected inverters. This distinction is important in determining the most suitable inverter type for specific applications, depending on whether the system needs to function in isolation or conjunction with a larger power network.

Grid-Tied Inverter

Grid-tied inverters are designed for systems that are directly connected to the grid. They serve two main functions: converting direct current and voltage from the solar panels into AC to power the load and feeding excess power back into the grid. These inverters are also referred to as synchronous inverters because they synchronize the frequency and phase of the AC to match the utility grid. In photovoltaic

(PV) applications, grid-tied inverters are advantageous for users who have easy access to the electrical grid, as they are easier to design compared to standalone inverters and have lower maintenance costs. Additionally, excess energy produced by the solar panels can be sold to the grid, making them a cost-effective solution. However, the primary disadvantage of grid-tied systems is their high dependence on the grid. During a power outage, the system cannot meet the user's load requirements, even if the solar panels are still generating power. This happens because of a safety mechanism that automatically shuts down the inverter if a power outage is detected on the grid. This feature prevents the inverter from feeding electricity back into the grid during an outage, ensuring the safety of utility workers who might be repairing the lines.

Standalone Inverter

Standalone inverters, or off-grid inverters, provide direct power to the load without any interaction with the grid or other components. They are particularly useful when connecting to the electrical grid is impractical or unavailable and are typically paired with energy storage systems. Solar standalone inverters are often coupled with battery banks to store solar energy, which can then be used during the night or on cloudy days. This ensures that the user's electricity needs are consistently met.

Standalone inverters are more reliable than grid-connected inverters, as they guarantee a continuous power supply. However, they can be expensive due to the need for significant energy storage, and they are generally more complex to design compared to grid-connected systems.

A trade-off between the positive and negative aspects of these two types of inverters is achieved through the hybrid inverter. The solar hybrid inverter offers a versatile solution that caters to a wide range of energy needs. By integrating the best features of both systems, hybrid inverters allow for energy independence while maintaining a connection to the grid. They can store excess solar energy in batteries for later use and feed surplus power into the grid, providing the flexibility to maximize energy efficiency. In the event of a grid outage, hybrid inverters automatically switch to battery power, ensuring a continuous electricity supply, similar to standalone systems [17].

Output Voltage Wise Classification

An ideal inverter is meant to be an inverter which converts DC signal into a pure sinusoidal AC output. The problem with practical inverters is that their output signals are not pure sinusoidal. Based on the output wave form, inverters are classified into 3 main categories.

Square Wave Inverters

Square wave inverters are the simplest type of DC-to-AC converters. They generate an AC output in the form of a square wave, which is not a pure sinusoidal waveform as required for most applications. Instead, this square wave output consists of high harmonic distortion, typically around 45%. This high distortion makes the output less suitable for sensitive electronic devices, but these inverters are cost-effective and have a simple construction, often using an H-Bridge topology. The basic operation involves turning switches on and off to alternate the current flow, producing the square wave at the output. Harmonics in the output can be reduced using filters, which improve waveform quality but add complexity and cost.

Quasi Sine Wave Inverter

Quasi-sine wave inverters, also known as modified sine wave inverters, produce a staircase-like approximation of a sinusoidal waveform. The output signal rises in discrete steps with positive polarity, reaches the peak, and then decreases stepwise before reversing polarity to reach the negative peak. The output signal is still far from a pure sinusoidal wave but the THD is approximately 24%, lower than

the previous square wave case. This quasi Sine wave output is reached using multilevel inverters, made by multiple half-bridge inverters connected in parallel to generate an output with several discrete voltage levels. The quasi sine wave output is shown in **Figure 2.17.**
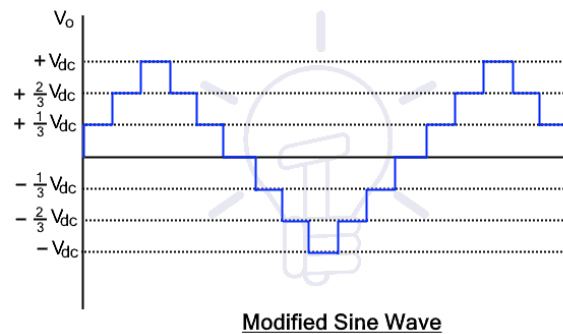

Figure 2.17: Modified Sine Wave Output for an Inverter, Source: [18]

Pure Sine Wave Inverter

Pure sine wave inverters convert DC to nearly ideal sinusoidal AC with very low harmonic distortion, making them suitable for sensitive electrical devices. The output waveform, although not perfectly sinusoidal, is smoother compared to square and quasi-sine wave inverters. Harmonics, which are undesirable sine waves at odd multiples of the fundamental frequency, can be minimized using PWM techniques and low-pass filters. These inverters are preferred for practical applications as they are less likely to damage electrical devices [18].

Pulse Width Modulation

Pulse Width Modulation (PWM) is a technique used in power electronics to control the switching of inverters and modify the shapes of output voltage waveforms to approximate a pure sine wave as closely as possible. PWM controls the switching of transistors or other switches in an inverter by varying the duration (width) of each pulse in a periodic signal. A high-frequency carrier wave, typically a triangular wave, is compared with a reference signal (often a sinusoidal waveform). When the reference signal exceeds the carrier, the width of the pulse increases, turning the switches ON for a longer period, allowing more power to flow to the load. Conversely, when the reference signal is lower than the carrier, the pulse width shortens, and the switches are OFF for a longer duration, reducing the power delivered.

In PWM Inverters, two important concepts are modulation amplitude ratio and modulation frequency ratio. These parameters help define the quality and behavior of the output waveform. The modulation amplitude ratio is the ratio of the peak amplitude of the reference signal to the peak amplitude of the carrier signal, determining how much the carrier wave is modulated by the reference signal. The formula is:

30) $m_a = \dfrac{V_{ref}}{V_{carrier}}$

This quantity must be equal or smaller than one to guarantee enough intersection between the two curves.

The modulation frequency ratio is the ratio between the frequency of the reference signal and the frequency of the carrier wave. It is given by:

31) $m_f = \dfrac{f_{carrier}}{f_{ref}}$

A higher modulation frequency ratio improves the waveform quality by increasing the number of pulses per cycle, while the amplitude ratio impacts how closely the output waveform matches the desired sine wave. For household applications, the carrier frequency is around 20kHz while the reference frequency is the electrical grid frequency (5oHz or 6oHz depending on the country).

The main PWM techniques are unipolar and bipolar modulation.

In a bipolar switching method, the carrier signal and the modulating signal are compared. The inverter switches turn on when the reference signal is higher than the carrier signal, and they turn off when the carrier signal is higher. The resulting gate pulse is sent to switches S1 and S4 of the inverter, while an inverted gate pulse is sent to switches S2 and S3.

In unipolar PWM, two sinusoidal signals with a 180° phase difference are used, both having the same magnitude and frequency. These sinusoidal signals are compared with a triangular pulse. The gate signal for switch S1 is created by comparing the positive reference signal with the triangular signal, while the gate signal for switch S3 is generated by comparing a 180° phase-shifted reference signal with the triangular signal. Switch S2 operates in the opposite way to switch S1, and similarly, switch S4 operates in the opposite way to switch S3 [19].

The functioning of the unipolar and bipolar techniques is shown below (on the left unipolar PWM, on the right bipolar PWM).
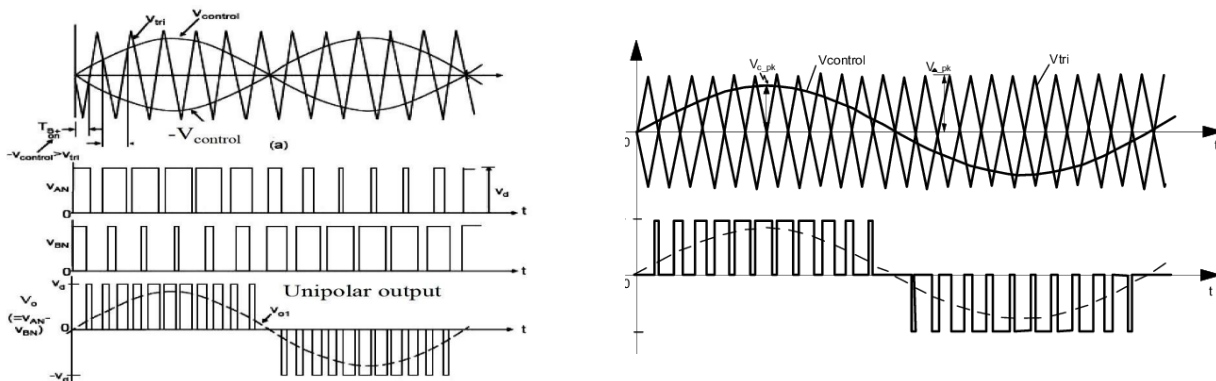

Figure 2.18: a) Unipolar PWM and b) Bipolar PWM, Source: Researchgate.net

2.6 LCL Filter

Nonlinear voltage drops, dead time, limited PWM resolution, and a lack of stiffness in the DC link can cause a non-linear behavior of the inverter, which leads to harmonic distortion in the output current and voltage waveform. Harmonic distortion presents significant challenges in photovoltaic systems, as it can adversely affect the functionality and efficiency of the electrical infrastructure. Harmonics are frequency components that exceed the fundamental frequency (60 Hz) and come from devices such as inverters used in photovoltaic arrays.

The following outlines the negative effects of harmonic distortion:

- Overheating: the presence of harmonics can result in elevated current levels, leading to increased thermal stress in conductors and transformers, diminishing their operational lifespan.
- Interference: harmonics may generate electromagnetic interference, which can disrupt the performance of adjacent electrical and electronic equipment.
- Reduced efficiency: distortion negatively influences inverter performance, leading to a decrease in the effective conversion of energy.
- Device Damage: the effects of harmonics can induce abnormal mechanical and thermal stresses in electrical devices, including motors and transformers, potentially resulting in premature failure.

In the case of photovoltaic systems, wind turbines, and other renewable energy sources, characterized by unpredictable and variable power production the stability problem is even more relevant: problems regarding voltage regulation are more probable because of sudden increased demand, switching of load, or faults.

The necessity to provide a proper filter becomes a fundamental challenge [20]. The most common topologies used are L, LC, and LCL filters. Here is an analysis of each type:

L Filter: The L filter is the simplest, consisting of a single inductor. Its function is to smooth the current by reducing the high-frequency harmonics produced by the switching actions of the converter. While it is easy to implement, its size and cost increase significantly for lower switching frequencies, as larger inductance is required to maintain effective harmonic suppression. This makes L filters bulky and less economical for grid applications, especially under strict harmonic standards like IEEE 519-2012.

LC Filter: The LC filter combines an inductor and a capacitor. This configuration improves filtering performance compared to the L filter, providing a better reduction of both voltage and current harmonics. However, the inductance value of the LC filter does not decrease as significantly, leading to similarly bulky designs as the L filter. The added capacitor helps smooth voltage ripples, making this filter more effective but still not the optimal solution for minimizing component size and cost at lower switching frequencies.

LCL Filter: The LCL filter consists of two inductors (one on the converter side and one on the grid side) and a capacitor. This third-order filter offers superior attenuation of harmonics compared to both L and LC filters, especially in high-frequency ranges. The primary advantage of the LCL filter is that it achieves better harmonic suppression with lower inductance values, thereby reducing both size and cost. It is particularly effective at addressing grid-connected voltage source converter harmonics without requiring large inductive components, making it ideal for modern grid applications.

However, the main disadvantage of the LCL filter is its potential for resonance due to the interaction between the inductors and the capacitor. This issue can be mitigated with damping strategies, such as

passive damping (using resistors) or advanced techniques like split-capacitor passive damping, which reduce losses while maintaining filtering performance.

In summary, while L and LC filters are simpler, they become impractically large and expensive for stringent harmonic standards. The LCL filter, with its superior performance and reduced size, is the preferred choice especially for grid-connected converters, despite its need for damping to prevent resonance [21].

The resonance is a phenomenon which occurs due to the interaction between the two inductors and the capacitor in the filter. When the resonance frequency is reached, the impedance of the filter can drop significantly, potentially leading to high currents and system instability. This resonance can cause excessive harmonic amplification, particularly at specific frequencies, which compromises the performance of the filter and the overall inverter system. The resonance frequency is defined as:

$$32)\ f_r = \frac{1}{2\pi}\sqrt{\frac{L_1+L_2}{L_1 L_2 C}}$$

This is a significant value that must be carefully managed during the design and control process of the inverter.

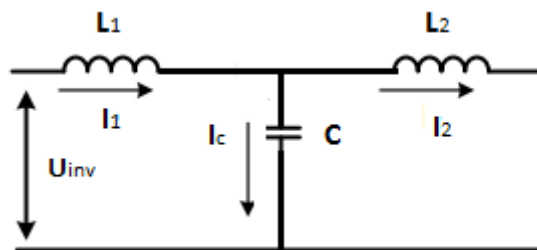The structure of the LCL filter is shown in **Figure 2.19**.

Figure 2.19: LCL filter Circuit, Source: Researchgate.net

3. Control of the Components

In this chapter, the control strategies implemented for the standalone PV system are presented. These strategies are crucial for ensuring optimal power flow between system components such as the PV panels, DC-DC boost converters, battery storage, the inverter, and the load. The design, implementation, and evaluation of these control mechanisms ensure system efficiency, stability, and reliability under varying operating conditions.

3.1 Open-Loop Control of the Boost Converter on PV Side

Open-loop control refers to a control system in which the controller operates based solely on predefined inputs or commands, without utilizing feedback to adjust its behavior based on the system's actual output. Using the Open-Loop control is advantageous in this primary phase because it is simple and allows us to easily validate the Boost converter operation. For real-world PV systems, open-loop control is not suitable since it does not account for the dynamic nature of solar energy generation, and it is used only in the first phase of control implementation.

As already said, the control in an open loop is simple to implement. In the case of the PV system considered in this project, the duty cycle between the PV output voltage (i.e., the DC-DC boost converter input voltage) and the desired Boost output voltage is calculated using *Equation 11)*. So, a pulse generator is employed to create the necessary control signal for the boost converter. The pulse generator produces a periodic signal with a period Ts, where the width of the pulse is proportional to the calculated duty cycle D. The generated signal is applied to the gate of the converter's switch (typically a MOSFET or an IGBT), causing the switch to alternately open (turn off) and close (turn on). Note that as the input voltage Vin changes (for example, due to a temperature or irradiance change) the duty cycle must be recalculated to obtain the desired output voltage Vout and allows the system to maximize power flow despite changes in operating conditions. If hourly irradiance variations throughout the day are considered, the computational effort required to continuously adjust the duty cycle becomes significantly higher. In addition, due to parameter variations (e.g., temperature and weather changes) and the lack of initial knowledge about system parameters and operating conditions, make open-loop control unsuitable. Alternatively, a fixed and constant duty cycle value can be imposed but, in this case, the control is not optimized, and it is not possible to extract the maximum power and thus maximize the system's efficiency. For these reasons, it is fundamental to implement closed-loop control.

3.2 Closed-loop Control of the Boost Converter on PV Side with MPPT Algorithm

In this work, to control the Boost connected to the PV array a direct duty ratio perturbation P&O algorithm is implemented. The P&O algorithm for Maximum Power Point Tracking (MPPT) in photovoltaic systems has three primary variants, categorized by the control variable used:

- Reference Voltage Perturbation: The PV array's voltage reference is the control variable; the duty ratio is regulated by a PI controller which has the error between Vref and V calculated as input. Reference Voltage perturbation presents a fast response to changes in irradiance and temperature, but it is significantly impacted by noise, particularly at low step sizes, which can destabilize the system. The use of low-pass filters for noise rejection may decrease the performance even more.
- Reference Current Perturbation: the output current reference is used as the control parameter. This algorithm is conceptually simple, but it has a slow transient response and high susceptibility to noise, leading to oscillations and inefficiencies in operation.
- Direct Duty Ratio Perturbation: the duty ratio of the MPPT converter serves as the control parameter in this method. It provides enhanced stability and greater energy utilization efficiency compared to the reference voltage technique, as it is less impacted by noise and avoids

oscillations caused by PI controllers. Furthermore, it supports high perturbation rates without sacrificing system stability. However, its slower transient response makes it less suitable for conditions with rapidly changing irradiance [22].

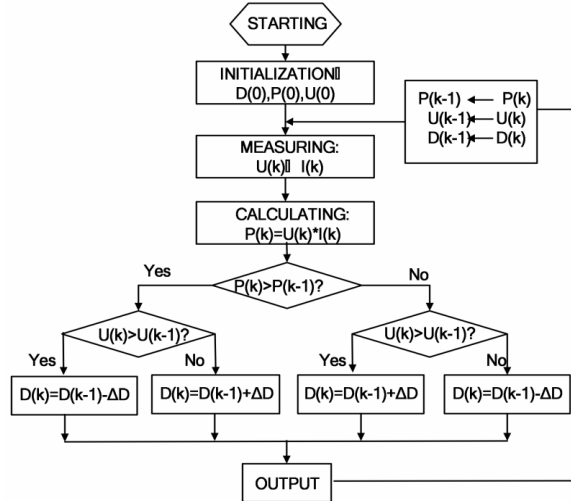The flow chart of the implemented algorithm is shown below.

Figure 3.1: P&O MPPT Algorithm Scheme, Source: Researchgate.net

3.3 Current Closed-Loop Control of the Boost Converter on Battery Side

The open-loop control for the boost has been already explained, so the model is directly implemented through a closed-loop control without the preliminary use of an open-loop control. A current closed-loop control is often preferred over voltage closed-loop control in boost converters due to its faster response and enhanced stability. By directly regulating the inductor current, current control enables quicker adjustments to dynamic changes in load or input conditions compared to voltage control, which depends on slower changes in the output voltage.

The concept behind the control is simple: the actual inductor current IL is measured and compared with the reference inductance current value IL_ref to calculate the error signal ε = iL_ref – iL. A PI controller then processes the error, which gives the duty cycle D as output. The current closed-loop control continuously regulates the inductor current to follow the desired reference value [23][24].

The conventional Proportional-Integral (PI) controller, widely recognized for its simplicity and effectiveness, is one of the most commonly used controllers for regulating the output voltage or inductance current of DC/DC power converters. This approach combines proportional and integral actions to generate an optimal control signal (u) and requires a thorough understanding of the system for effective implementation.

The current IL_ref is the current at the boost converter equilibrium point, which can be expressed by the two equations

33) $\frac{u-1}{L} V_{o,ref} + \frac{V_{in}}{L} = 0$

34) $\frac{1-u}{C} I_{L,ref} - \frac{1}{RC} V_{o,ref} = 0$

where u is the optimal duty cycle, $V_{o,ref}$ is the output reference voltage, $I_{L,ref}$ is the inductance reference current, V_{in} is the input voltage, R is the load, L the inductance and C the capacitor. Note that

32

these equations represent a classical boost linked with a R load but in my case, the load R is substituted by a DC voltage source which represents the battery.

The output voltage $V_{o,ref}$ is imposed by the DC voltage generator, while the reference current is calculated using the power equation:

35) $P_{in} = V_{in}I_{L,ref}$ where P_{in} is the battery power in nominal condition and, V_{in} is the battery voltage in nominal conditions, so $I_{L,ref}$ can be found

The error ε is calculated and processed by the controller C2 to produce the optimal duty cycle *u*. The C2 block represents the PI controller defined as:

36) $PI_{curr} = k_{p,curr} + \frac{k_{i,curr}}{s}$ where $k_{p,curr}$ is the proportional gain and $k_{i,curr}$ is the integral gain. Note that they are expressed in the Laplace domain rather than in the time domain, allowing the controller's behavior to be represented in terms of transfer functions and frequency analysis.

The proportional gain reacts proportionally to the instantaneous error, while the integral gain accounts for the accumulation of error over time to eliminate the steady-state offset.
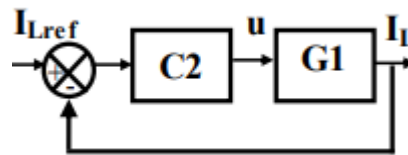
The current closed-loop control scheme is:

Figure 3.2: Boost Current Closed-Loop Control, Source: [23]

The transfer function in the Laplace domain between IL and u is calculated in equation *37)*. It allows the recalculation of the measured IL from the duty cycle u, closing the loop.

37) $G1(s) = \frac{V_o(1+sCR)+I_LR(1-u)}{R(1-u)^2+sL(1+sCR)}$

To verify that the control is consistent, the behavior of the Average, Switching, Steady-State & small-signal model of a Boost converter is analyzed. The control works well for all the 3 models since the controlled current shows a similar pattern. The switching model's current oscillates around the average current value, while the Steady-State & small-signal model current and the average current are initially overlapped. If a step is applied to the reference current, instead, there will be a discrepancy between the currents of the two models. This is because the small-signal model comes from the linearization around a specific point of the nonlinear boost converter model. The basic assumption behind this model is that the boost works across its equilibrium state without significant perturbations, and it is possible to approximate the system behavior as linear. However, when a step (sudden change in the inductor current) is applied the operating point shifts because of the significant variation in the duty cycle. This means that parameters like inductance current and output voltage, calculated at the initial operating point, no longer accurately reflect the system's behavior under the new operating conditions. Since the small-signal model is derived based on the initial operating point, it introduces errors in predicting the steady-state behavior after the operating conditions change and so the linearization model diverges from the real system behavior, represented better by the average model which instead uses average equations without accounting for small-signal linearization.

Since the average model remains accurate even with consistent duty cycle changes, it is preferable to use it compared to the steady-state + small-signal model. In addition, it provides an easier

interpretation of the system dynamics compared to the switching model, which accounts not only for the mean quantities but also for the ripple caused by the switches.

Performance analysis

The performance of a closed-loop control system is crucial for ensuring that the system behaves as expected under various operating conditions, such as changes in input, reference, or disturbances. In the case of the inductor current control, performance is typically evaluated by examining key aspects such as bandwidth, stability, and the system's ability to reject disturbances or follow the reference signal accurately. This performance analysis is typically carried out using the closed-loop transfer function Wcurr, which describes the relationship between the output (inductor current) and the reference input. By analyzing the step response, frequency response, and steady-state error, it is possible to assess the system's effectiveness and optimize the controller design for desired performance. The following sections will address these key performance metrics in more detail.

First, it is essential to properly define Wcurr, as it serves as a key tool for analyzing the system's response to control inputs and disturbances. The closed-loop transfer function is calculated using the following formula:

38) $W_{curr} = \frac{OL_{curr}}{1+OL_{curr}}$ where OL_{curr} is the open-loop transfer function defined as

39) $OL_{curr} = PI_{curr} * G$

Bandwidth and Responsiveness

The bandwidth of the closed-loop system is a key performance metric. It is defined as the frequency range over which the system can effectively follow the reference input or reject disturbances while maintaining high performance. This range is directly linked to the gain crossover frequency fc, which is the frequency at which the magnitude of the open-loop transfer function OL(s), or equivalently Wcurr, becomes equal to one (0 dB). Below this frequency, the system can effectively track the reference signal. A high bandwidth indicates the system can respond quickly to changes in the reference or reject disturbances, while a narrower bandwidth can lead to slower system responses. It is crucial to ensure that the PI controller is designed to achieve a high loop gain over the broader frequency range. However, it is important to ensure that the crossover frequency is not set too close to the switching frequency fs, as this could lead to undesirable effects which will explained in more detail in the Design Chapter.

Stability

An essential aspect of closed-loop control is ensuring system stability. The closed-loop transfer function Wcurr must not have poles with positive real parts, as this would lead to instability and cause the system's dynamic response to diverge. To analyze the system's stability, the Nyquist diagram of the open-loop gain OL(s) can be used. The Nyquist diagram provides a graphical representation of the frequency response of the open-loop transfer function, showing how the gain and phase change as a function of frequency. By analyzing the rotation of the Nyquist plot around the point −1+0j, it is possible to verify the stability of the system. If the open-loop transfer function is stable and the loop gain intersects the real axis at a single point, stability can be further evaluated by examining the phase margin.

The phase margin is defined as:

40) $m_\phi = \pi + \angle OL(jw_c)$

where $\angle OL(jw_c)$ is the open-loop transfer function evaluated at the gain crossover frequency expressed in rad/s.

If the phase margin is positive, the closed-loop transfer function is stable. This stability will be assessed through Bode plot analysis during the simulation in MATLAB.

<u>Steady-State Error</u>

The steady-state error of the system is another critical performance metric. It refers to the difference between the desired output (the reference current iL,ref) and the actual output (the controlled inductor current iL) once the system has settled into a steady state after a change in the reference or input perturbation. For a properly designed PI controller, the steady-state error for a step input should be zero, meaning the output tracks the reference with no error in the long term. This is because the integral action of the PI controller eliminates the steady-state error by accumulating the error over time and adjusting the output accordingly. Therefore, the design of the PI controller is crucial in minimizing the steady-state error while ensuring that the system responds correctly to disturbances or changes in the reference input.

The output of the PI controller from the average model simulation will be compared to Wcurr to ensure that the simulation results align with the theoretical system dynamics.

<u>Time-Domain Metrics for Performance Evaluation</u>

Another way to evaluate the performance of the control is through time domain metrics. These metrics are particularly useful to assess the dynamic response of the system, which means how quickly and accurately it reaches its desired state and how it behaves during the transient phase before stabilizing.

The main time domain metrics are discussed:

- **Rise Time** is the time taken from the output controlled current to rise from 10% to 90% of the reference value. It indicates how quickly the system responds to a step input or a sudden change in the reference signal and it is a critical measure of responsiveness. It strongly depends on the controller's parameters. High proportional gain typically reduces rise time by increasing the system's response speed. However, if the proportional gain is too high, it may cause overshoot and lead to instability. The integral gain helps eliminate steady-state error but can increase rise time if set too high. There is also a relationship between the rise time tr and the bandwidth Bw, expressed in Hz, of the control that can be expressed as:

$$41) \; Bw = \frac{0.28}{tr}$$

This highlights that the bandwidth is inversely proportional to the rise time: a wider bandwidth enables faster responses, reducing the rise time, while a narrower bandwidth slows the system's response.

For the current-controlled loop in a boost converter, this relationship provides a practical guideline for designing the control system. The constant 0.28 reflects the typical dynamics of second-order systems and is derived from the correlation between the system's natural frequency, damping ratio, and transient response characteristics. This equation helps balance the trade-off between system responsiveness and potential issues like noise sensitivity or instability.

- **Settling Time** is the amount of time taken by the system to settle within a specified error band (often ±2% of the reference value) after a disturbance or change in the input. Essentially, it's the time the system needs to stabilize and stay close to the desired value without oscillating or overshooting beyond

the error band. It is important because it is a measure of how quickly the system reaches a steady state after a disturbance or change in the reference input.

- **Overshoot** measures how much the system's output exceeds the reference value during the transient phase (the period immediately after a change in the input). It's typically measured as the percentage by which the peak value exceeds the reference value. Excessive overshoot indicates a lack of damping in the system, which can cause instability or unnecessary wear on the components. Keeping overshoots under control is important for ensuring smooth operation and preserving the lifetime of the system.

These time-domain metrics can be easily evaluated by simulating the system in Simulink. The Rise Time, Settling Time, and Overshoot can be automatically extracted from the response curve to a step variation and the Steady-State Error can be calculated by comparing the steady-state value of the output with the reference.

3.4 Inverter Control Strategies: Implementation of a new control type

The control of single-phase standalone inverters plays a critical role in ensuring reliable and high-quality AC power supply in off-grid systems. Unlike grid-connected inverters, which rely on the grid as a stable reference for voltage and frequency, standalone inverters must independently regulate these parameters. This autonomy introduces additional challenges, such as maintaining voltage stability, frequency accuracy, and robust performance under varying and often nonlinear load conditions. Furthermore, standalone inverters must operate as voltage sources, while grid-tied inverters function primarily as current sources, injecting power into the grid according to grid-imposed constraints.

The control of standalone inverters is a crucial area of research, but the field of grid-connected inverters is far more developed. Despite the relevance and importance of studying and analyzing standalone systems, the majority of research efforts have been dedicated to grid-tied technologies. This trend is evident from the considerably higher number of published articles on grid-tied inverters. For instance, a search on IEEE Xplore over the last 25 years (2000–2024) reveals approximately 18,000 publications related to "grid-connected inverter control" or "grid-tied inverter control," compared to only about 3,500 articles on "standalone inverter control" or "off-grid inverter control." The further interest in grid-connected inverters comes from their widespread applications, particularly in industrialized regions where power supply is generally reliable, and the electrical grid infrastructure is well-established. Furthermore, grid-tied inverters are subject to stricter requirements, including synchronization with the grid and advanced fault-tolerant control strategies, which make them a focal point for researchers.

Research on three-phase inverters is also more advanced compared to single-phase inverters. This is largely due to the greater complexity of controlling three-phase systems and their predominant use in industrial applications. A similar literature analysis on IEEE Xplore over the period from 2000 to 2024 highlights this difference: approximately 19,000 articles were published on three-phase inverters, compared to around 11,200 articles on single-phase inverters.

The increasing deployment of standalone systems in off-grid rural areas makes the research on standalone single-phase inverters an important challenge. These systems face unique challenges, including intermittent power generation from renewable sources, highly variable load profiles, and the need for energy storage integration. Addressing these issues requires innovative control approaches to ensure stable, reliable, and efficient operation under diverse conditions.

This chapter focuses on the control strategies specific to single-phase standalone inverters with an LCL filter, which is particularly challenging due to the lack of literature on this topic.

A double-loop control is developed to offer both voltage and current regulation and it is initially developed using two PI controllers. The functioning of the PI regulator has already been explained in Boost Converter control's paragraph.

Double-loop control is widely used in standalone inverters to achieve precise voltage and current regulation. The control scheme is based on the sensing of the capacitor current as an inner loop with an added output voltage feedback loop to ensure a sinusoidal and well-regulated output voltage.

The outer voltage loop ensures that the inverter maintains a stable and sinusoidal output voltage, even under load variations. The inner current loop enhances system stability and dynamic response, preventing overcurrent conditions and improving robustness against disturbances. This configuration is particularly effective for inverters with LCL filters, as the inner loop actively damps resonance while the outer loop focuses on the voltage waveform quality. Together, these loops ensure high performance and reliability in standalone applications [25].

Using the capacitor or inductor current as the reference current in inverter control is preferred over the load current (io) because it directly relates to the dynamics of the LCL filter. The capacitor and inductor are part of the inverter-side components and provide better feedback for controlling the switching behavior, ensuring stability and damping filter resonance. The load current, being influenced by the connected load's impedance, can introduce variability and delay, reducing control accuracy and dynamic response. Therefore, capacitor or inductor current offers faster, more precise control. Moreover, the capacitor current feedback in the inner current loop ensures much lower output impedance compared to the inductor current feedback approach.

The initial control is structured in this way: the output voltage is measured and compared with the reference voltage which is sinusoidal with 110RMS V and a frequency of 60Hz, which is the frequency of the electrical grid in the USA and in Canada, for which the electrical AC loads devices are designed. The error between the reference and the real output voltage is calculated and processed by a PI controller which gives as output the reference current on the capacitor. This reference capacitor current is compared with the measured one, the error is computed and processed by another PI controller which gives as output the carrier wave for the PWM control. A combination of the PWM techniques and a second-order filter LCL is used to create a sinusoidal output waveform with a minimum total harmonic distortion. It is important to design correctly the proportional and integral control gain of the PI controller to get a stable operation of the closed loop system. From the transfer function calculated from the circuital model in **Figure 2.19** (considering a resistive load in series with the L2), the PI controller variables are calculated using Formula 36).

The Gdic transfer function derived from the circuital model applying the Kirchoff law and the Laplace transform is:

42) $G_{dic}(s) = \frac{U_{dc}(sLC+RC)}{(s^2LCR+s(2L-C)+R)}$

Where Udc is the voltage on the DC side, L is the inductance, C the capacitor and R the resistive load

This function is used to design the inner current control loop.

The closed- loop function W_{curr_inv} is calculated as for the boost control, using Formula 38) and 39).

The transfer function Gicvo between the output voltage and the capacitor current used for the control is computed and it is:

43) $G_{icvo}(s) = W_{curr\_inv} \frac{(R+Ls)}{sCR}$

The PI parameters for the outer voltage loop control are given from this transfer function.

The PI controller design for the outer voltage loop of an inverter requires careful attention, especially compared to the case of a boost converter. Unlike boost converters, where the bandwidth and phase margin of the control system can be evaluated simply as a function of the switching frequency (fsw), inverter control must also account for the resonance frequency of the LCL filter. To ensure stable and responsive tracking of the input signal, it is critical to operate the system at a frequency far from the resonance point. Operating near the resonance frequency can lead to significant peaks and instability. A general guideline is that the bandwidth of the inner current loop should not exceed half the resonance frequency. The outer voltage loop, on the other hand, is typically designed with a bandwidth of approximately one-tenth that of the inner current loop. This separation ensures stability and proper dynamic response of the overall control system.

Using the PI controller is not an optimal choice for these applications since it gives a steady state error which refers to a non-optimal tracking of the reference signal. This is due to the AC behavior of the inverter's signal which does couple well with the PI controller functioning. When the reference signal is a DC quantity, the gain of the open loop transfer function at the reference frequency (0 Hz) is infinitive. The tracking error is defined as the inverse of the open loop transfer function's gain at fundamental frequency so for DC quantity is almost 0. Instead, an inverter manages AC quantities with a reference frequency f of 60Hz or 50Hz. The open loop transfer function's gain for $s = j2\pi f$ is not infinite, leading to a no zero steady-state error. For this reason, proportional resonant (PR) controllers are more suitable for AC applications' control since they can reach an infinitive gain at the fundamental frequency and hence achieve a zero steady-state error. Moreover, the PR controller has a better disturbance rejection capability, resulting in higher performance than the PI controller.

The PR controller can be developed by transforming an ideal synchronous frame PI controller to the stationary frame and achieve an infinitive gain at AC frequency $\omega_o = 2\pi f$. The proportional gain kp is the same as the PI controller while the resonant gain kr considers also the given reference frequency. The ideal PR controller is defined as:

44) $PR(s) = k_p + \frac{2k_i s}{s^2 + \omega_o^2}$

The ideal PR controller acts like a network with an infinite quality factor which is a dimensionless parameter that measures how sharply a system resonates at its natural frequency. A high-quality factor means that the system response is very narrow and strong at a specific frequency, and it quickly decays away from that frequency. For this reason, the real construction of an ideal PR controller with infinitive quality facto is not possible due to physical hardware limitations (like damping in analog systems) or computational constraints (such as the need for finite precision in digital systems). To solve this problem a non-ideal PR with a high-gain low pass filter is usually preferred. Its structure is shown in the equation below:

45) $PR(s) = k_p + \frac{2k_i \omega_c s}{s^2 + 2\omega_c s + \omega_o^2}$

where ω_c is the cut off frequency which acts as a filter for undesired harmonic. At other harmonic frequencies, the response of the non-ideal PR controller is comparable to that of the ideal PR controller.

The Proportional-Resonant (PR) controller has three main parameters kp, ki, and ω_c that affect its behavior and that must be tuned in the right way. It is noted that keeping kp and ω_c constant, an increase of ki will raise the magnitude of the controller's gain without affecting its bandwidth. This means that ki directly scales the gain while leaving the controller's frequency selectivity unchanged. On the other hand, if kp and ki do not change, varying ω_c influences both the magnitude and phase of the controller's

response, with both increasing as ω_c grows. Importantly, the same gain can still be achieved at the resonant frequency by adjusting ω_c. Finally, an increase of kp enhances the overall magnitude of the controller and creates a peak at the resonant frequency, while simultaneously reducing the phase magnitude. This behavior indicates that increasing kp enhances harmonic impedance, helping to suppress harmonic components. A higher kp improves the system's ability to track sinusoidal references accurately and reject disturbances effectively. Thus, the values of kp, ki, and ω_c should be carefully chosen to balance gain, bandwidth, harmonic suppression, and overall control performance [26].

3.5 DC Bus Voltage Regulation

The DC bus is an electrical connection point in a power system that operates in direct current (DC). It serves as a central hub for transferring energy between components like photovoltaic (PV) panels, batteries, and inverters. Typically, a capacitor is placed on the DC bus to filter voltage ripples and stabilize the system by compensating for fluctuations caused by dynamic power exchanges. This ensures consistent operation and prevents excessive stress on connected components. The stability of DC bus voltage is essential to guarantee the correct functioning of the system because a high variation of the voltage can damage the linked devices, such as the inverter or the boost converters. This DC bus is extremely important for decoupling the AC inverter quantities from the DC ones.

To maintain the DC bus voltage almost constant it is necessary to implement a control able to balance the absorbed or released power on the bus, which is expressed better as the power on the capacitor filter. The load is assumed constant for the duration of the simulation and absorbs power from the PV system or the battery. If the solar irradiance is high enough to provide exactly the required user power, the battery does not work. If the power produced by solar panels array is lower than the user requirement, the battery provides the power needed to satisfy user demand. If the solar panels produce more energy than the consumed ones, the excess power is absorbed and stored in the battery.

A control must be implemented to keep the power Pc on the DC bus capacitor filter equal to the zero, to keep the voltage across the capacitor (and so on the bus) constant. The relationship between the capacitor voltage and power is:

46) $P_c = V_{DC} C \frac{dV_{DC}}{dt}$

A double-loop control strategy is implemented using a PI controller. The inner loop regulates the inductor current of the boost converter, which corresponds to the current flowing into the battery. Meanwhile, the outer loop maintains a stable DC bus voltage by adjusting the system's operation accordingly. The real DC voltage is measured and compared with the reference DC value, the error between them is managed by the PI controller which gives as output the power on the battery which is defined as:

47) $P_{pv} - P_{load} = P_c = -P_{bat}$

It is assumed as convention that a power is positive if it is given/produced, and it is negative if it is absorbed. For example, if the PV array produces more power than the power absorbed by the load, there is an increase of power on the capacitor on the bus that must be immediately absorbed by the battery.

The power of the battery is divided by the nominal battery voltage to compute the reference inductor current which is compared with the measured inductor current to produce the error $e_i(t)$ processed by the second PI controller. The output of the inner PI block is the duty cycle of the boost connected with the battery which opens and closes to guarantee the right current flow [27]. The tuning of the proportional and integral gains is carried out using the respective transfer function.

For the inner loop the transfer function between the duty cycle and the inductor current is defined by *Formula 37)*. The bandwidth of the control is assumed to be one-tenth of the switching frequency as already explained in the Inverter control section.

For the output loop the used transfer function is calculated using Formula *46)* and *47)* and is:

$$48)\; P(s) = -\frac{1}{sCV_{DC}}$$

Since this transfer function depends only on the capacitor value and the DC voltage (it is a fixed parameter) it is extremely important to design the capacitor filter in the right way. The capacitor must be able to filter effectively the voltage ripple, maintaining the DC voltage stable and ensuring a smooth operation of the system.

The bandwidth choice for the outer loop controller is very important in power systems that convert DC to AC, especially in setups with batteries and inverters. If the controller's bandwidth is too high, it might react too quickly to small, repetitive fluctuations, like the 120 Hz ripple caused by the inverter. This can lead to unnecessary actions, instability, wasted energy, and added stress on system components, reducing efficiency and their lifespan. To prevent this, the outer loop controller's bandwidth is set to a low value, typically around 15 Hz or less. This helps the controller focus on larger, slower changes and ignore smaller, fast ripples.

When an inverter operates at 60 Hz, it creates a 120 Hz ripple on the DC bus. This occurs because the inverter draws power from the DC bus in pulses that align with the peaks of the AC sine wave. Since the AC sine wave completes a cycle 60 times per second, these power pulses occur twice per cycle—once at the positive peak and once at the negative peak—resulting in a ripple frequency of 120 Hz. The power drawn by the inverter is sinusoidal with a frequency twice that of the grid frequency and an average value equal to the inverter's rated power.

By keeping the outer loop controller's bandwidth low, the controller effectively ignores these small ripples and reacts only to bigger, more important changes in the DC bus voltage. This reduces unnecessary corrections, improves stability, and ensures the battery operates more smoothly. In the long term, this approach improves efficiency, reduces energy losses, extends battery life, and ensures the overall system performs better. Setting the bandwidth low is a key step to achieving this balance.

To validate the control behavior, a comparison between the measured DC Voltage oscillations on the bus and the theoretical oscillation computed by the formula is done.

Considering the power absorbed by the inverter as an external disturbance on the bus, the closed-loop transfer function is calculated as:

$$49)\; CL(s) = -\frac{P(s)}{1+P(s)PI}$$

where PI is the control and P(s) the open loop transfer function defined in Equation *48)*.

The attenuation of the voltage oscillation given at the reference frequency f =120 Hz is calculated by imposing s = jω (where ω=2πf) in the transfer function and multiplying the given attenuation for the power of the inverter. If the theoretical attenuation and the measured one are close to each other, it means that the control works properly.

4. System Design

First of all, it is necessary to design the different components of the PV system that will be used later in the Simulink simulation. Initially, the PV system's location and usage must be chosen.

4.1 Design of the Photovoltaic System

It is assumed that the PV system is used for household applications to completely cover the electrical needs of a house in the Mauricie National Park area of Shawinigan, a small town 200km north of Montreal, Canada. Even though the area is not far from big cities, it is still located in an inaccessible place, making it preferable to use a standalone system.
Choosing the right size for solar panels is important to ensure they can provide enough energy to satisfy user's electricity demand. This means figuring out how many panels you need and how powerful they should be to produce enough electricity based on factors like how much energy you use, how much sunlight you get, and how efficiently the system runs.
The first thing to do is calculate how much energy is needed by the user. This can be done by looking at its past electricity usage or estimating how much energy its appliances and devices use. Energy needs are usually measured in kilowatt-hours (kWh) daily or monthly. After knowing your energy needs, the next step is to look at how much sunlight is available, which is referred to as solar irradiance. This amount can change based on the geographical location, the time of year, and the positioning and inclinations of solar panels. Solar irradiance is measured in peak sun hours (PSH), which indicates how many hours of strong sunlight your panels can get in a day.

Evaluation of the electrical load

Since the plant taken into account is a standalone system, the electrical user's requirement must be completely satisfied by the photovoltaic panels. It is necessary to calculate how much electrical energy is used, on average, by the user. The electrical loads include lighting, a small refrigerator, a fridge, an electrical stove for cooking, a computer, a TV, and other ordinary household electrical appliances as shown in **Figure 4.1**.

LOAD type	n of units	n of hours	Watt used	Wh/day
Lights	6	12	15	180
Fridge	1	8	70	560
Refrigerator	1	8	80	640
Home appliances	6	3	2000	6000
Computer	1	4	250	1000
Electrical stove	1	2	1500	3000
TV	1	2	100	200
			TOT	11580

Figure 4.1: Evaluation o Electrical Load, Source: Excel Calculation

The load is assumed to be constant at 11580 Wh/day all over the year to simplify the sizing of the PV panels.

After assessing the customer's willingness to install a system of a specified power, it is essential to conduct a detailed economic analysis based on the site's characteristics.
To ensure that the site is "efficient," it must be verified that it is oriented between SOUTH-EAST and SOUTH-WEST. Alternatively, the possibility of installing two photovoltaic arrays oriented towards WEST

and EAST should be considered. It is assumed that no shading will influence the power production of the system.

The global solar irradiance available to produce electricity must be evaluated for the given location for every hour of the day. Note that this quantity depends on the season and the orientation and inclination of the solar panels.

The irradiation data are taken from the Photovoltaic Geographical Information System website of the European Commission [28].

The website provides:

- Monthly Irradiation Data: the total monthly global irradiation for the given location

- Average Daily Irradiance Data

- Hourly radiation Data

For this work, the PVGIS-ERA5 solar radiation database is considered. The optimal orientation and inclination for the PV panels are calculated by the software: the panel is inclined at 40°C and is facing South (azimuth angle equal to 0°). The comparison between the optimal configuration and the horizontal one is shown in **Figure 4.2.**
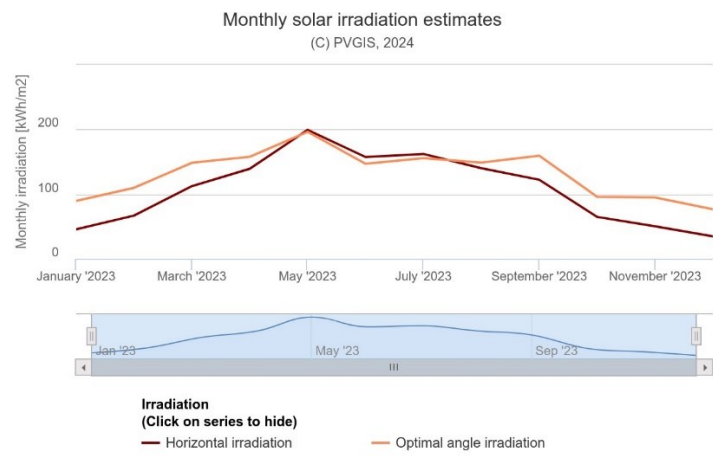
Figure 4.2: Estimation of Monthly Solar Irradiation in Shawinigan, Quebec, Source: [28]

To simplify the procedure, the average daily solar irradiation is calculated from the total monthly irradiation divided by the number of days of the month. The results are shown in **Figure 4.3.**
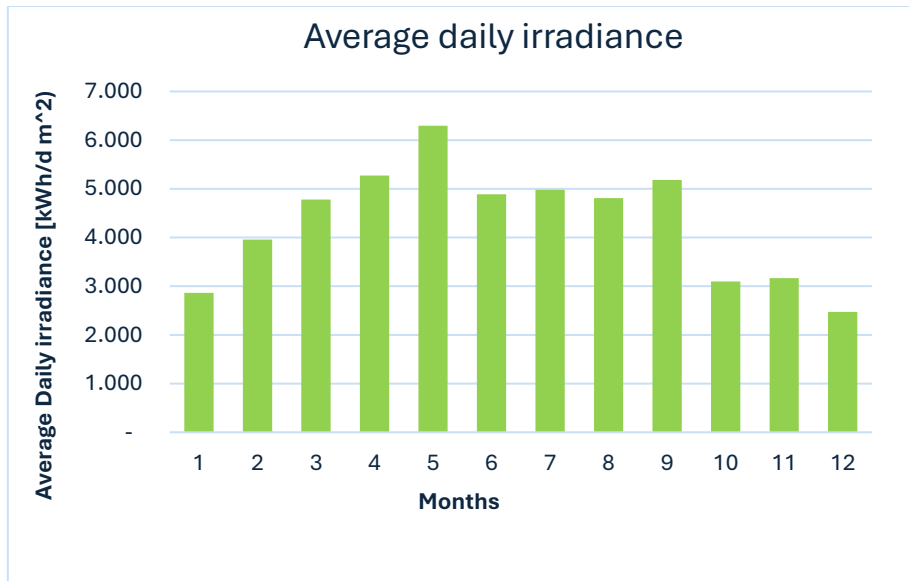
Figure 4.3: Average Daily Irradiance in Shawinigan, Quebec, Source: Excel Calculation

The sizing of the solar plant is done taking into consideration that also during winter, when the solar radiation facing the panels is lower, the user requirement for electricity must be satisfied. From the graph, it is clear that the worst situation occurs in December when the average daily solar irradiation is 2473 Wh/m^2 day. This value is taken for the calculation.

The area occupied by the PV is calculated with the following formula:

$$50)\ PV_{area} = \frac{E_{el}}{I*\eta_{out}*\eta_{pv}*TCF} = 23.6\ m^2$$

where Eel is the electrical load defined before, I is the average solar irradiation in December, and TCF is the temperature correction factor assumed equal to 1.14, $\eta_{out} = 0.83$ is the output efficiency (comprise the battery and inverter efficiencies) and $\eta_{pv} = 0.21$ is the efficiency of the panel [29].

Note that TCF is bigger than one because the mean temperature of the cell during winter, due to the negative external air temperatures is lower than the standard cell temperature of 25°C and this enhances the system performance.

The selected modules are Jinko Solar Co. Ltd JKM250P-60, mono-crystalline silicon with the following specifications at standard test conditions (i.e., 1000 W/m2 and 25°C and AM=1.5), taken from the product datasheet:

- Max Power mod_{peak}: 250.1 W
- Cells per module: 60
- Open Circuit Voltage Voc: 37.7 V
- Short-circuit current Isc: 8.85 A
- Voltage at maximum power point Vmp: 30.5 V
- Current at maximum power point Imp: 8.2 A
- Temperature coefficient of Voc: -0.306 %/°C

The peak power of the PV system is calculated as:

$$51)\ PV_{peak} = PSI * PV_{area} * \eta_{PV} = 4970\ Wp$$

43

Where PSI is the maximum solar radiation intensity assumed equal to 1000 W/m².

The peak power is used to evaluate the number of panels that must be installed as:

$$52)\ n_{mod} = \frac{PV_{peak}}{mod_{peak}} = \ 20$$

The peak power of the single module is considered equal to 250 Wp.
The modules must be coupled in parallel and in series to reach the desired output voltage and current:

$$53)\ n_{serie} = \ \frac{V_{nom}}{V_{mp}} = 7$$

Where $V_{nom} = 213.5\ V$ AND $V_{mp} = 30.5\ V$
Approximating, the number of parallel panels is set equal to 3, so the final number of panels is 21.

4.2 Battery Sizing

Batteries play a crucial role in the PV system and renewable energy sources, especially, due to their unpredictable behavior. In this contest, batteries are necessary to decouple the PV energy production from the load demand; thanks to energy storage the user needs are satisfied even during cloudy days, characterized by a lower solar irradiance and a lower electrical production. Therefore, a good sizing of energy storage is fundamental to ensure the continuity of the power supply and better efficiency of the systems.

Although less efficient than other battery types, Lead-Acid batteries are more cost-effective due to their lower initial capital cost, making them a better choice for small-scale residential systems where budget considerations are a priority.

The capacity of the battery is evaluated from the equation below:
$$54)\ C_{batt} = \frac{E_{el}N_C}{DOD\ V_{batt}\ \eta} = 1100\ Ah$$

Where Eel is the electrical load required every day, Nc = 3 is the number of consecutive cloudy day, DOD=0.7, η=0.8is the energetic efficiency and Vbatt=370 V is the battery nominal voltage.

4.3 Boost Converter Design

The sizing of the DC-DC converter is an essential step in the design of the plant. Usually, in this kind of application is preferable to use Boost converters, which would raise the input voltage to the desired output one. The input voltage, measured directly from the PV array, is usually too low and must be boosted to feed correctly the load and the battery. Moreover, a higher voltage level and a lower current lead to a more efficient power transfer between electrical devices, due to the smaller conduction losses in the wires.
A particular focus must be maintained during the sizing of the boost, to guarantee that the DC-DC converter works always in CCM mode, no matter which are external solar conditions.
The initial assumption for the design of the boost on the Pv side are:

- Vin = 213.5 V,

- Vout = 750V,
- Fsw = 30000 Hz.

Starting from these initial assumptions, the inductor and capacitor size will be evaluated using the mathematical formula.

55) $L = \frac{V_{in}D}{\Delta I_L * fs}$ = 4.1 mH

Where it is assumed that the current ripple ΔI_L is 5% of the inductance current I_L, defined as:

56) $I_L = \frac{Ppv}{V_{in}} = 24.6\ A$

The minimum capacitor is found assuming an output voltage ripple ΔV_{out} = 1%

57) $C_{min} = \frac{V_{out} * D}{f_s * \Delta V_{out} * I_o}$ = 22.3 μF

where D is the duty cycle

58) $D = \frac{(V_{out} - V_{in})}{Vout} = 0.7153$

And

59) $I_o = I_L(1 - D) = 7\ A$ is the output current

The same process is used for the sizing of the 2nd boost, linked with the battery.

In this case, the input voltage value is the nominal voltage of the battery Vbatt, the duty cycle D is 0.5067, then inductor L is equal to 4.3mH , the capacitor C is 15.7 μF, and ILbatt is 28.77 A. The output voltage is the voltage on the DC bus.

To avoid DCM, the inductance L must be big enough to keep the fluctuation of current across it constant as much as possible and avoid the current going to zero. The minimum value of inductance is therefore calculated at the boundary condition between CCM and DCM. Moreover, large inductance values tend to increase the start-up time slightly while small inductance values allow the coil current to ramp up to higher levels before the switch turns off. Large inductances are more expensive too.

The key factors in selecting the output filter capacitor are its capacitance and equivalent series resistance (ESR). Since the ESR influences the efficiency of the system, using low-ESR capacitors is necessary for optimal performance. To further reduce ESR, multiple capacitors can be connected in parallel. The output filter capacitors should be selected to not only meet the specified output voltage ripple requirements but also to handle the ripple current stress effectively.

4.4 Inverter and LCL Filter Design

Under the assumption of ideal components in the circuit (with no losses, parasitic elements, or commutation time), the nominal power of the inverter is considered equal to the power generated by the photovoltaic (PV) system. The inverter operates at a switching frequency fs=20kHz. To prevent interaction between harmonics, a different switching frequency for the boost converters and the inverter is preferred. Additionally, switching frequencies below 20 kHz are avoided because they fall within the audible range.

However, several factors can introduce nonlinear behavior in the inverter, leading to harmonic distortion in both the output current and voltage waveforms. These factors include nonlinear voltage drops, dead time, limited PWM resolution, and the lack of stiffness in the DC link. Harmonic distortion presents

significant challenges in photovoltaic systems, as it can negatively impact the functionality and efficiency of the entire electrical infrastructure. Harmonics are frequency components that extend beyond the fundamental frequency (60 Hz), often generated by devices like inverters in photovoltaic arrays.

The negative effects of harmonic distortion are as follows:

- Overheating: Harmonics can increase current levels, resulting in higher thermal stress on conductors and transformers, which reduces their lifespan.

- Interference: Harmonic distortion can create electromagnetic interference, disrupting the performance of nearby electrical and electronic devices.

- Reduced Efficiency: Distortion degrades the inverter's performance, decreasing the effective conversion of energy.

- Device Damage: The stresses caused by harmonics can lead to abnormal mechanical and thermal loads on electrical devices such as motors and transformers, potentially causing premature failure.

In renewable energy systems like photovoltaics and wind turbines, where power production is often unpredictable and variable, the issue of stability is even more critical. Sudden fluctuations in demand, load switching, or faults can exacerbate voltage regulation problems, further compromising the reliability and performance of the system.

The necessity to provide a proper filter becomes a fundamental challenge [30].

For these reasons, it is chosen an LCL filter in this application.

60) $L = \frac{V_{DC}*D_{max}}{\Delta I*f_{sw}}$ = 39 mH

Where $V_{DC} = 750V$ is the voltage on the DC bus side, Dmax=0.2 is the max duty cycle (calculated between the DC bus voltage and he RMS output voltage), f_{sw} is the switching frequency and ΔI is the current ripple and it's considered equal to 40%I_{ref}, calculated as:

61) $I_{ref} = \frac{P_{inv}}{Vload} = 47.75\ A$ considering $V_{load} = 110\ RMS\ V$ that is the voltage of the load (AC load are usually designed to be connected to the gird, in a standalone system the inverter must "replace" the grid)

In an LCL filter, it's often suggested to use two inductors that have the same value—one on the converter side and one on the grid side. Keeping them equal is important because it leads to:

- Better Harmonic Cancellation: The two inductors work together to filter out unwanted harmonics. If they are the same size, they do a better job of equally reducing these harmonics on both sides, which means the filter works more effectively.
- Lower Inrush Currents: When the filter connects to the grid, there can be a big surge of current. If both inductors are equal, they help balance this surge, which lowers the chance of damaging the filter or the converter.
- Less Resonance Problems: Resonance can happen in LCL filters due to interactions between the inductors and the capacitor. Having equal inductors helps prevent uneven resonance frequencies, making it easier to manage and control these effects.

- Easier Capacitor Sizing: With both inductors being the same, it's simpler to choose the right size for the capacitor. The capacitor smooths out voltage changes, and having balanced inductors simplifies calculations and adjustments, leading to a more efficient design.

In summary, using equal inductors helps enhance performance, reduces instability risks, and makes it easier to design the LCL filter [31].

To size the inverter the following formula is used:

62) $C = \frac{Q_{max}}{2\pi f_g * V_{load}^2} = 11.5 \, \mu F$

With $f_g = 60 Hz$ is the load frequency, and Q_{max}=0.01P_{inv} is the maximum allowable reactive power that the inverter can handle, expressed as a function of the rated active power.

Since the capacitor and inductors values have been computed, the resonance frequency can be evaluated as:

63) $f_{res} = \frac{1}{2\pi} \sqrt{\frac{2L}{L^2 C}} = 3347 \, Hz$

A resonant frequency value too close to the grid frequency can cause resonance, amplifying grid harmonics and leading to voltage distortion, while if the resonant frequency is too similar to the switching frequency it can cause interaction between harmonic, leading to a destabilization of the system. For this reason, it must be verified that the switching frequency is far enough from the other 2 frequencies considered. A good value for the resonant frequency is considered within the range:

64) $10f_g \leq f_{res} \leq 0.5f_{sw}$

Keeping the resonant frequency within these limits minimizes harmonic distortion, ensures efficient filtering, and improves overall inverter performance and grid stability [32].

In this case, it is verified that the filter is designed correctly since fres is within the established range.

Other important parameters to design are the capacitor filter on the PV side, the load, and the DC bus capacitor.

A capacitor on the PV side (C_{pv}) is needed to smooth the voltage from the photovoltaic (PV) array, which fluctuates due to changes in sunlight, temperature, and other factors. Without this capacitor, the voltage from the PV array would be too unstable, so the MPPT algorithm would not track accurately the maximum power point and extract the maximum power. The value of the capacitor on the PV side should be close to the boost capacitor to ensure consistent filtering. If the capacitance values differ significantly, it can cause a mismatch in voltage response and interference between the two capacitors, potentially introducing ripple or instability. Matching the capacitor sizes ensures that both capacitors work together smoothly to stabilize the voltage, helping the boost converter and MPPT algorithm operate efficiently. For this reason, C_{pv} is assumed equal to half of the boost converteSmoothing out high-frequency fluctuations and acting as an energy buffer r capacitor.

A Cbus filter on the DC bus between an inverter and a boost converter serves to reduce voltage ripples, improve power quality, and protect system components. By smoothing out high-frequency fluctuations and acting as an energy buffer, it stabilizes the DC bus voltage, enhances system dynamics, and ensures efficient, reliable operation.

The Cbus is sized by using the formula:

65) $C_{bus} = \dfrac{P}{\omega_{sw}\Delta V_{DC}} = 1400\ \mu F$

Where P is the power managed by the DC bus (since it is assumed to have ideal components, the nominal power of the PV array or boosts, can be independently used), ω_{sw} is the switching frequency of the inverter expressed in rad/s, and $\Delta V_{DC} = 1\% V_{DC}$ where V_{DC} is the average value.

Finally, the resistive AC load on the inverter is calculated from the formula:

66) $R_{load} = \dfrac{V_{load}}{P_{inv}} = 2.3\ \Omega$

In addition, in the Simulink implementation a small resistive element $r = 1 m\Omega$ will be added in series with the DC bus capacitor.

5. Simulink Implementation and Simulation

After analyzing the main components of the photovoltaic system, including their theoretical characteristics, control strategies, and sizing criteria, this chapter focuses on the simulation of the system in the Simulink environment. The goal is to develop a model that accurately represents the system's behavior, integrating the photovoltaic generator, the energy storage system, and the associated control algorithms. The simulation allows for evaluating the system's performance under various operating conditions, assessing its efficiency, stability, and ability to respond to changes in load and solar irradiation.

The PV array block is already present in Simulink, so it is simply added to the workspace. Note that the block requires 2 input variables: the irradiance and the cell temperature. Initially, the irradiance is represented by a step block which imposes an initial value of 500 W/m^2, and at the midpoint of the simulation, the irradiance value is set as 1000 W/m^2. The temperature is assumed to be constant and equal to 25°C (standard conditions).

The boost converter is instead modeled from the basic components block from the Simscape Electrical Specialized Power System library: the series RLC branch blocks are used to represent the inductance and capacitor. The switch and the diode do not appear in the model because the average model is used to represent the boost converter.

Initially, in the simulation, a DC voltage generator (Vout = 750V) is used along with the photovoltaic panel and the Boost converter, instead of a load, to verify the correct functioning of the power conversion system. This configuration allows focusing on the dynamics of the PV and Boost without additional complications from the load behavior. In this way, it was possible to test the interaction between the photovoltaic panel and the Boost converter, ensuring that the system operated correctly and reached the Maximum Power Point (MPP) in response to variations in irradiance and other environmental conditions.

The model of the PV array integrated with the boost and the DC voltage generator is shown in **Figure 5.1.**
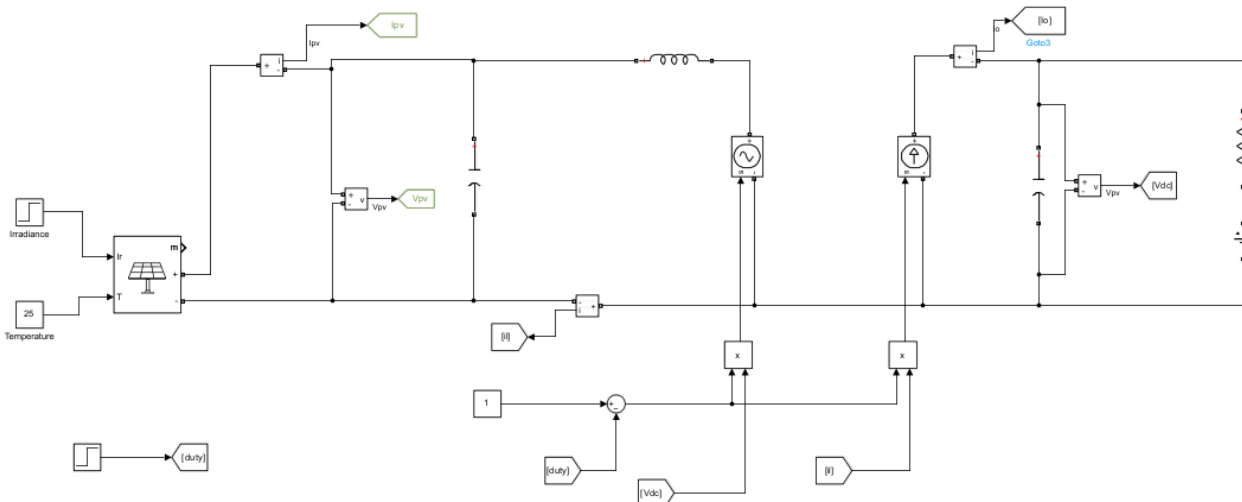

Figure 5.1: Simulink Model of PV array and Boost Converter

The system is initially simulated in the open loop: the duty cycle value is calculated from the formula and regulated "manually", instead of being dynamically adjusted in response to real-time system feedback.

5.1. Simulation of Photovoltaic Array and Boost Converter on PV Side

The duty cycle is calculated from Formula 9) for each input voltage (so the output of the PV array which depends on irradiance and temperature). The simulation is carried out considering 2 different irradiance values, so:

- For Irr = 500 W/m^2, Vin = 215.9 V (found from the characteristic curve in **Figure 2.7**) → the duty cycle is D1= 0.7120
- For Irr = 1000 W/m^2, Vin = 213.5 V (from **Figure 2.7**) → the duty cycle is D2= 0.7153

In Simulink, the step block is used to change the duty cycle from D1 to D2 at Tsim/2.

Using the Open-Loop control is advantageous in this primary phase because it is simple and allows easy validation of the Boost converter operation. The provided simulation results **Figure 5.2** illustrate the behavior of a photovoltaic (PV) panel connected to a boost converter under open-loop control.
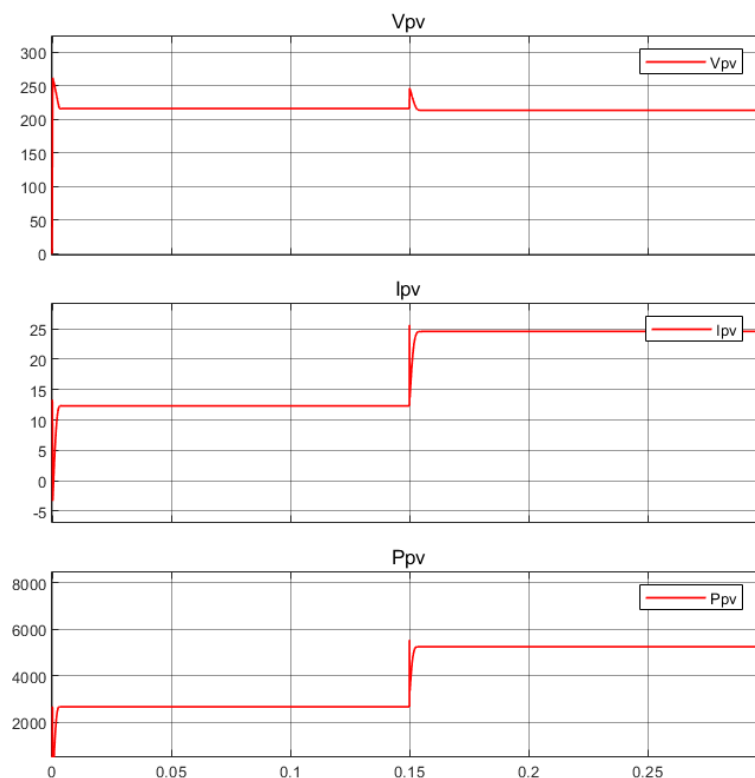
Figure 5.2: PV Voltage, Current, and Power Trends with Open-Loop Control

The graphs represent:

- The Voltage at the PV output: it is initially equal to 215.6 V and then it stabilizes around 213.5 V. This means that the open control voltage with the defined D values works properly because it's equal to the theoretical value from the characteristic curve.
- The current is equal to 12.33 A at the beginning and when the external conditions (and the duty cycle) vary, it stabilizes around 24.57 A. This is coherent with the theory.
- The power is initially equal to 2661 W and then as the external conditions change, the PV power rises to 5462 W, really close to the theoretical values of 5252W. Moreover, the presence of the small resistance r and the second capacitor will introduce some losses (really small but bigger

50

than zero). The power difference is negligible and does not compromise the overall performance of the system.

The system shows stable operation conditions under open loop control and stabilizes after the disturbance application reaches the new power, voltage, and current value. However, this control does not change the duty cycle automatically when external conditions vary, and it is not optimal especially if several values of irradiance and temperatures are considered during the simulation. The relationships between power, voltage, and current are consistent with the PV panel's behavior under changing conditions:

- An increase in the current leads to a slight voltage decrease
- Even under different external conditions, the voltage value stays almost constant at around 215V
- The increase in power reflects the higher current output, since P=I*V;

Closed-loop control

In reality, during the day, irradiance and temperature values can change rapidly and unpredictably. This makes open-loop control impractical, as demonstrated in my simulation, where I had to manually adjust the irradiance and simultaneously modify the corresponding duty cycle to ensure the system operated at the Maximum Power Point (MPP). In this open-loop simulation, everything was straightforward because only two different irradiance values were considered, so calculating the duty cycle for these two cases was neither extremely time-consuming nor inefficient. However, if real irradiance variations throughout the day are considered, the computational effort required to continuously adjust the duty cycle becomes significantly higher, making open-loop control unsuitable. Alternatively, a fixed and constant duty cycle value can be imposed but, in this case, the control is not optimized, and it is not possible to extract the maximum power and thus maximize the system's efficiency. For these reasons, it is fundamental to implement closed-loop control.

Starting from the flowchart in **Figure 3.1** the control has been implemented in Simulink as shown in **Figure 5.3.**
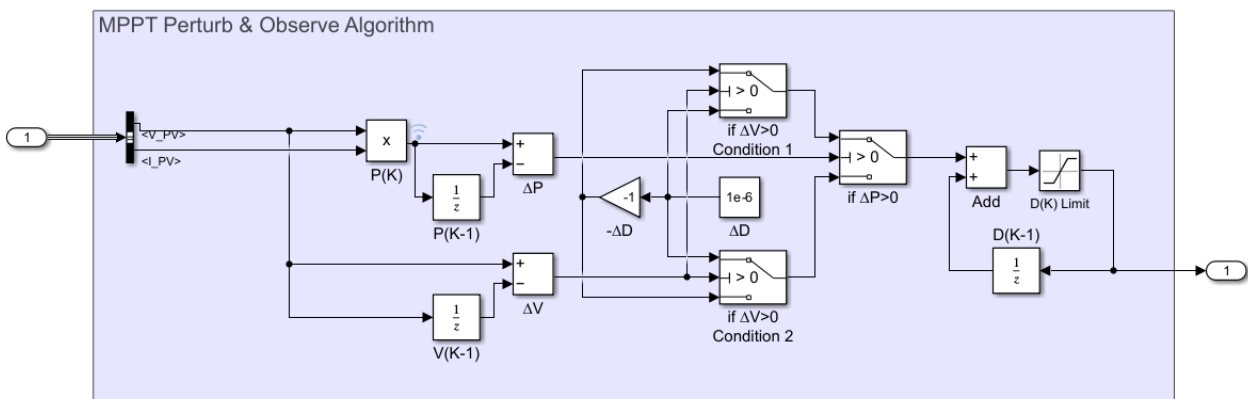

Figure 5.3: Simulink Implementation of MPPT Perturb & Observe Algorithm

The model takes as input the voltage (V_PV) and the current (I_PV) from the PV panel at each time step and gives as output the updated duty cycle D(K) used to control the DC-DC converter connected to the PV system.

The current Power P(K) is calculated as the product between voltage and current at the same time instant K, then variations of PV power ΔP and voltage ΔV are calculated through the comparison

51

between the value at the K step and the value at the previous step K-1. The memory block is used to store variable values at the K-1 step. The switching block is used to consider the different conditions, and the algorithm compares ΔP and ΔV to determine how to adjust the duty cycle D(K) to move toward the Maximum Power Point (MPP).

An appropriate choice of step size for the duty cycle adjustment ΔD is crucial for the efficiency and stability of the P&O algorithm because it affects how quickly the algorithm can follow the MPP and how stable the system is once it reaches the MPP. Generally, a large ΔD provides faster tracking but larger oscillation and instability while a small ΔD allows smaller oscillation and consequently higher steady-state efficiency but the slow tracking of the MPP may be problematic under dynamic conditions.

A comparison of the simulation results found using two different ΔD values is shown below. On the top (**Figure 5.4**) ΔD = 1e-6, the voltage ripple is ΔV = 0.5% so the oscillation is very small. On the bottom (**Figure 5.5**) ΔD = 1e-5, the voltage ripple is ΔV = 5% so the oscillation increases 10 times. The transient response is not very visible, especially because the Voltage variation is quite small in the 2 situations.
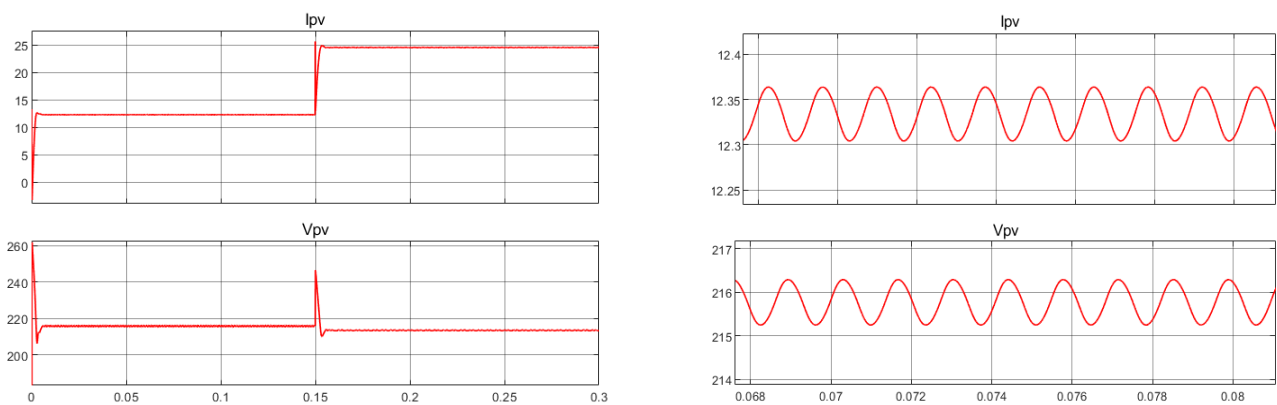
Figure 5.4: Simulation result using MPPT Algorithm with a duty cycle variation ΔD = 1e-6
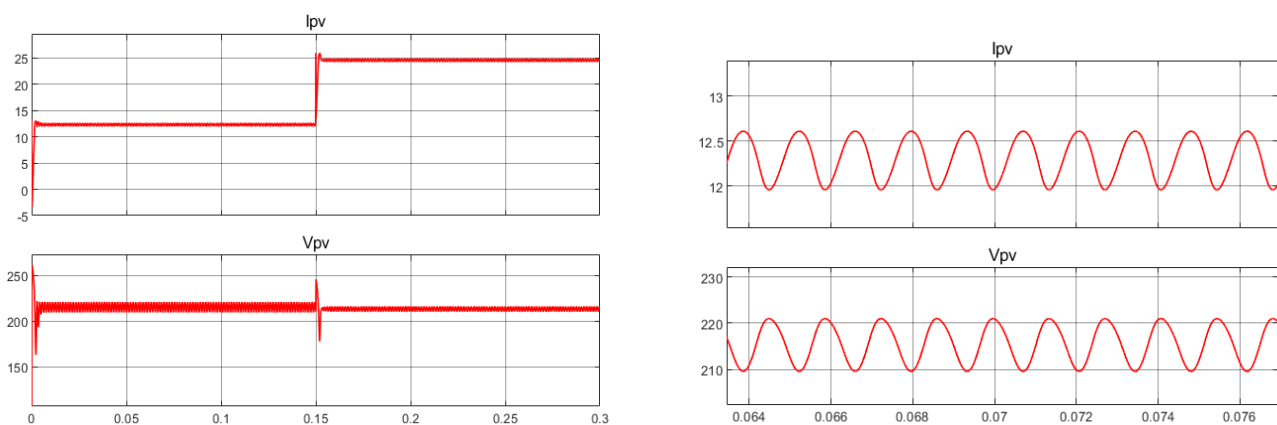
Figure 5.5: Simulation result using MPPT Algorithm with a duty cycle variation ΔD = 1e-5

To optimize the performance of a PV system, the selection of an appropriate step size (ΔD) for the converter is crucial. The optimal value depends on various factors: like

- System Dynamics: Low-inductance converters with faster dynamics can tolerate larger ΔD values, while systems with slower dynamics benefit from smaller values for better stability.
- Environmental Conditions: Under steady irradiance and temperature, a smaller ΔD minimizes oscillations around the Maximum Power Point (MPP). For rapidly changing conditions, a larger ΔD helps track the MPP more quickly.
- Switching Frequency: For converters with high switching frequencies, smaller ΔD values can be used as the control loop can make frequent adjustments.
Carefully balancing these factors ensures a fast response with minimal oscillations, achieving efficient MPP tracking**.**

The simulation is done with ΔD =1e-6 considering the following array of irradiance [500,1000, 800, 1200 W/m^2] to verify that the MPP algorithm works well in different operating conditions and can track correctly the MPP. The results are shown in **Figure 5.5**.
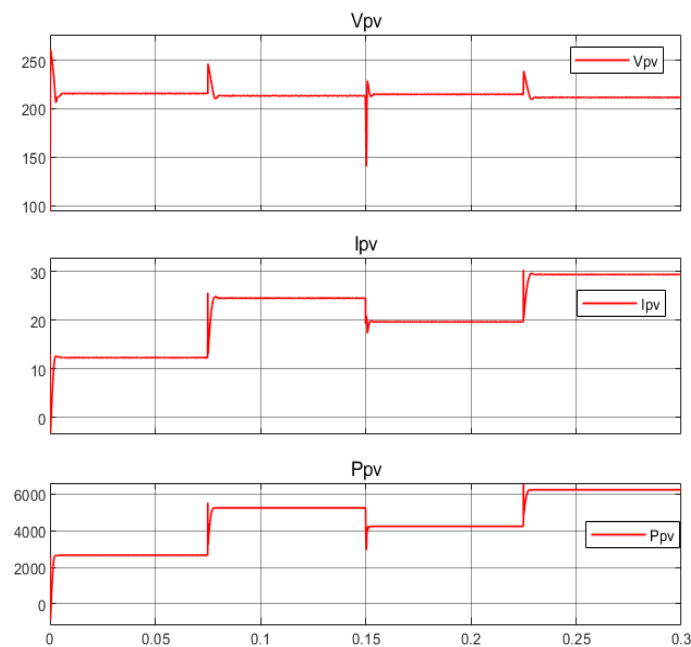
Figure 5.6: MPPT Simulation Result under Different Solar Irradiance Conditions

Then, the response of the MPP value is analyzed varying the temperature cell value (expressed in °C). The array of values [10, 25, 30] is considered while the irradiance value Irr =1000 W/m^2 is kept constant for the duration of the simulation. The results are shown in **Figure 5.7.**
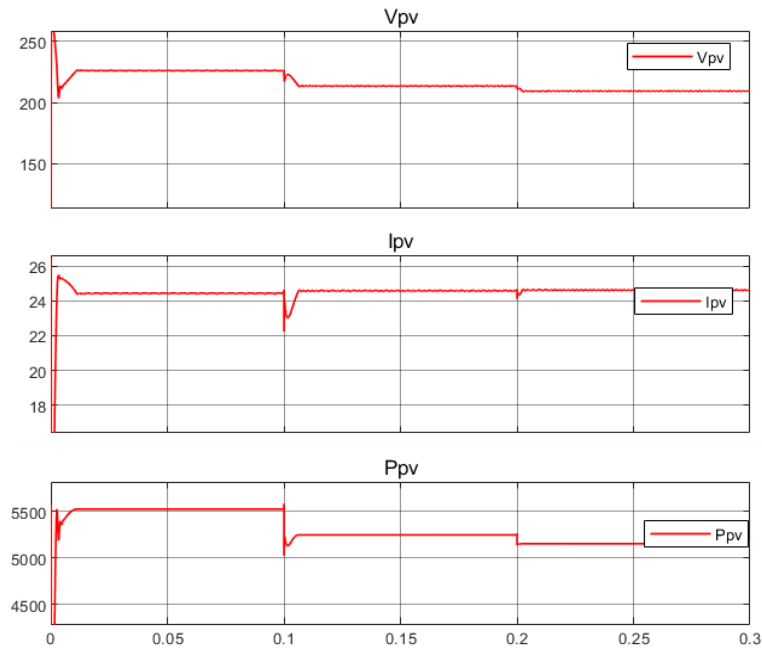
Figure 5.7: MPPT Simulation Result under Different External Temperature Conditions

Note that in cold climates, such as Montreal, the low temperatures enhance the efficiency of photovoltaic (PV) panels. This is because lower temperatures lead to higher output voltage, but the current is not highly affected by temperature variation, so the power production increases. This can be verified from the characteristic curve. This temperature effect is particularly beneficial during winter when solar irradiation is lower due to shorter daylight hours and a lower sun angle. The improved efficiency from colder temperatures helps to partially compensate for the reduced solar energy input, allowing for better overall energy production under these conditions.

5.2 Simulation of the Boost Converter on Battery Side

The average model of the Boost converter is implemented in Simulink using the basic ideal components as already explained in the part concerning the PV array. The load R is substituted by another DC voltage generator which represents the battery. The battery can be seen as a DC voltage source because both provide a DC voltage, a current which varies depending on the load and that can be seen as an energy source. Since the open-loop control for the boost has been already explained, the model is directly implemented through a closed-loop control. A current closed-loop control is often preferred over voltage closed-loop control in boost converters due to its faster response and enhanced stability. By directly regulating the inductor current, current control enables quicker adjustments to dynamic changes in load or input conditions compared to voltage control, which depends on slower changes in the output voltage. For this reason, a current closed-loop control is implemented. The transfer function G1 is used as a reference in the PID tuner tool of MATLAB to evaluate the optimal parameters ki and kp.

In the PID Tuner tool, the two key parameters that can be adjusted to design properly the controller in the frequency domain are the Phase Margin and the Bandwidth. Generally, the control bandwidth must be a maximum of one-sixth of the switching frequency, to avoid interaction with the switching frequency but at the same time does compromise too much the speed of the controller. The Bandwidth is set equal to 3kHz (1/10fsw) while the Phase margin is assumed equal to 60°.

The value of the proportional gain and the integral gain are respectively 0.1916 and 2086.

To verify that the current closed-loop control implementation is correct the Average, Steady State & small signal, and Switching model of the boost converter are implemented, and their response to a small perturbation of the reference current is analyzed (a 0.5 value step is applied at Tsim/2).
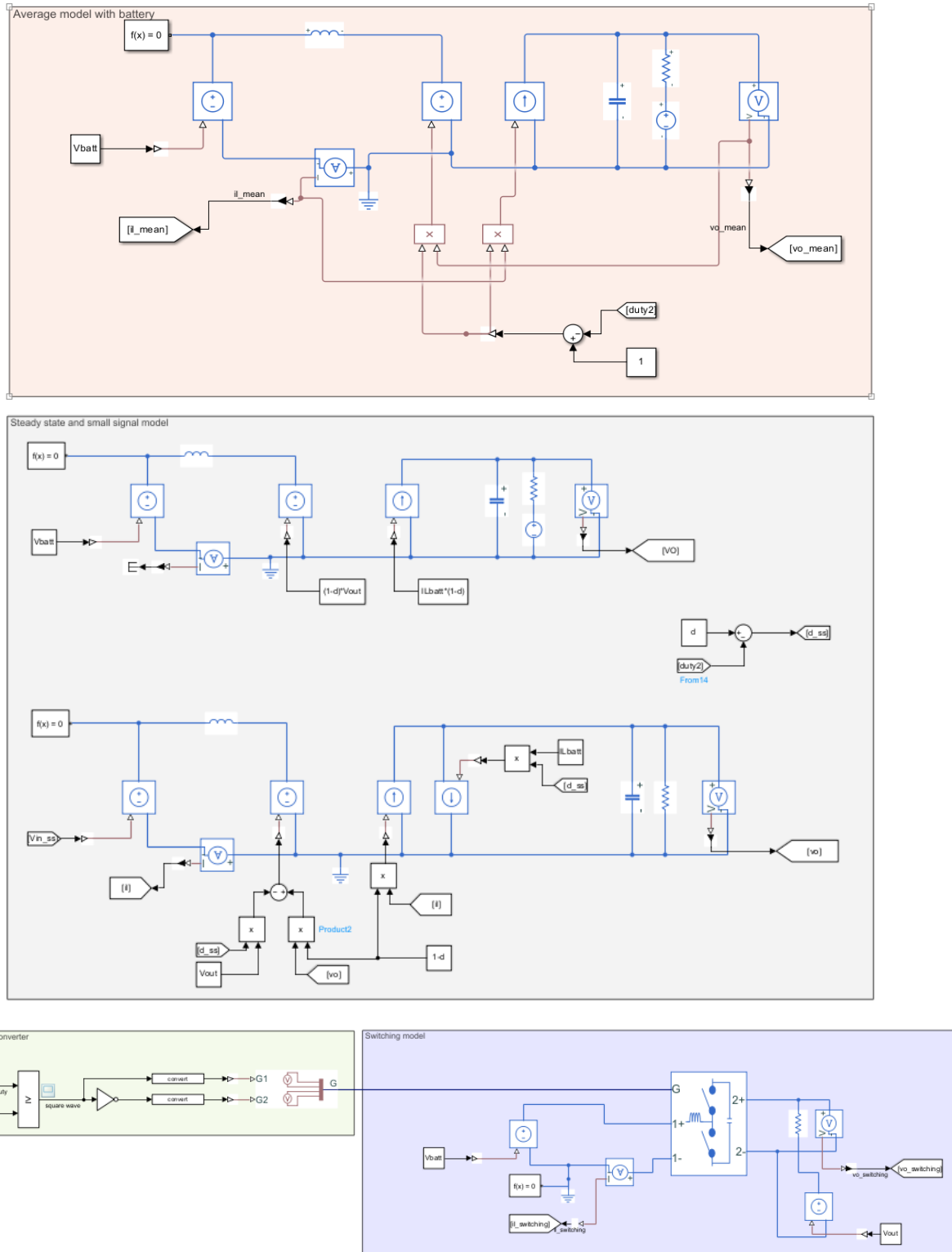
The scheme of the models is the following:

Figure 5.8: Implementation of Average, Steady State & small signal, and Switching model of the boost converter

From the simulation, it is possible to note that the 3 models work properly and give the same results. The closed-loop control is correct, and the simulation results are shown below. The switching model follows the mean current value. For small disturbance appliances, the SS state + ss model is equivalent to the average model.
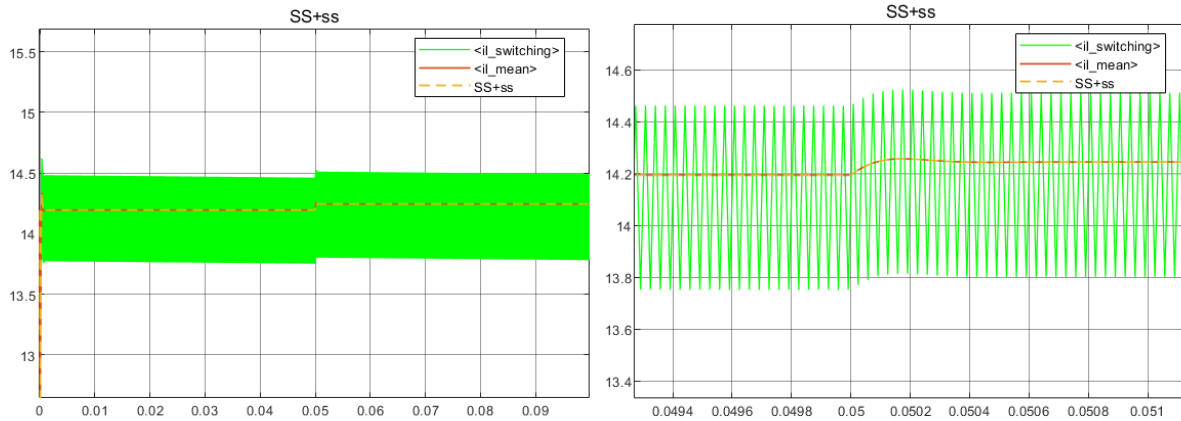
Figure 5.9: Controlled current comparison between Average, Switching, and Small Signal Model

Now, the inductor current of the average model is compared with the close loop transfer function W_currCTRL (defined in Equation 36) to verify that the simulation result is consistent with the theoretical expected value. From **Figure 5.10** is notable that there is a superimposition between the two curves, so the close loop control works as predicted. The rise time tr after the transient is calculated to find some information about the system's responsiveness. The time needed to pass from 10% to 90% of the reference value is 67μs over a simulation period of 0.1 seconds. The real Bandwidth of the control can be evaluated using Formula 39) and it is equal to 4180 Hz.
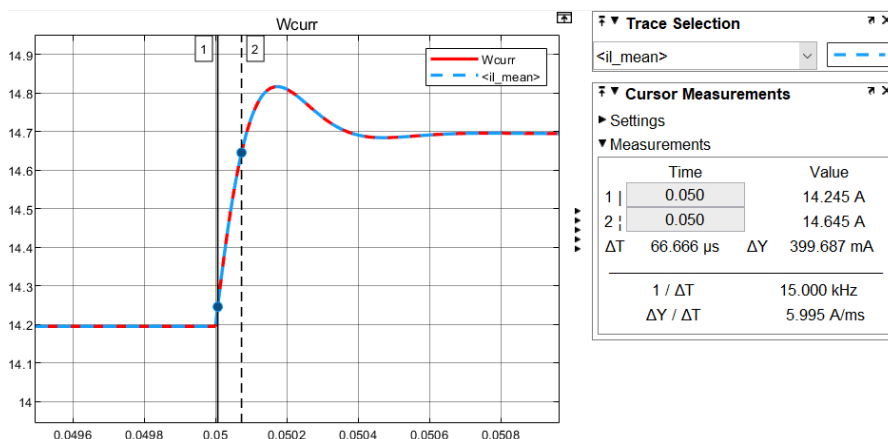
Figure 5.10: Step response of the controlled current (kp= 0.1916; ki= 2086)

If a different bandwidth is used for the tuning of the PI controller parameters, this will affect the responsiveness of the system. For example, a Bandwidth of 2500Hz is used and the new values of the integral and proportional gain are calculated (ki = 1448 and kp=0.1597). The new rise time is calculated, and it is 80μs as can be seen from **Figure 5.11.**

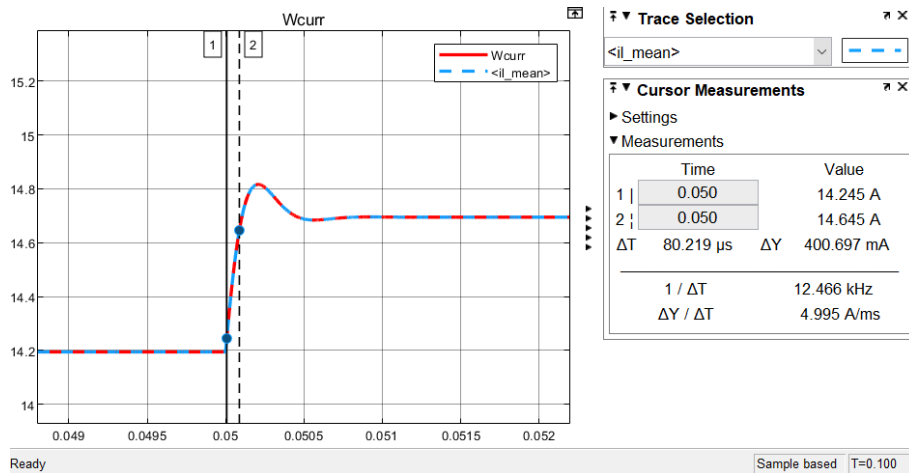*Figure 5.11: Step response of the controlled current (kp= 0.1597; ki= 1448)*

It is verified by Simulation what is already said in the *Control of the Boost's* paragraph. Generally, a higher proportional gain means a faster response while a higher integral gain slows down the system response. Note that the effect of ki dominates on kp since, even if both ki and kp are increased, the rise time has increased too, leading to a smaller responsiveness of the system. The new Bandwidth is 3181 Hz.

To validate this, the bandwidth obtained from the simulation is compared with the real bandwidth of the closed-loop transfer function. The real bandwidth is determined from the Bode plot of the closed-loop system, specifically by identifying the frequency where the magnitude of the transfer function drops to -3 dB. This frequency is known as the cutoff frequency.

From the Bode plot of the closed-loop transfer function, the frequency at -3 dB was approximately 26,000 rad/s, equivalent to 4300 Hz as shown in **Figure 5.12**. This result closely matches the bandwidth estimated from the simulation, which was derived using the relationship between bandwidth and rise time. The agreement between these values confirms the accuracy and validity of the model.
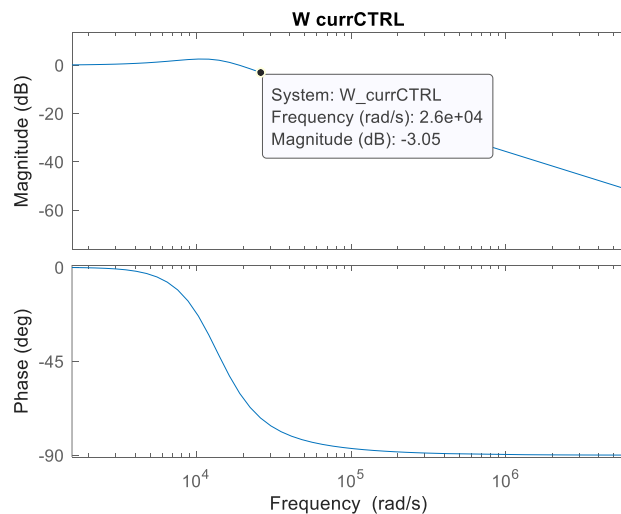

Figure 5.12: Bode Plot of the Closed Loop transfer function W_currCTRL

The stability analysis is conducted by evaluating the open-loop transfer function (**Figure 5.13**). At the gain crossover frequency (the frequency where the magnitude of the open-loop transfer function is equal to 0 dB), the phase is measured as −120°, as shown in the figure below. The stability of the closed-loop transfer function is assessed using Formula (38).

Since the phase margin is positive ($m_\phi = 60°$) the closed-loop transfer function is stable.

It is important to note that a phase margin of 60° was chosen during the design of the PI controller parameters. This design decision ensures stability and satisfactory dynamic performance of the system. Consequently, the phase margin observed in the stability analysis aligns with the design phase margin, as the closed-loop system's behavior directly depends on the controller tuning.
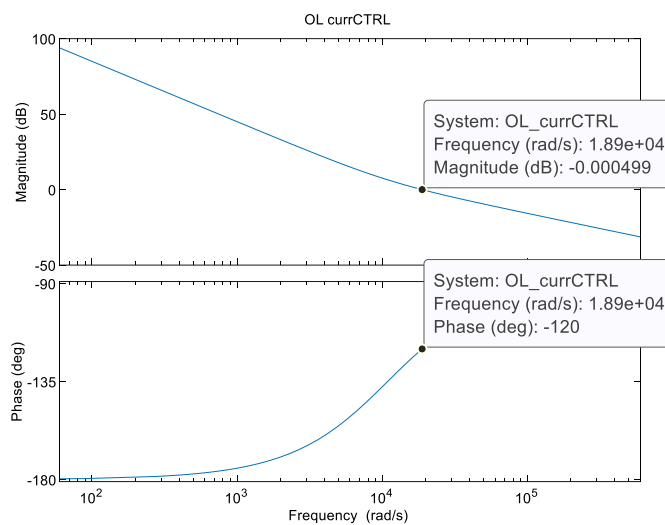
Figure 5.13: Bode Plot of the Open Loop Transfer Function OL_currCTRL

The final verification is performed by checking the steady-state error of the PI controller. For proper operation, the steady-state error at the reference frequency (0 Hz, since the system is DC) should be zero. This implies that the closed-loop transfer function's gain at s=0 should be equal to one. The closed-loop transfer function evaluated in MATLAB is:

$$W_{\text{currCTRL}}(s) = \frac{1.632e04\ s^2 +\ 1.035e12\ s\ +\ 1.127e16}{s^3 + 6.343e07s^2 + 1.035e12\ s + 1.127e16}$$

So $W_{\text{currCTRL}}(0) = \frac{1.127e16}{1.127e16} = 1$

The good performance of the closed loop boost converter control is verified.

5.3 Simulation of the Single-Phase Standalone Inverter

The single-phase full-bridge inverter is implemented in Simulink using fundamental building blocks. Initially, the inverter is modeled independently, without connections to other system components, to analyze its behavior in isolation and eliminate potential interactions with the larger system. In this setup, the DC bus is replaced by a 750 V DC voltage source. The full bridge consists of four IGBT/diode blocks controlled by a PWM scheme. An LCL filter is then connected to a resistive load. The Simulink model of the inverter is illustrated below.
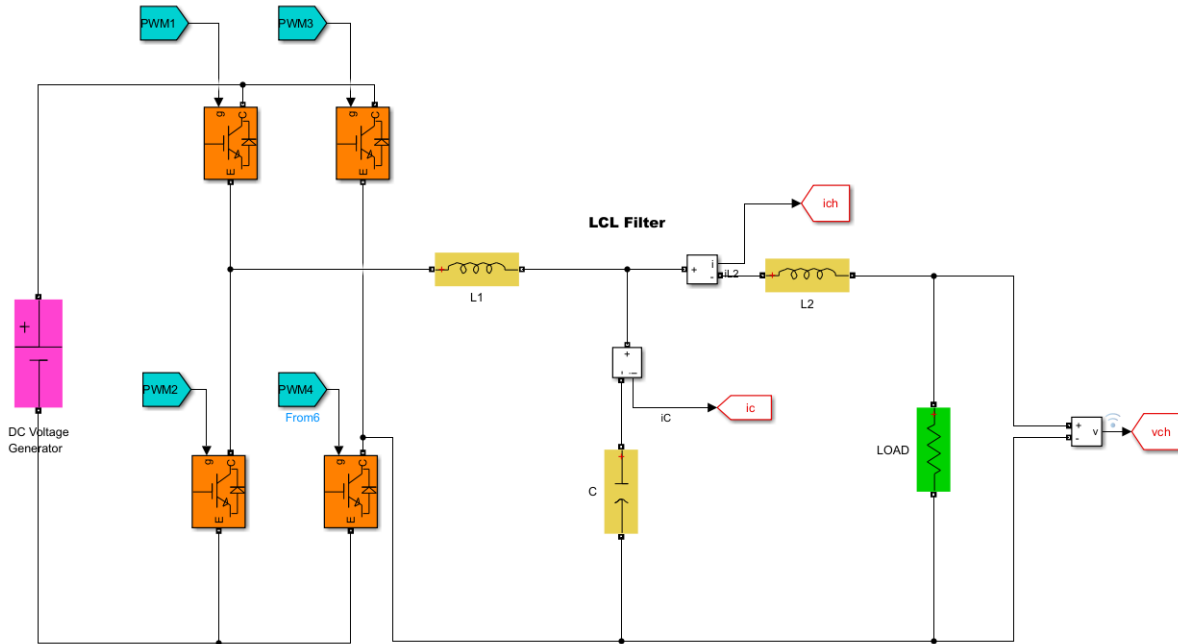
Figure 5.14: Simulink Implementation of the Single-Phase Standalone Inverter

Then the closed-loop control must be implemented. Firstly, the transfer function between the capacitor current and the duty cycle d is used to evaluate ki and kp. The bandwidth for the inner loop is assumed to be 18000 rad/s while for the outer loop, it is 3000 rad/s, and the phase margin is assumed to be 60° for both. For the inner loop: ki=217.6 and kp=0 (so an integral control will be used), while for the outer loop ki=114.7 and kp= 0.03274. From the PID tuner tool is seen that this bandwidth ensures stable behavior of the system.

The control diagram is built in Simulink (**Figure 5.15**). The system begins by comparing the measured voltage on the load (Vch) with a sinusoidal reference signal that represents the desired output waveform. The error between these two signals is processed by a PI controller, which generates the reference current for the capacitor. The measured capacitor current (ic) is then compared with this capacitor current reference, and the resulting error is processed by the current controller. The output of the current controller determines the duty cycle required to drive the inverter.

This duty cycle is used in a pulse-width modulation PWM process, where it is compared to a triangular carrier signal to generate the appropriate switching signals for the inverter. The resulting PWM signals are complementary, with logical operations (such as NOT gates and signal inversion) ensuring correct and safe switching of the full-bridge inverter's switches.
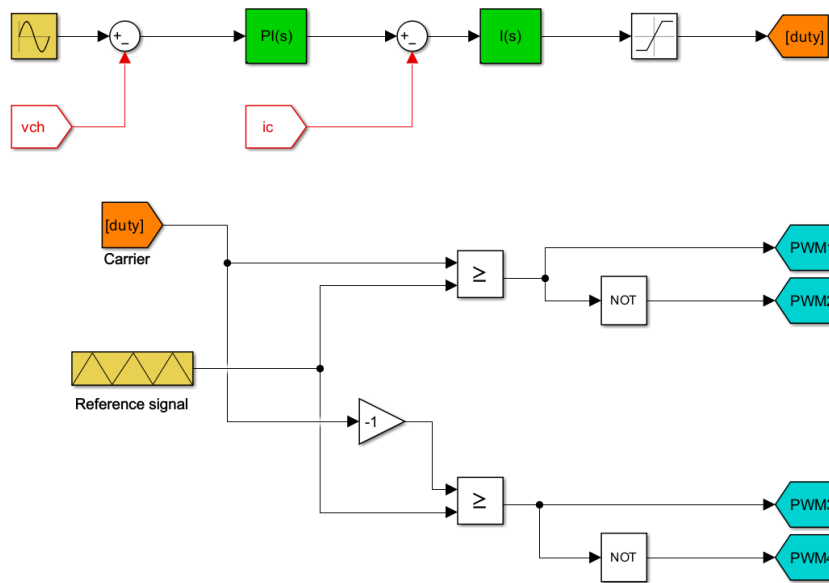
Figure 5.15: Simulink Implementation of Inverter Control
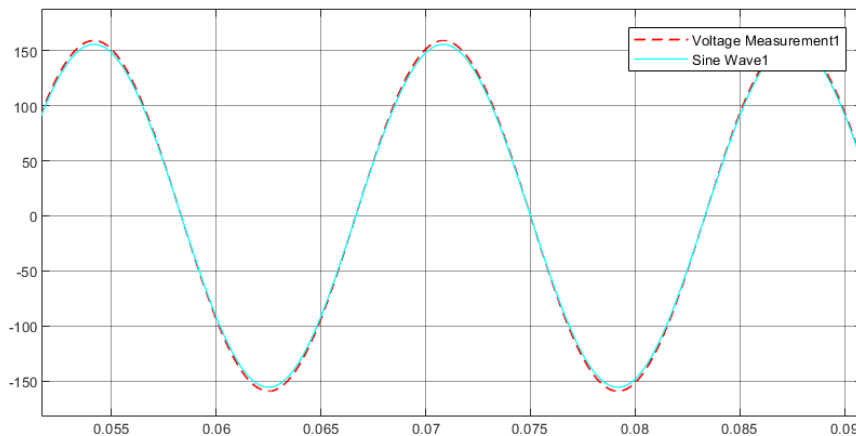
The voltage and current waveforms are shown below:

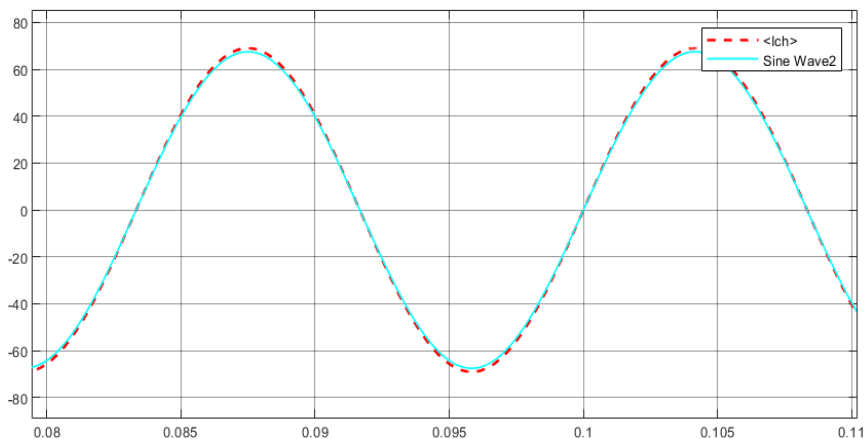*Figure 5.16: Output Voltage Waveform using a PI controller*

Figure 5.17: Output Curren Waveform using a PI controller

The output current and voltage are sinusoidal waveforms that follow the reference signal; however, the peak values of both voltage and current exceed the reference values. For instance, the voltage measures 112.4 V RMS instead of the desired 110 V RMS. This discrepancy is due to the tracking error, as the PI controller is designed primarily for DC quantities, whereas in this case, the reference signal has a frequency of 60 Hz. Consequently, the steady-state error is not zero. From the Bode plot of the open-loop transfer function (**Figure 5.18**), it is evident that the gain at 60 Hz is not sufficiently high to achieve zero steady-state error.
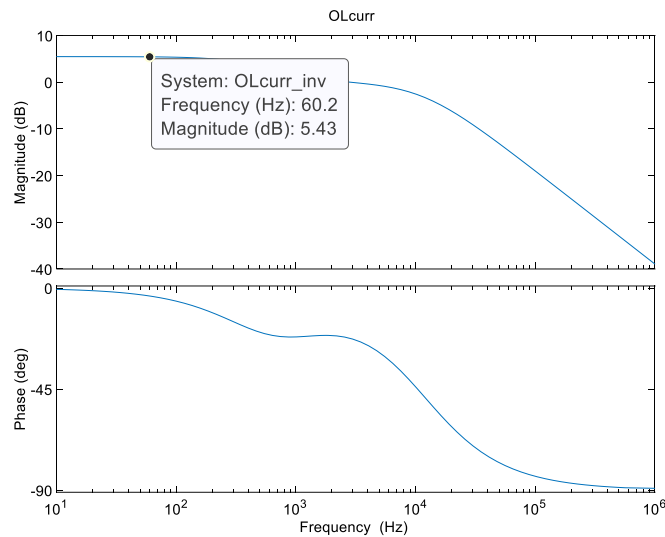

Figure 5.18: Bode Plot of Open Loop Transfer Function OL_currINV using a PI controller

While this error does not significantly compromise the performance of the control system, using a PR controller (Proportional-Resonant) would improve performance. A PR controller introduces an infinite gain at the target frequency, eliminating the tracking error and enhancing overall system precision. So, the integral control for the current loop is substituted by the PR controller calculated using Formula 42). From the bode plot of the open loop transfer (**Figure 5.19**) function defined using formula 37) it can be verified that the PR control ensures an infinitive gain at f=60Hz.
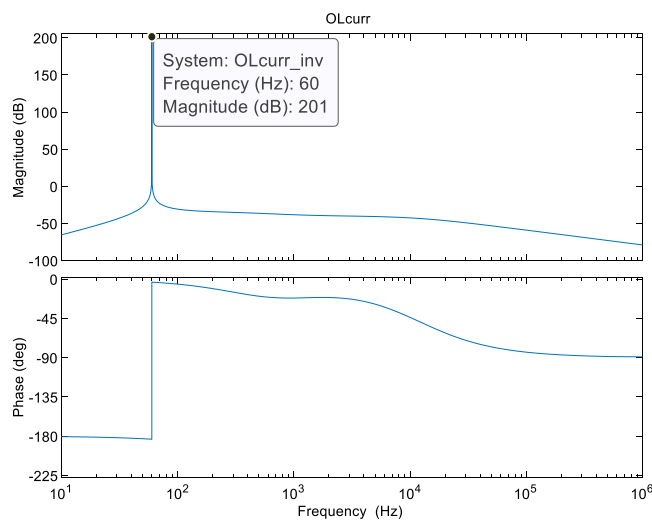

Figure 5.19: Bode Plot of Open Loop Transfer Function OL_currINV using a PR controller

The new parameters for the voltage control loop must be tuned again from formula 41) using the W_curr calculated using the PR control. The bandwidth and phase margin are kept as before, obtaining ki=3743 and kp=1.594. The Simulink simulation is done again and now the controlled voltage and current are perfectly equal to the reference waveform (**Figure 5.20** and **Figure 5.21**).
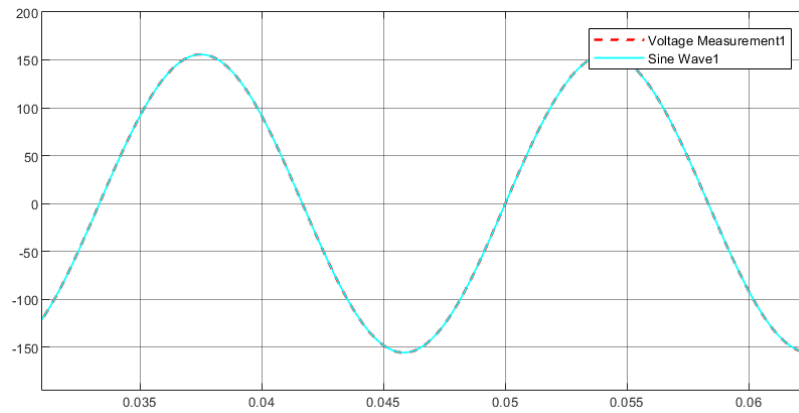

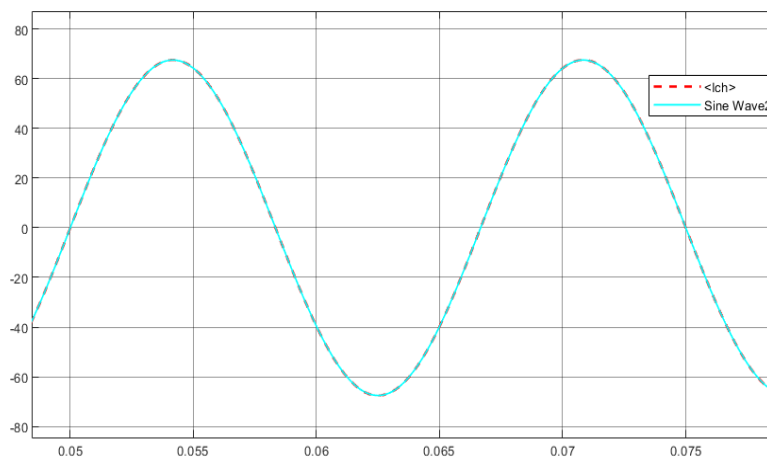*Figure 5.20: Output Voltage Waveform using a PR controller*

Figure 5.21: Output Current Waveform using a PR controller

The RMS value of the output quantities is exactly what is expected (110 V RMS for the voltage and 47.77 A RMS for the current)

5.4 Simulation of the DC Bus Voltage

Once the implementation of the various components is done, the control of the entire linked system must be built. In particular, it must be verified that the battery absorbs or provides the required energy to maintain the power at the bus equal to zero, keeping the DC Voltage constant.

Initially, the control is made on a simplified circuit that replaces the PV array and the battery, simulating their behavior and allowing an easier understanding of the control dynamics.

The basic circuit comprises the capacitor filter at the DC bus, and two current generators, one representing the PV panels and the other the battery. Given a certain amount of power by the PV array, the control must measure the voltage across the capacitor and provide the reference battery power (and so the current) to the battery to balance the power on the bus. The scheme is shown in the Figure below:
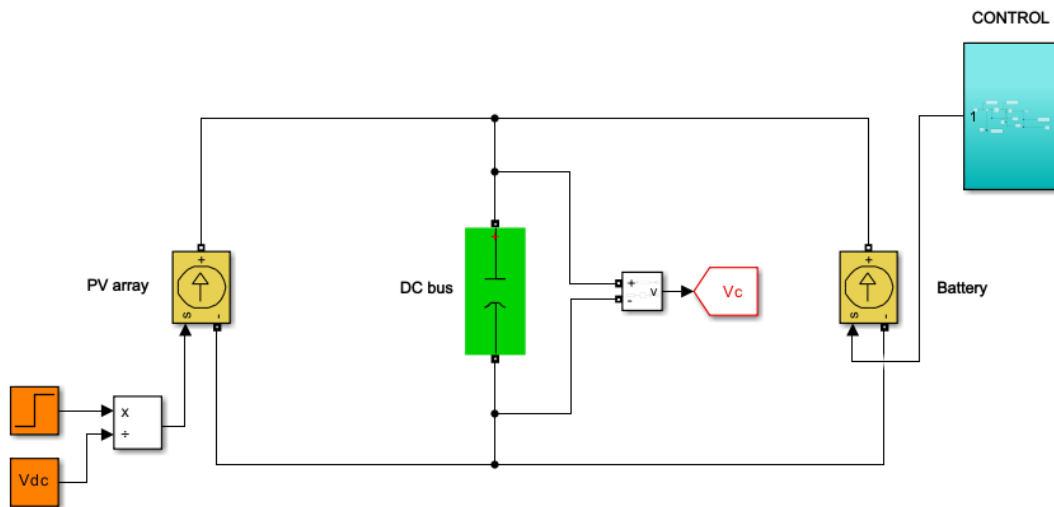

Figure 5.22: Basic Circuit (current generators and capacitor filter) for DC bus Voltage Control

The capacitor is already assumed completely charged at 750 V, a Step is applied at Tsim/2 to the input power to see the transient response of the system and to verify that the control response is fast enough. The closed-loop control starts with the measurement of the capacitor voltage which is compared to the reference Vdc to compute the error, processed by the PI block. The output of the control block is the battery power divided by the voltage to get the current flowing from/to the battery. The control scheme is shown below. Ki and kp are tuned through the PID tuner tool using the transfer function in Formula 46), a Bandwidth of 1/fsw, and a phase margin of 60°.
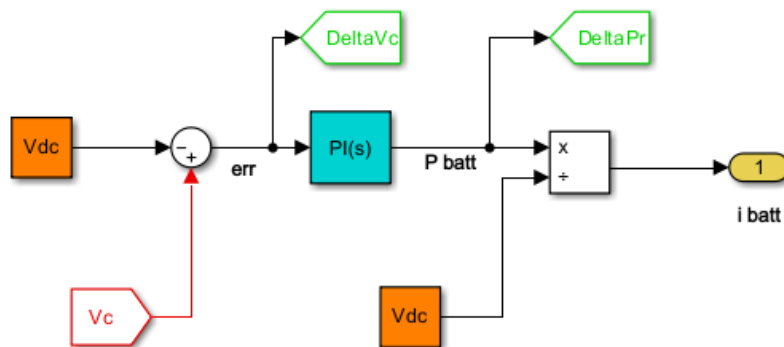

Figure 5.23: Voltage Closed Loop Control scheme for the Basic Circuit

The current generated by the solar panel flows directly into the battery, for the convention used the PV current is positive while the battery one is negative. The real voltage control made by the PI block is compared with the theoretical one using the close loop transfer function CL defined in formula 47) and they perfectly overlap as shown below (note that the voltage variation is considered due to the variation of input power of 375 W).
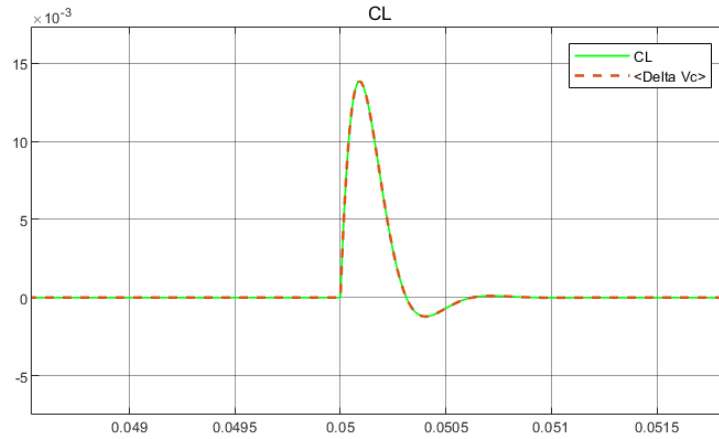

Figure 5.24: Voltage response after a Disturbance (in Basic Circuit)

The power variation on the battery is compared with the variation of the input power (represented by the step block) as shown below:
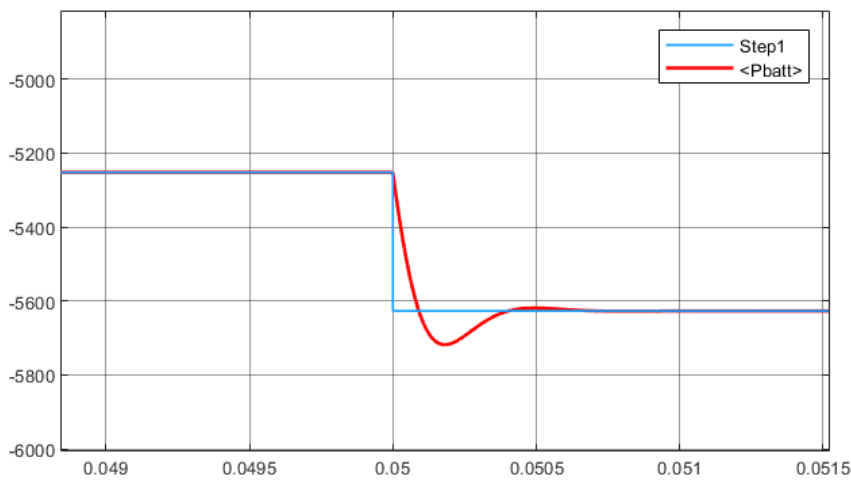

Figure 5.25: Battery Power response after a Disturbance (in Basic Circuit)

This basic circuit helps understanding how the voltage control of the DC bus must work, and it is used as a base to implement the integrated system with all the components. Then the control is carried out using all the DC components (PV, boost converters, and battery). In the case of a more complex system, the double-loop voltage and current must be implemented. Even in this case, the PID tuner tool from MATLAB is used to compute ki and kp for both voltage and current control. The internal loop bandwidth is 1/10 fsw while the external loop bandwidth is 1/100 fsw and the phase margin is 60° for both the controller.
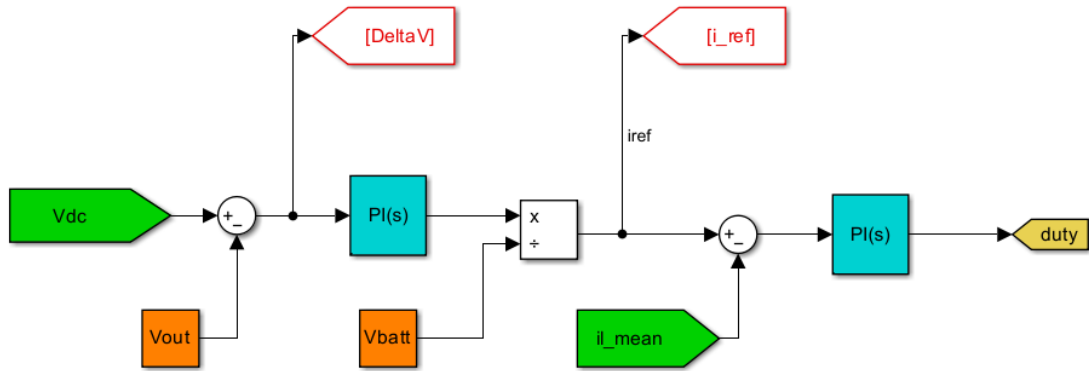
The control scheme is shown below:

Figure 5.26: Double Inner Current and Outer Voltage Loop Control Scheme

The simulation is carried out, the voltage behavior is the same as in the case of the basic circuit with only the 2-current generator. The inner loop current control has already been explained in the section about the boost converter (on the battery side) control. The only difference here is that the reference current is calculated as a function of the voltage variation instead of being a constant reference value, calculated by the basic Kirchoff low. Note that in this case a small resistance is added in series with the filter DC capacitor, but this does not affect the performance and behavior of the system.

Initially, the measured voltage is 750V since the filter capacitor's initial value is set to 750V and the power produced by the PV panels is totally absorbed by the battery. At Tsim/2, the generated power increases due to an increase in solar irradiance which passes from 1000W/m^2 to 1100W/m^2. So, the voltage on the capacitor shows a transient behavior: it increases suddenly because of the higher injected power, but then the measured voltage stabilizes again around 750V because the control varies the current in the battery, to compensate for the excess of power. The voltage trend is shown below (the red curve is the measured DC voltage, the blue one is the reference constant voltage):
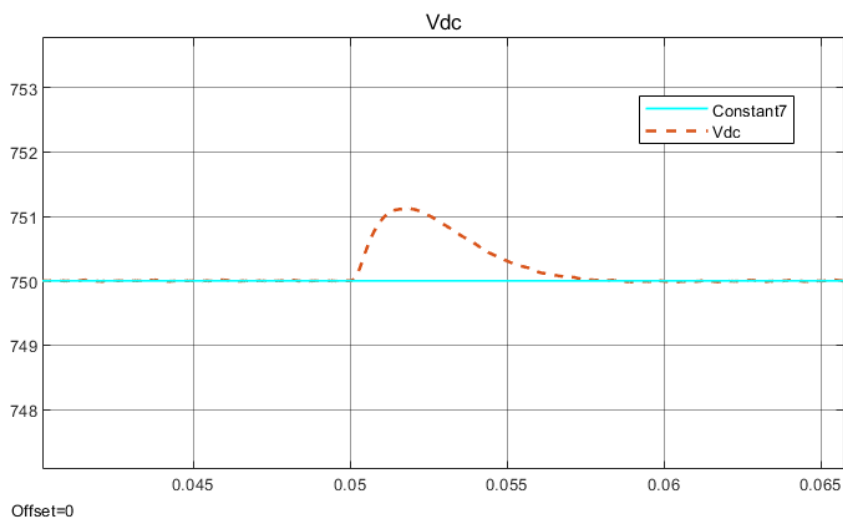

Figure 5.27: DC Voltage Simulation Result of the Double Loop Control

The battery current (a negative sign for how the system is built) increases in absolute value after the appliances of the external disturbance because more current flows to the battery to compensate the variation in power and keep the power on the capacitor filter Pc equal to zero. The current trends is shown below:
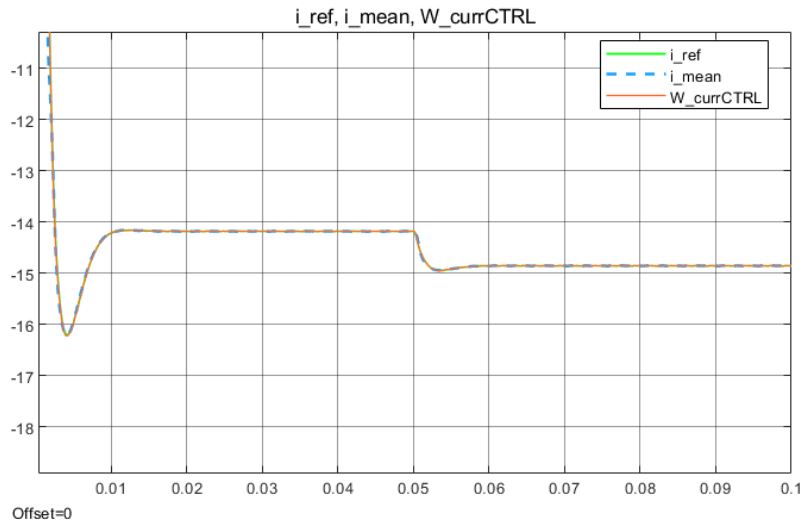

Figure 5.28: Battery Current Simulation Result of the Double Loop Control

After the initial transient, the measured battery current (denoted as i_mean in **Figure 5.28**, since the Average Boost Model is used, and the control operates on mean values) aligns with the reference value. The closed-loop transfer function, W_currCTRL, is used to evaluate the performance of the control system. Throughout the simulation, there is consistent overlap between the reference current, the measured current, and the transfer function, indicating that the control system effectively minimizes error. As a result, the measured current quickly and accurately follows the reference signal, demonstrating the responsiveness and accuracy of the control.

5.5 Simulation of the complete PV System

The last step is adding the inverter and the resistive load to the simulation, the integrated system is shown below:
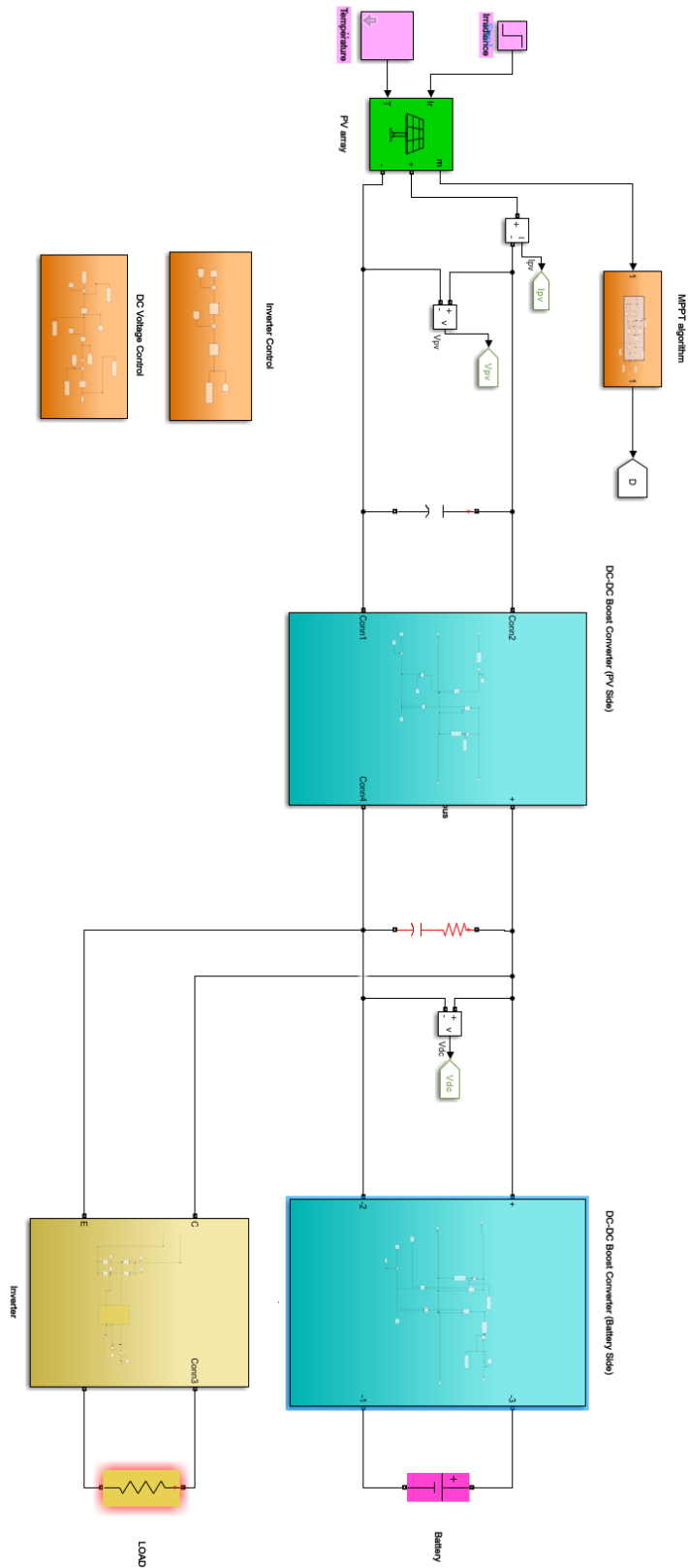

Figure 5.29: Simulink Implementation of the overall PV system

To do this some important aspects must be considered:

- The inclusion of the inverter necessitates adjustments to the voltage control parameters, specifically the proportional (Kp) and integral (Ki) gains. Previously, a bandwidth of 300 Hz ensured a fast response to DC voltage variations. However, with the inverter now linked to the DC bus, AC components are introduced, causing inherent oscillations in the bus voltage. A high control bandwidth would make the controller overly reactive to these natural oscillations, potentially destabilizing the system. To address this, the bandwidth is reduced to 10 Hz, allowing the controller to respond more gradually and mitigate its reaction to AC oscillations. Despite this adjustment, the phase margin is maintained at 60° to ensure stability and adequate transient response. In this case, kp_volt= -40.45 and ki_volt = -1401.
- The inverter and resistive load draw power from the DC bus, requiring dynamic management of power balance. When the photovoltaic (PV) array does not generate sufficient power to meet the load demand, the battery must quickly supply the deficit. Conversely, during periods of high solar irradiation, when the PV array produces excess power, the battery must absorb the surplus energy. This dynamic interaction ensures voltage stability but requires the battery system to respond promptly to real-time variations in power flow.
- The integration of the inverter inevitably introduces AC ripple effects on the DC bus. While the voltage control regulates the average DC voltage, it cannot eliminate oscillations caused by the AC component. Consequently, the battery current, controlled based on voltage variations, oscillates at the frequency of the DC voltage ripple. This results in non-constant battery power, even when power generation and consumption are balanced on average. To minimize battery power fluctuations, a compromise is made by allowing slightly larger oscillations in the DC voltage. This trade-off reduces high-frequency variations in battery current and power, enhancing system stability.

The DC voltage slowly stabilizes after a long transient because of the narrow bandwidth for the Voltage loop control which asset for the AC behavior of the inverter but slows down the response. When a variation of PV power occurs, the voltage experiences another transient and it slowly stabilizes again around 750V. Note that a Voltage ripple of 14.4 V is still present, however this is low considering the DC Voltage value. The attenuation of the voltage oscillation given at the reference frequency f = 120 Hz is calculated by imposing s = jω (where ω=2πf) in the disturbance rejection function and multiplying the given attenuation for the power of the inverter, so $P_{inv}ATT = 6.09$. The two values are closed so the theory validated the simulated model.
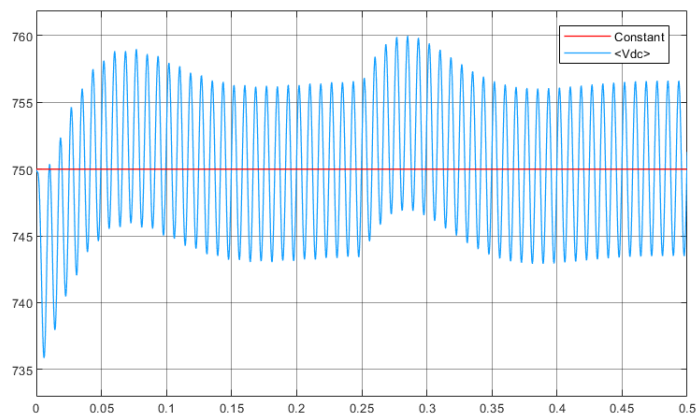

Figure 5.30: Overall System Simulation Result (DC Voltage)

The battery current is influenced by the narrow bandwidth of the outer control loop, resulting in a slow transient response before stabilization. The current exhibits a small ripple, primarily due to the AC behavior of the inverter, as the power generated by the PV system is fully absorbed by it. Following the application of an external perturbation, such as an increase in PV power, the battery current rises in absolute terms to absorb the excess power generated. The frequency of oscillation is 120 Hz as already explained in the control theory paragraph. The current trend is shown below:
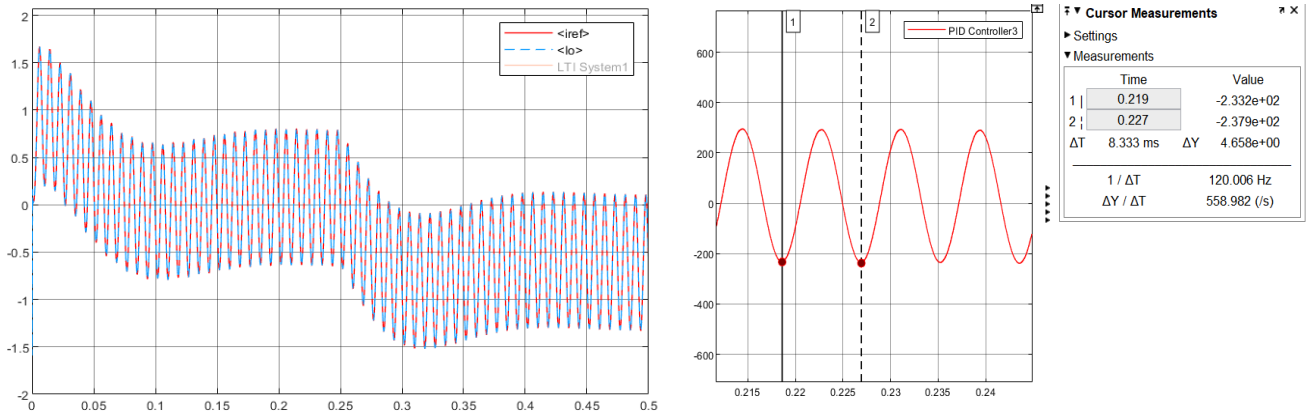

Figure 5.31: Overall System Simulation Result (Battery Current)

The battery power assumes values equal to Vbatt*ibatt, where the battery voltage is constant and equal to 370V, while the battery current oscillates.
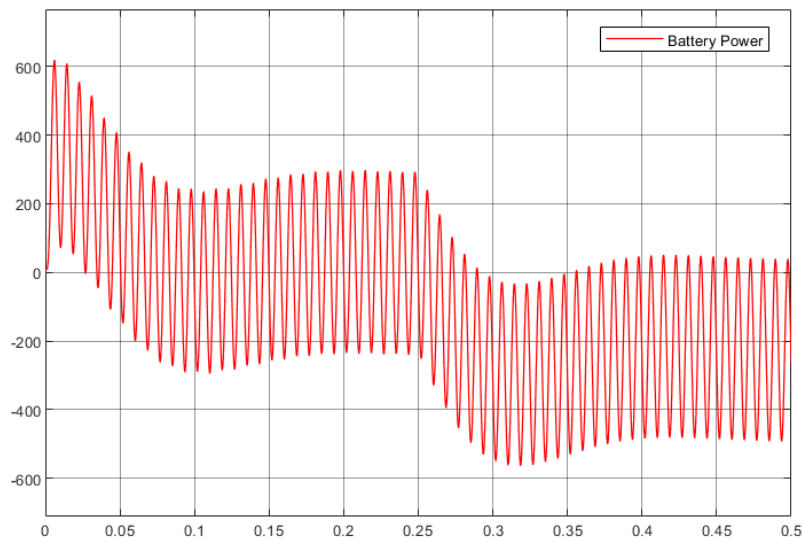

Figure 5.32: Overall System Simulation Result (Battery Power)

6. Conclusion

The integration of renewable energy sources with the power grid, or their direct connection to alternating current loads, poses a significant challenge in the context of global decarbonization and the advancement of green energy technologies. This thesis deals with on the design and analysis of a standalone photovoltaic system intended for residential applications. One of the primary challenges associated with standalone systems is the variability in energy production resulting from unpredictable meteorological conditions, which significantly impact the performance of solar panels. To ensure a continuous supply of electricity during periods of inadequate sunlight, such as during inclement weather or nighttime, an energy storage system, typically implemented as batteries, is integrated into the setup. Additionally, meeting the demand for AC loads necessitates the incorporation of an inverter, which introduces considerable control complexity due to its integration with direct current components such as solar panels, batteries, and boost converters.

The work starts with a literature review aimed at clarifying the general architecture of standalone PV systems and analyzing the importance and functionality of their principal components. A detailed theoretical description of each component was provided, followed by the mathematical formulation of control algorithms. In particular, a Perturb and Observe algorithm was executed to regulate the operation of the boost converter on the PV side, ensuring maximum power point tracking.

However, the main emphasis was placed on the control mechanisms of the single-phase standalone inverter. A dual-loop voltage-current control strategy was implemented, utilizing the capacitor current of the LCL filter as the reference in the control loops. Proportional-resonant controllers were employed to enhance system performance, given their superior ability to track sinusoidal references in comparison to traditional Proportional-Integral (PI) controllers. The parameters of the control blocks were optimally tuned using transfer functions derived from the mathematical model of the inverter.

The regulation of the DC bus voltage and the battery current was of central importance. The DC bus voltage was maintained around a specified reference value via the battery-side boost converter. The batteries either absorbed surplus power or delivered additional power to ensure balance in the total power on the bus. While oscillations in the DC bus voltage were noted due to the AC power output from the inverter, these fluctuations were managed by dynamically adjusting the battery current, thereby guaranteeing that load requirements were consistently satisfied.

The system design process begins with the sizing of the PV array, considering the energy requirements of a household user in Shawinigan, Quebec (Canada). Solar irradiation data, such as daily average irradiance, and optimal panel tilt angle were obtained from the PVGIS-ERA5 database provided by the European Commission. The PV array was sized to meet energy demands based on the worst-case scenario, specifically considering the average daily radiation in December. The remaining system components were sized under ideal conditions to verify the underlying assumptions of the control models.

The theoretical models were validated through simulations conducted in MATLAB/Simulink. The MPPT algorithm effectively tracked the maximum power point under varying irradiance and temperature conditions. Increases in irradiance led to elevated power generation, while lower temperatures enhanced panel efficiency, although this came at the expense of reduced battery performance in cold weather. The boost converter was assessed using multiple models (Average, Switching, and Small Signal models) to confirm their accuracy. Performance metrics, including rise time, steady-state error, and Bode diagrams of transfer functions, underscored the stability and reliability of the control strategies. The inverter generated sinusoidal voltage and current outputs that closely aligned with

reference values, achieving zero tracking error and validating the efficacy of the dual-loop control approach.

The DC bus voltage generally conformed to the reference value; however, the AC outputs produced by the inverter introduced fluctuations in the DC bus. Consequently, the DC bus voltage oscillated around its desired reference value, influenced by the inverter's AC power production which varied in response to changes in solar generation. These voltage oscillations impacted the battery current, prompting the battery to either supply or absorb power to uphold the DC bus voltage at a stable level. The battery dynamically compensated for these fluctuations to maintain the overall power balance on the bus, stabilizing the capacitor voltage even when power production from the PV array varied. Despite these oscillations, the system effectively satisfied load demands as the battery continually adjusted to maintain voltage stability on the DC bus.

Future enhancements include the experimental validation of the system utilizing a laboratory test bench. This setup will feature a real inverter, an LCL filter, and variable AC loads to evaluate the system's response to practical disturbances such as changes in load and power generation fluctuations. These experiments will assess voltage quality, control stability, and the overall performance of the proposed algorithms, providing critical insights for the improved practical integration of standalone PV systems.

This thesis contributes to the advancement of sustainable energy solutions by presenting a comprehensive framework for the design, control, and validation of standalone photovoltaic systems. The obtained results emphasize the significance of robust control strategies and precise system design in ensuring reliable energy delivery for residential applications, thereby facilitating progress in the integration of renewable energy sources.

Bibliography

[1] International Renewable Energy Agency (IRENA). "Renewable energy integration in power grids," 2015. URL: https://www.irena.org/publications/2015/Apr/Renewable-energy-integration-in-power-grids

[2] McKinsey & Company. "How grid operators can integrate the coming wave of renewable energy," 2024. URL: https://www.mckinsey.com/industries/electric-power-and-natural-gas/our-insights/how-grid-operators-can-integrate-the-coming-wave-of-renewable-energy#

[3] M. A. Basit, S. Dilshad, R. Badar, et al. "Limitations, challenges, and solution approaches in grid-connected renewable energy systems", *International Journal on Energy Research*, 2019. URL: https://onlinelibrary.wiley.com/doi/epdf/10.1002/er.5033

[4] M. Shafiullah, S. D. Ahmed, F. A. Al-Sulaiman, "Grid Integration Challenges and Solution Strategies for Solar PV Systems: A Review," *IEEE Transactions on Smart Grid*, 2022. URL: https://ieeexplore.ieee.org/document/9773105

[5] S. Mohammed, D. Devaraj et al. "Simulation and analysis of stand-alone photovoltaic system with boost converter using MATLAB/Simulink," *IEEE International Conference on Circuit, Power and Computing Technologies*, 2014. URL: https://ieeexplore.ieee.org/document/7054991

[6] V. Tamrakar, S.C. Gupta, Y. Sawle, "Study of characteristics of single and double diode electrical equivalent circuit models of solar PV module**"**, *IEEE International Conference on Energy Systems and Applications*, 2015. URL:https://ieeexplore.ieee.org/document/7503362

[7] A. Nandi, A. Manna, A. Mohapatra et al. "Analysis of Effect of Partial Shading on PV Array and Location of Local Maxima in PV Characteristics", *IEEE Power Electronics & IoT Applications in Renewable Energy and its Control International Conference*, 2022. URL: *https://ieeexplore.ieee.org/document/9726575*

[8] Y. Chaibi, A. Allouhi, M. Malvoni, et al. "Solar irradiance and temperature influence on the photovoltaic cell equivalent-circuit models", *Solar Energy Journal*, 2020. URL: https://www.sciencedirect.com/science/article/pii/S0038092X19306590

[9] M. Y. Worku, M. A. Hassan, L. S. Maaraba et al. "A Comprehensive Review of Recent Maximum Power Point Tracking Techniques for Photovoltaic Systems under Partial Shading", 2023. URL: https://www.mdpi.com/2071-1050/15/14/11132

[10] Y. Rais; A. Zakriti; A. Khamlichi. "Maximum Power Point Tracking in Photovoltaics: Overview and Application*" Renewable Energies, Power Systems & Green Inclusive Economy*, 2018. URL: https://ieeexplore.ieee.org/document/8488818

[11] IntegraSources. "DC-DC converters: Functions, types, design, applications, and challenges," IntegraSources, 2022. URL: https://www.integrasources.com/blog/dc-dc-converters-functions-types-design-applications-challenges/

[12] B. T. Lynch, "Under the Hood of a DC/DC Boost Converter", Texas Instruments, URL: https://www.ti.com/download/trng/docs/seminar/Topic_3_Lynch.pdf

[13] Electronics for Energy Notes, AA 2014/2015

[14] H. E. Oliveira Farias, L. Neves Canha "Battery Energy Storage Systems (BESS) Overview of Key Market Technologies", *IEEE PES Transmission & Distribution Conference and Exhibition - Latin America*, 2018. URL: https://ieeexplore.ieee.org/document/8511796

[15] R. Teja, "Difference Between Single Phase and Three Phase," *ElectronicsHub*, 2024. URL: https://www.electronicshub.org/difference-between-single-phase-and-three-phase/

[16] "Single Phase vs Three Phase; What's the Difference?," *ChintBlog,* 2021. URL: https://www.chintglobal.com/global/en/about-us/news-center/blog/single-phase-vs-three-phase.html

[17]"Grid Tied, Off Grid, Hybrid Solar Inverter," *SolarCtrl*, 2023. URL: https://www.solarctrl.com/blog/grid-tied-off-grid-hybrid-solar-inverter/

[18] "Types of Inverters and their Applications," *Electrical Technology*, 2020. URL: https://www.electricaltechnology.org/2020/06/types-of-inverters.html

[19] J. Soomro, T. D. Memon, M. A. Shah "Design and analysis of single phase voltage source inverter using Unipolar and Bipolar pulse width modulation techniques", *IEEE 2016 International Conference on Advances in Electrical, Electronic and Systems Engineering,* 2016. URL: https://ieeexplore.ieee.org/document/7888052

[20] U. P. Yagnik, M. D. Solanki, "Comparison of L, LC & LCL filter for grid-connected converter", *IEEE International Conference on Trends in Electronics and Informatics*, 2017. URL: https://ieeexplore.ieee.org/document/8300968

[21] C. Chen, J. Lai, Y. Wang, et al. "Design and Control for LCL-Based Inverters with Both Grid-Tie and Standalone Parallel Operations", *IEEE Industry Applications Society Annual Meeting*, 2008. URL: https://ieeexplore.ieee.org/document/4659114

[22] M.A. Elgendy, B. Zahawi, D. J. Atkinson, et al. "Assessment of Perturb and Observe MPPT Algorithm Implementation Techniques for PV Pumping Applications", *IEEE Transactions on Sustainable Energy*, 2011. URL: https://ieeexplore.ieee.org/document/6102293

[23] O. Rabia, B. H. Mouna, S. Lassaad. "Cascade Control Loop of DC-DC Boost Converter Using PI Controller", *International Symposium on Advanced Electrical and Communication Technologies*, 2018. URL: https://ieeexplore.ieee.org/document/8618859

[24] M. Ishaq, M. Waqar, M. H. Afzal. "Design of Double Closed-Loop Boost Converter Controller to Reduce Transient Voltage Dip for Sudden Load Connection", *International Conference on Emerging Power Technologies*, 2023. URL: https://ieeexplore.ieee.org/document/10152449

[25] N.M. Abdel-Rahim; J.E. Quaicoe, "Analysis and design of a multiple feedback loop control strategy for single-phase voltage-source UPS inverters," *IEEE Transactions on Power Electronics*, 2002. URL: https://ieeexplore.ieee.org/document/506118

[26] H. Cha, T. Vu, J. Kim et al. "Design and control of Proportional-Resonant controller based Photovoltaic power conditioning system", *IEEE Energy Conversion Congress and Exposition*, 2009. URL: https://ieeexplore.ieee.org/document/5316374

[27] R. D. Bhagiya, R. M. Patel. "PWM based Double loop PI Control of a Bidirectional DC-DC Converter in a Standalone PV/Battery DC Power System", *2019 IEEE 16th India Council International Conference*, 2019. URL: https://ieeexplore.ieee.org/document/9028974

[28] European Commission, Joint Research Centre. "Photovoltaic Geographical Information System (PVGIS)," 2023. URL: https://re.jrc.ec.europa.eu/pvg_tools/it/?lat=&lon=&startyear=&endyear=&raddatabase=&angle=&browser=&outputformat=&userhorizon=&usehorizon=&js=1&select_database_month=PVGIS-ERA5&mstartyear=2020&mendyear=2023&selectrad=1&mangle=30#PVP

[29] DIY Solar Forum. "PV Array Temperature Correction Table (NEC 2017.78)," 2017. URL: https://diysolarforum.com/resources/pv-array-temperature-correction-table-nec-2017.78/#:~:text=There%20are%20calculators%20like%20this%20one%20made%20by%20@upnorthandpersonal%20which

[30] A. Reznik, M. Godoy Simões, A. Al-Durra et al. "LCL Filter Design and Performance Analysis for Grid-Interconnected System", *IEEE Transactions on Industry Applications*, 2013. URL:

https://xplorestaging.ieee.org/document/6571219

[31] W. Wu, F. Blaabjerg, H. Chung, Y. He, M. Huang, Control and Filter Design of Single-Phase Grid Connected-Converters, *IEEE Press Editorial Board*, 2023, pp. 54-55